SAINT-PETERSBURG UNIVERSITY

Yasser Elsayed Shaaban Mohamed

CHARACTERISTICS OF THE STRUCTURE OF GROUNDWATER FLOW IN ARID REGIONS (BASED ON THE EXAMPLE OF THE NORTHERN PART OF SINAI PENINSULA, EGYPT)

Scientific specialty 1.6.6. Hydrogeology

Thesis

to apply for a scientist PhD degree in geological and mineralogical sciences

Translation from Russian

Scientific adviser-
candidate of geological-min. sciences,
assistant professor
N.A.Vinograd

Saint-Petersburg
2023

TABLE OF CONTENT

Page

INTRODUCTION

Relevance of the research. The Arab Republic of Egypt is entirely located in the arid climate zone. Lack of water for drinking, industrial and agricultural purposes is a major problem. Currently, the provision of water resources is carried out mainly through surface water - the river Nile. However, problems have recently arisen between countries geographically connected to the Nile River (Egypt, Ethiopia and Sudan) due to the construction of the Ethiopian Dam, which will further reduce the availability of water from the river Nile for Egypt due to increased water withdrawal by these countries. In this regard, the problems of groundwater extraction in various territories of Egypt, including the Sinai Peninsula, are of paramount importance.

Goal of the research. Regional hydrogeodynamic and hydrogeochemical characteristics of the territory of one of the administrative units of the Arab Republic of Egypt - North Sinai, which is approximately half the size of the Sinai Peninsula, with the aim of further justifying the possibility of predicting the production and management of groundwater resources in this territory.

Main objectives of the research:

- Collection, synthesis and systematization of all materials on the geological structure and hydrogeological conditions of the study area.
- Creation of databases on hydrodynamic and hydrogeochemical characteristics of aquifers.
- Statistical processing of data on the hydrogeodynamic characteristics of aquifers and the chemical composition of groundwater.
- Identification of genetic types of groundwater developed within North Sinai.
- Zoning of the territory of North Sinai according to the values of filtration parameters of aquifers and the value of groundwater mineralization. Construction of a map-scheme of general and local filtration flows of groundwater within the territory of North Sinai.

Object of the research is the aquifers developed in the territory of North Sinai.

Factual material on hydrogeological, hydrogeodynamic and hydrogeochemical indicators for about 500 wells for various purposes in the territory of North Sinai was collected by the author during 2009−2020. in various centers and departments associated with the Egyptian Ministry of Water Resources and Irrigation, as well as in selected non-governmental organizations.

Research methods. To solve the problems, the following methods were used:

- Study of the geological structure and hydrogeological conditions of the territory of North Sinai based on the results of a synthesis of published and stock materials.
- Creation and updating of databases on hydrogeodynamic characteristics, filtration parameters and chemical composition of waters of the main aquifers.
- Obtaining various statistical characteristics of the distribution of values of hydrogeodynamic and hydrogeochemical indicators and corresponding correlation dependencies using the SPSS Statistics 17.0.0 program.
- Computer physical and chemical modeling of the state of groundwater with assessment of the degree of their saturation in relation to the main carbonate and sulfate minerals using the “PHREEQC interactive 3.5.0.14000” program.
- Construction of computer maps of hydrogeological purposes using the GIS software package “ArcGIS Desktop 10.6-version 10.6.0.8321”.
- Zoning of the study area according to reasonable criteria (gradations) of various hydrogeodynamic and hydrogeochemical indicators.

Scientific novelty:

- For the first time, based on data from more than 500 wells, a generalized description of the conditions of occurrence of aquifers, hydrogeodynamic and hydrogeochemical features of the entire northern part of the Sinai Peninsula is given.

- Based on the collected material, a unified database on hydrodynamic characteristics, filtration parameters and chemical composition of aquifer waters was created.
- Computer maps of the roof-base were constructed for all aquifers identified in North Sinai.
- The main statistical characteristics of the distribution and correlation dependences of the filtration coefficient, mineralization and concentrations of macrocomponents on various rock parameters were obtained.
- The territory of Northern Sinai has been zoned according to the filtration coefficient and mineralization of groundwater.
- The main genetic groups of groundwater developed within North Sinai have been identified and substantiated.
- Based on 250 hydrogeological wells, a regional map of the generalized filtration flow within North Sinai was constructed, which shows that the general direction of this flow for all horizons in the aggregate is determined mainly by the presence of the main regional drain - the Mediterranean Sea - with an average hydraulic slope of about 0.002. Internal, local directions of groundwater flows are determined by the presence of local drains confined to the wadi valleys.
- The most promising water supply areas based on Quaternary and pre-Quaternary aquifers are shown. (Quaternary - Wadi El Arish and the northwestern part of North Sinai; pre-Quaternary - El Qusaima, Gebel El Magara, Rafah and Sheikh Zuwayid, Baghdad, Gebel Libni and Gebel Arif El Naga).

Theoretical and practical significance of the research. This work allows us to assess the regional hydrogeodynamic and hydrogeochemical features of the territory of North Sinai. The results will provide a basis for the administrative authorities of the Arab Republic of Egypt in drawing up a plan for the sustainable

development of North Sinai, taking into account the availability of groundwater for water supply to various residential, agricultural and industrial sites.

Defense provisions:

1. The territory was zoned according to the values of filtration coefficients for each aquifer in order to determine the most promising areas for groundwater extraction. Through statistical justification for 180 hydrogeological wells, characteristic values of filtration coefficients for various types of rocks were identified.

2. Up to the maximum tested depth, mineralization and concentrations of the main macrocomponents in both Quaternary and pre-Quaternary aquifers were examined. The formation of the chemical composition of groundwater is influenced by several factors: infiltration feeding by atmospheric precipitation and/or surface waters, metamorphization (evaporation), intrusions of sea water from the Mediterranean Sea, dilution of the original sedimentogenic waters with infiltration waters. Most likely, most water are mixed genesis.

3. The flow of groundwater is directed from south to north, towards the Mediterranean Sea, the Gulf of Suez and the Gulf of Aqaba, as well as (in a local sense) to the valleys of the main wadis. The average hydraulic slope is about 0.002. A database has been created on the level regime of groundwater, quaternary and pre-quaternary aquifers. Maps of hydro-isohypsum and hydro-isopyesis were constructed using GIS.

Personal contribution of the author. Work directly on the dissertation was carried out by the author, starting in 2017, at the Department of Hydrogeology of St. Petersburg State University (SPbSU) during postgraduate studies. It is based on materials collected personally by the author for the period (2017-20), as well as, and mainly, during his work at the Department of Hydrology of Zagazig University (Egypt) as an assistant (2009-14) and junior teacher (2014–16). The creation of appropriate databases, their statistical processing, compilation of computer maps, identification of genetic groups of groundwater, as well as zoning

of the territory of North Sinai according to various parameters was carried out directly by the author.

Credibility scientific provisions and conclusions are justified by the quality of primary geological, hydrogeological, hydrogeodynamic and hydrogeochemical information collected by the author from stock materials, as well as by approbation of work at conferences on earth sciences.

Approbation of research results. On the topic of the dissertation, 2 articles were published in peer-reviewed journals from the Higher Attestation Commission list, 1 article in peer-reviewed journals from the Web of science list, as well as 3 works indexed in the RSCI. The author participated in the conferences: “Geology, geoecology, evolutionary geography” (St. Petersburg, 2020), “XVII Great Geographical Festival” (St. Petersburg, 2021) and in the XXIII meeting “Underground waters of the East of Russia” (Irkutsk, 2021).

Structure and scope of the research. The work includes an introduction, 5 chapters and a conclusion. The total volume of the dissertation is 140 pages, including 96 figures and 25 tables.

Acknowledgment. The author expresses gratitude to the scientific supervisor, Ph.D., Associate Professor N.A. Vinograd for general scientific and organizational leadership of the work and many useful ideas; scientific consultant Ph.D. A.A. Potapov for identifying many scientific approaches and great assistance in processing the results; to the entire teaching staff of the Department of Hydrogeology of St. Petersburg State University for consultations in the process of writing the work, as well as to assistant A.S. Ivleva for valuable assistance in preparing the dissertation.

Publications in journals reviewed by the Higher Attestation Commission:

1. Mohamed Y.S., et al., (2020). Assessment of filtration conditions through earthen dams when changing their parameters using the Z_SOIL program // Bulletin of Voronezh State University. Series: Geology. No. 2. pp. 90-97. DOI: https://doi.org/10.17308/geology.2020.2/2863

2. Mohamed Y.S. et al., (2021). Natural and man-made factors in the formation of filtration flows of groundwater in Northern Sinai // Bulletin of Voronezh State University. Series: Geology. No. 4. pp. 71-81. DOI:https://doi.org/10.17308/geology.2021.4/3792

Publications in the journals Web of Science Core Collection, Scopus, RSCI:

3. Mohamed Ya. Sh., Lisetskii F. N., Budarina V. A., Vinograd N. A., Potapov A. A., (2021). Justification for Effective Water Planning and Management in the North of the Sinai Peninsula, Egypt // Journal Bioscience Biotechnology Research Communications. Vol. 14, No. 03, pp. 986-992. DOI: http://dx.doi.org/10.21786/bbrc/14.3.13

Other publications:

4. Mohamed Y.S., et al., (2020). Structure of groundwater filtration flows in the North of the Sinai Peninsula. Geology, geoecology, evolutionary geography: Collective monograph. Volume XIX / Ed. EAT. Nesterova, V.A. Snytko. -SPB.: Publishing house of the Russian State Pedagogical University named after. A.I. Herzen. No. 36. pp. 259-262. ISBN 978-5-8064-2986-6.

5. Mohamed Y.S. and Vinograd N.A., (2021). Tracking the natural direction of groundwater flow in North Sinai // From the 23rd XVII Great Geographical Festival, dedicated to the 195th anniversary of the Russian round-the-world trip F.P. Litke (1826-1829) - (St. Petersburg, St. Petersburg State University, Institute of Earth Sciences). C. 205-209. ISBN 978-5-4386-2045-7.

6. Mohamed Y.S. and Vinograd N.A., (2021). Zoning of the north of the Sinai Peninsula according to the filtration properties of pre-Quaternary water-bearing rocks // Underground hydrosphere: Materials of the XXIII All-Russian meeting on groundwater in eastern Russia with international participation. – Irkutsk: Institute of the Earth's Crust SB RAS, 2021. –P. 93-95. DOI: 10.52619/978-5-9908560-9-7-2021-23-1-93-95

CHAPTER 1. THE CASE STUDY OF NORTH SINAI AND FACTUAL MATERIALS

The Arab Republic of Egypt is entirely located in the arid climate zone and its area is mainly represented by deserts. Only 3% of the land (mostly in the Nile River valley) is cultivated [60]. The lack of water for drinking, cultural, domestic, technical and agricultural needs is considered a big problem for Egypt, whose territory is located in a region with an arid climate.

In 1966, renewable water resources in Egypt were 2189 m^3 per capita per year. Currently, Egypt's water resources have decreased to approximately 670 m^3/person/year [15]. This is mainly due to the constant annual population growth of 2.2%. Egypt's population is expected to grow to approximately 105 million by 2025, which will lead to decreased per capita water availability and water scarcity if overall water availability remains unchanged. In this regard, the problems of groundwater extraction and water resource management are of paramount importance.

Moreover, the problems that have arisen in recent years between states territorially connected with the river. Nile (Egypt, Ethiopia and Sudan) threaten to reduce water availability in the Republic of Egypt. These problems are expressed, for example, in an increase in water withdrawal from the river. Nile for irrigation. A particular challenge is the construction of the Ethiopian Dam, which will require filling the Nile Reservoir with an area of about 70 billion m^3 [15].

Thus, today there is an urgent need to find additional sources to solve the problem of projected water shortages in the Republic of Egypt. One of these sources is groundwater. Currently, in the Republic of Egypt, fresh groundwater resources account for less than 20% of the total balance of used water resources [15].

To cope with the challenges associated with population growth and the development of the social economy, the Egyptian government has focused on the development of the Sinai Peninsula, which is believed to have high potential for mineral resource development, tourism and agricultural activities.

The Arab Republic of Egypt is entirely located in the arid climate zone. Lack of water for drinking, industrial and agricultural purposes is a major problem. Currently, the provision of water resources is carried out mainly through surface water - the river. Nile. However, problems have recently arisen between states geographically connected to the Nile River (Egypt, Ethiopia and Sudan) due to the construction of the Ethiopian Dam, which will further reduce the availability of water from the river. Nile for Egypt due to increased water withdrawal by these countries [32; 91]. In this regard, the problems of groundwater extraction in various territories of Egypt, including the Sinai Peninsula, are of paramount importance.

On the Sinai Peninsula, located at a considerable distance from the main source of water - the river. Nile, other sources of water supply other than groundwater are practically absent, at least for most of the year outside the flood period. The territory of Sinai is completely represented by desert lands, with the exception of its very northeastern part. In general, the Sinai Peninsula is characterized by an arid climate - annual precipitation in various areas is estimated at 40 - 300 mm (the latter in the northeast).

The development of surface water in the Sinai has so far been carried out in some areas through the construction of dams and the organization of temporary reservoirs that operate only during flood periods. In some areas, such as El Arish in the northeast and El Tour in the southwest, groundwater is used as drinking and irrigation water, extracted mainly from Quaternary sediments from a depth of 50-100 m or more [81]. At the same time, excessive pumping of groundwater in recent years has significantly deteriorated its quality, and, in addition, aquifers in

the coastal zone of the Mediterranean Sea are susceptible to the intrusion of sea salt water.

The problem of water shortage in Egypt can be partially solved by collecting and storing flood water in earthen dams. In the Arab Republic of Egypt (ARE), the use of earthen dams to prevent flood risk and surface water storage is widespread, including in the Sinai Peninsula [49; 80]. All earthen dams with reservoirs are characterized by water filtration through their embankments, foundations and adjacent sides of the valley - creating an artificial aquifer. Quantifying this process is a major hydrogeological challenge; It is also necessary to solve many hydrological and geoecological problems. The Z-SOIL program used to solve the problem numerically is implemented based on the finite element method. The program is designed to simulate non-stationary filtration with the ability to change the water level, the size of the filtering object and the properties of its constituent soils. North Sinai has a group of important dams that collect and store surface water during floods. One of the most important dams in North Sinai, which is located on Wadi Arish, is Al-Rawfaaha Dam with a reservoir capacity of $5x10^6$ m^3. In addition, there are many sand dams in the Wadi Gharafi area [4; 5].

Seepage flow through an embankment with unstable boundary conditions is of interest for solving many hydrological and environmental problems, such as the stability of earthen dams or slopes with unstable water level boundary conditions in civil engineering, Interaction of surface water with groundwater in water resource scenarios. , groundwater pollution and its infiltration into the environment, sediment intrusion, oil production and seawater intrusion due to tidal fluctuations in the coastal aquifer [29; 59; 61; 64; and etc.].

An experiment on modeling filtration and soil permeability was carried out by the author on a physical model of the dam in laboratory conditions. Then the numerical geofiltration model was calibrated in Z-SOIL by comparing model and experimental data. Finally, the effect of changing the dam geometry on the water

level in the reservoir was assessed. As a result of research was found that the Z-SOIL numerical model allows one to simulate unsteady seepage through an earthen dam with a high degree of accuracy.

According to the results of numerical modeling, an increase in the crest width and height of the dam base, as well as an increase in the ratio of the horizontal and vertical filtration coefficients of the base and embankment (k_x/k_y) of the dam significantly reduce the average value of the groundwater head gradient in the dam body. Moreover, in the case of non-stationary filtration, the rate of change in pressure decreases along the length of the filtration path, i.e. the maximum changes are observed in the upper pool.

The results obtained are in good agreement with the practice of construction and operation of sand dams [29; 61; 86; 95; 97; 103; and etc.], therefore the Z-SOIL numerical model can be used for design and construction.

The Sinai Peninsula (area: 61,000 km^2, population: 559,071 in 2020) is divided into two administrative governorates: North Sinai Governorate (population: 450,528 in 2020) and South Sinai Governorate (population: 108,543 in 2020) (Fig. 1.1).

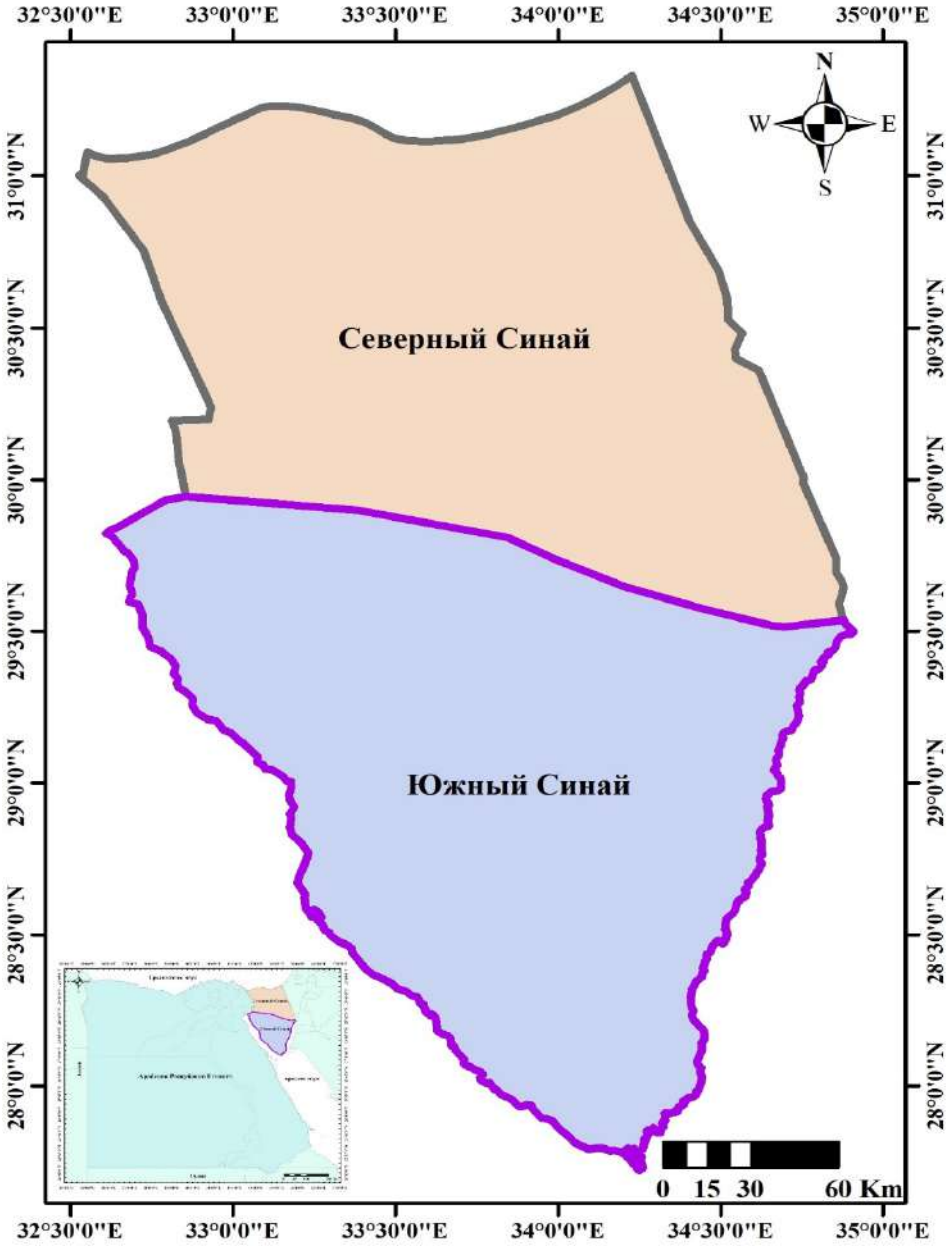

Fig. 1.1. Administrative provinces of the Sinai Peninsula

The presented work examines the hydrogeological conditions for the development of various aquifers within North Sinai, divided into five administrative regions: El Arish, Rafah, Sheikh Zuwayid, Bir El Abd, El Hassana and Nakhl (Fig. 1.2). The area of North Sinai is more than 26,000 km^2. It is located between 29° 35' and 31° 20' north latitude and 32° 30' and 34° 53' east longitude and extends from the borders of Ismailia governorate in the west to the Palestinian-Israeli borders in the east, between the Mediterranean Sea in the north to the provincial border South Sinai in the south.

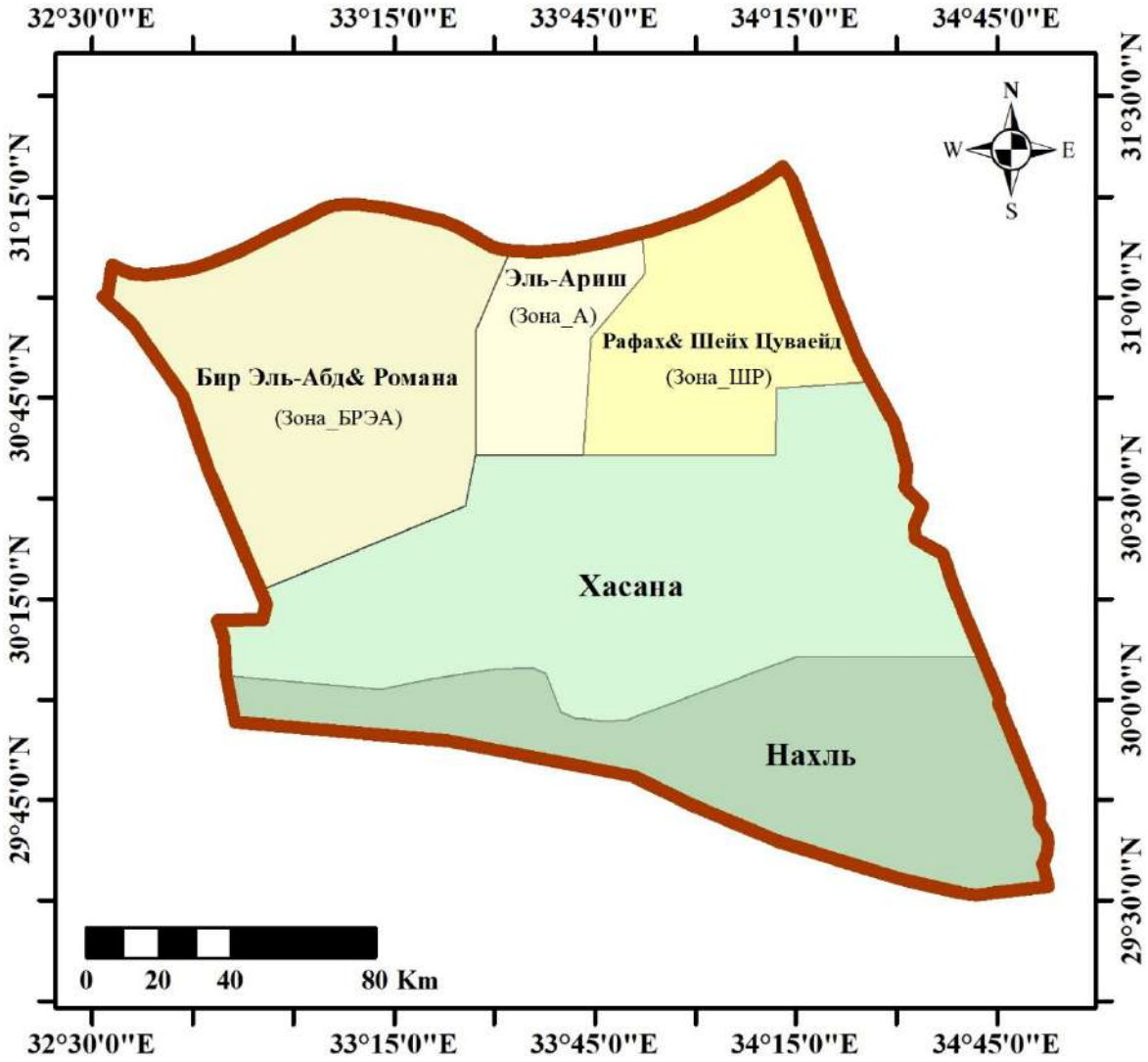

Fig. 1.2. Administrative regions of North Sinai Province

Most of the factual material for these studies on the geological structure and hydrogeological conditions, on the filtration and hydrochemical properties of the North Sinai aquifers was taken from the results of many years of work carried out by the Water Resources Research Institute (WRRI) in the Ministry of Irrigation and Water Resources of the Republic of Egypt [7; 28; 87; and etc.]. As part of these works, primary data on about 500 wells located in North Sinai were presented (Fig. 1.3) [31; 34; 71; 72; 73; 101; and etc.].

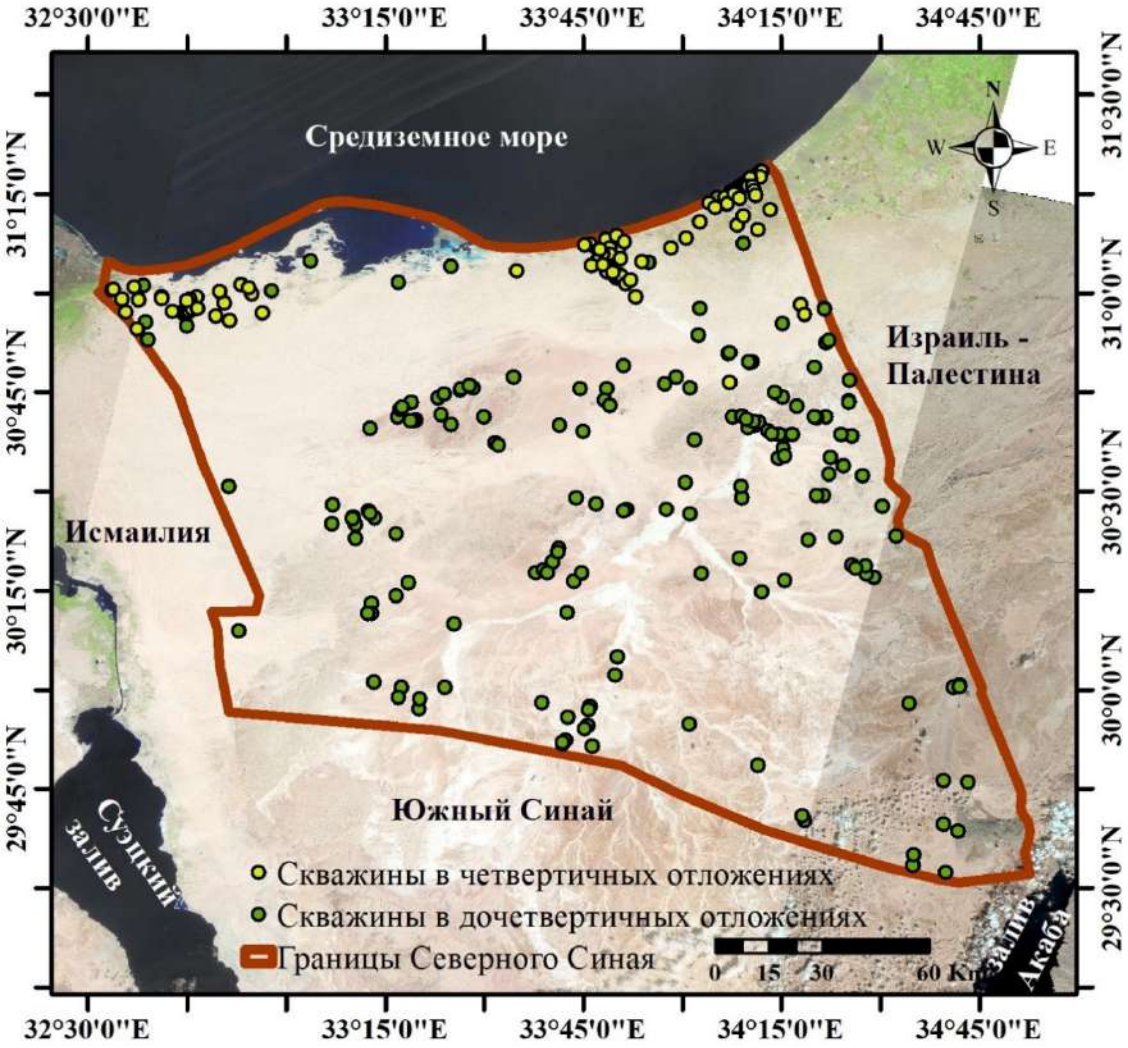

Fig. 1.3. Location of research wells in North Sinai Province

At the initial stage of research there were addition, updating, adjustment, rejection and systematization of information on all existing hydrogeological wells in the North Sinai region were carried out. The result of this systematization was the corresponding databases on various hydrogeological parameters. The research methodology is described in detail in the relevant chapters of the work. The research results were published by the author [1; 2; 3; 4; 5; 76; and etc.].

CHAPTER 2. GENERAL GEOLOGICAL AND GEOGRAPHICAL CHARACTERISTICS OF NORTH SINAI

2.1.Topographical and geomorphological description

The Sinai Peninsula is located between two branches of the Red Sea: The Gulf of Suez and The Gulf of Aqaba. Sinai has the shape of a triangle with a base extending along the Mediterranean coast from Port Fuad in the west to Rafah in the east, a length of 200 km (Fig. 2.1 and 2.2). The apex of the triangle lies in the extreme south at Ras Mohamed, which is located 390 km from the Mediterranean coast. The western bank stretches for approximately 510 km, while the eastern bank extends no more than 240 km. The imaginary line of the eastern political border between Sinai and Palestine, from Rafah in the north to Taba on the Gulf of Aqaba, extends 215 km. The total area of Sinai is 61,000 km^2. This is three times the area of the Nile Delta. The study area in this work is the northern half of the peninsula, which belongs to the administrative province of North Sinai with a total area of 27574 km^2 (Fig. 2.1) [72].

The Sinai Peninsula as a whole, as can be seen on topographic maps, according to topographic and geodetic characteristics, can be divided into the following parts:

– A triangular-shaped massif in the south, constituting the mountainous part of the peninsula. Mounts Moses and Mount Katarina are the highest points of the peninsula with absolute elevations of 2629 m above sea level.
– The central limestone plateau of central Sinai with absolute elevations of about 1000 m above sea level, consisting mainly of Mesozoic and Tertiary sediments. It is deeply dissected by valleys bounded by steep slopes. The beds of these valleys have a sharp slope, creating waterfalls during floods.

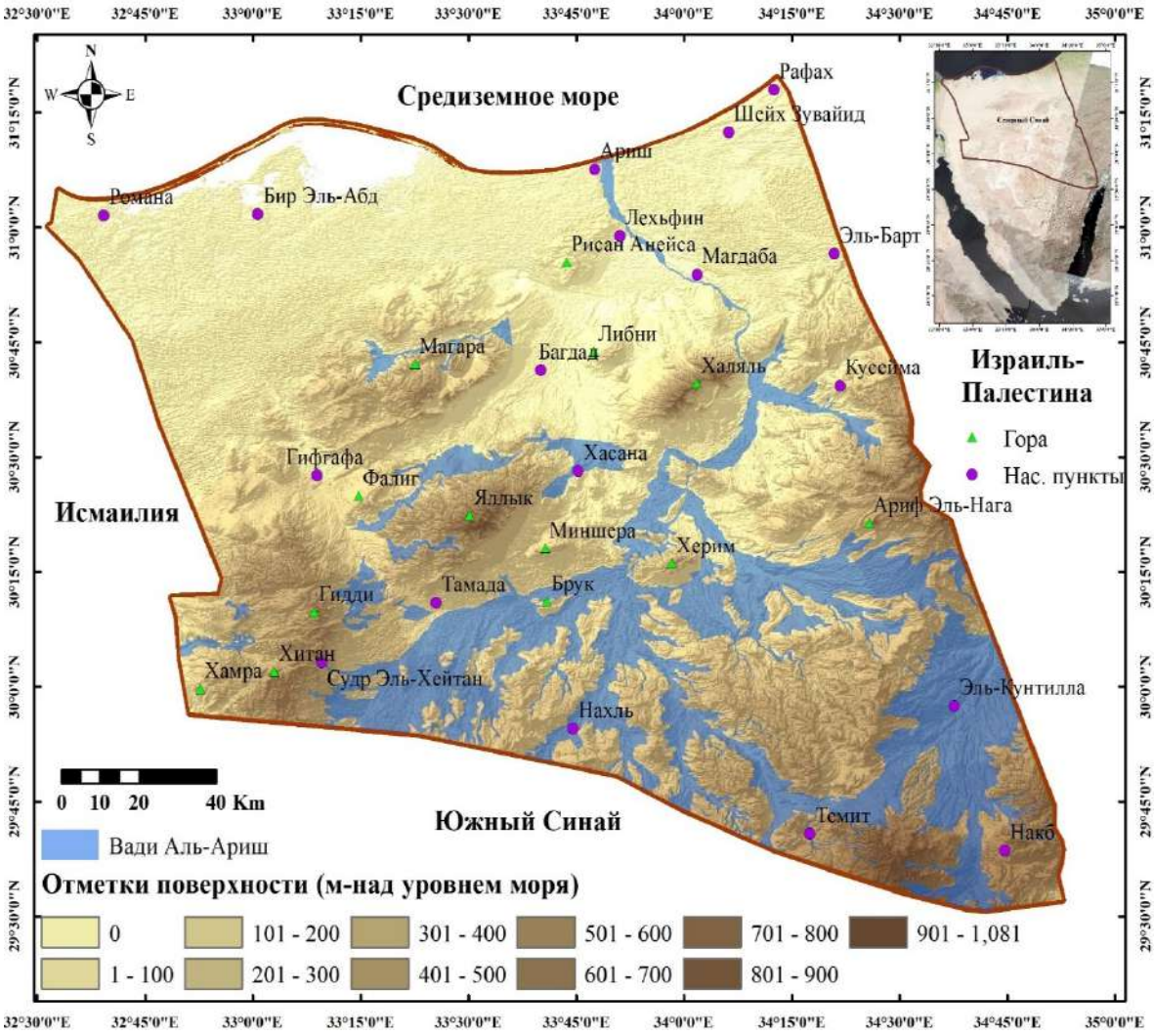

Fig. 2.1. Topographic map of the Sinai Peninsula

– The Rangdom Hills extend from northeast to southwest and are bounded by the dune plain in the north and the El Tih and Egma plateaus in the south. They have steep and moderately steep slopes.
– A dune plain that stretches from the Suez Canal in the west to Rafah in the east and from the Mediterranean coast in the north to the Rangdom Hills in the south. These wind dunes quickly change their shape and position.
– Coastal plains extending along the Mediterranean Sea and along the Gulf of Suez and the Gulf of Aqaba.

In the northern part of the Sinai Peninsula, the regional slope is divided into many large hills and ends in the north with a belt of lowlands with high sand dunes

along the Mediterranean coast. Various morphological features are observed in the study area of North Sinai [34; 60].

Thus, the main geomorphological units of the Sinai Peninsula as a whole are the central plateau, fold belt and coastal plains (Fig. 2.2) [99].

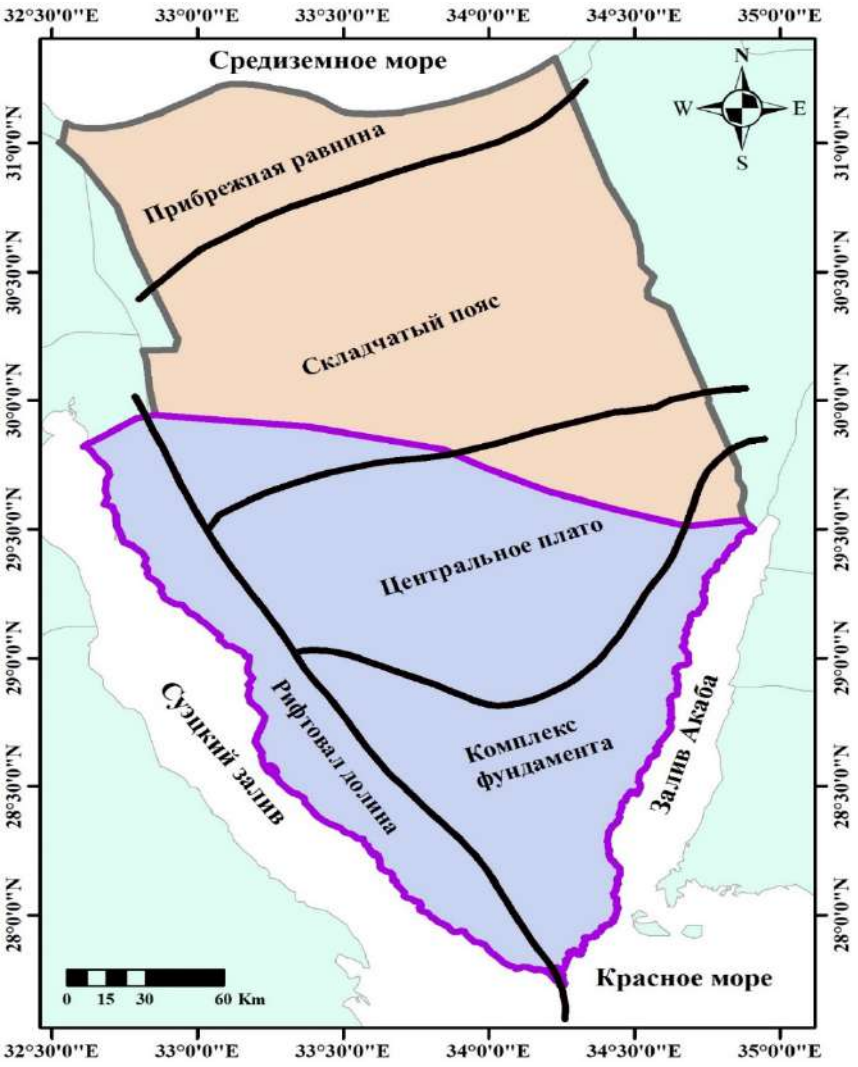

Fig. 2.2. Geomorphological units of the Sinai Peninsula

Central Plateau

Most of the surface of the plateau is covered with Paleogene limestone. On the other hand, relatively soft rocks such as chalk and Upper Cretaceous marl are distributed in and around the valley. They are easily eroded.

Fold belt (Syrian arc zone)

The area is characterized by large mountain blocks that belong to the Syrian Arc Zone. Gebel Maghara, Halal and Yellek are located successively along the main axis from northeast to southwest. They consist of double submerged anticlinal structures, where the north side typically has a slight slope of 10-20 degrees, and the south side is faulted and folded. Most of these mountains are mainly composed of limestones, marls and sandstones, ranging in age from the Jurassic to the Upper Cretaceous. Hills surround these mountainous areas. Many hills composed of Tertiary and Quaternary colluvial sediments are located in the upper reaches of the Wadi El Arish drainage system.

Coastal Plains

The area is a vast plain composed of alluvial sediments and sand dunes. As a rule, the plain slopes slightly to the north. A narrow sand spit, surrounded by lagoons that form a lagoonal lowland, stretches along the Mediterranean Sea. The coastal lowlands are found along the Sabkhet el Bardawil lagoon and other areas along the Mediterranean coast.

Fig. 2.3. Images of Wadi El Arish during the flood period[youm7.com]

Wadi El Arish

Wadi is a common term in North Africa and can be defined as a river that is dry for most of the year except during the rainy season [36; 41; 51; and etc.]. This is, as a rule, a low-lying, wide area in the desert, which, when precipitation falls, fills with water, forming an oasis (Fig. 2.3).

In addition to the above geomorphological units on the peninsula, the Wadi El Arish drainage system is also one of the main, largest of the wadis, characteristic units of the morphology of the region in general and North Sinai in particular. The source originates from Gebel Egma in the central plateau, passing through the Syrian Arc Zone and the northern coastal plain to the Mediterranean Sea. The total length of the wadi is 310 km. The catchment area is about 20,000 km^2, which is one third of the entire peninsula (Fig. 2.4) [73]. The tributaries of the Wadi El Arish system, including their floodplains, are composed of sand and gravel. Groundwater is presenting here only during periods of floods.

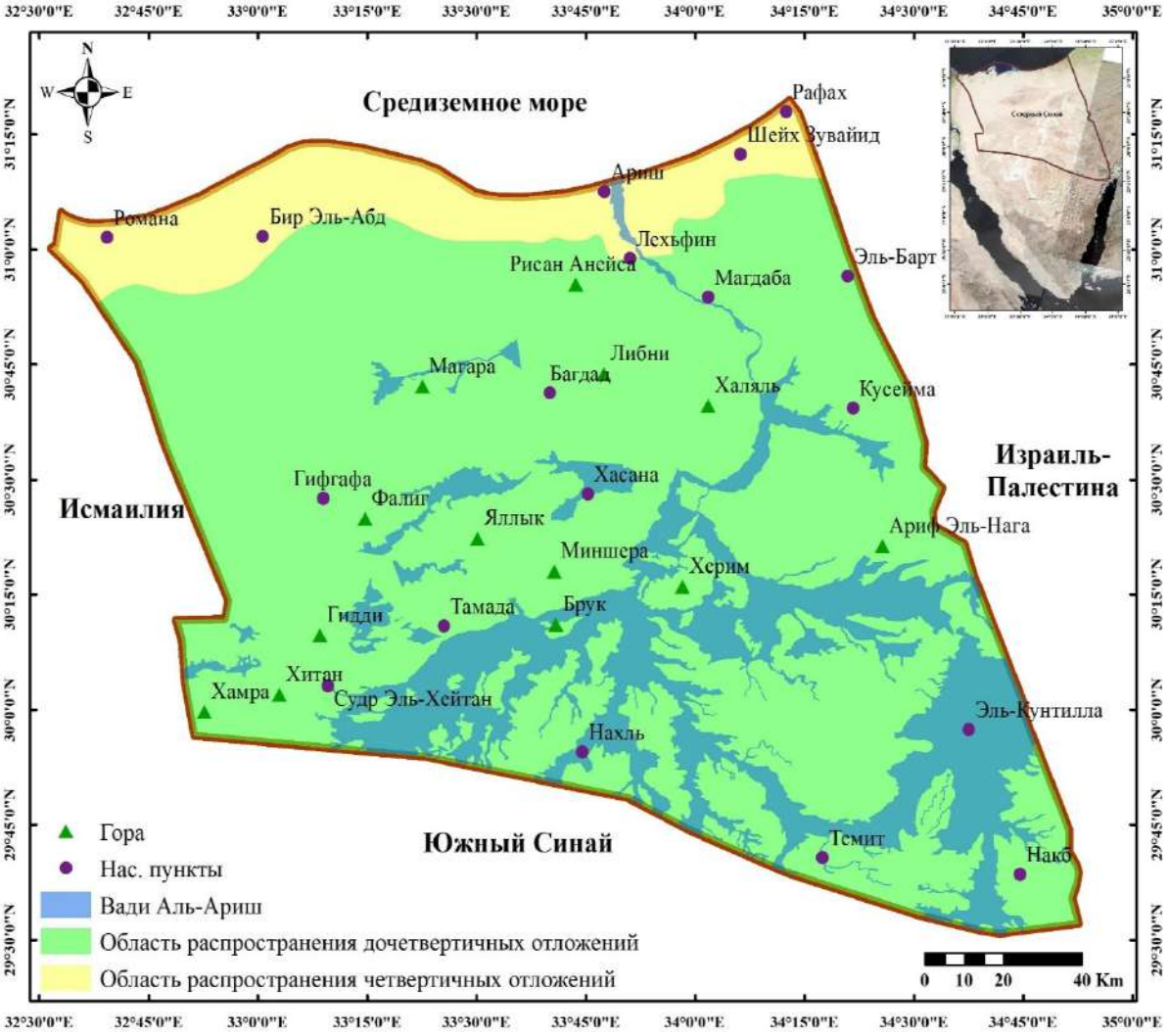

Fig. 2.4. Wadi El Arish drainage area

2.2.Climatic characteristics

Air temperatures in northern Sinai are generally higher than in the interior of the peninsula. The average temperature decreases in winter and reaches its minimum in January, increasing in summer to a maximum in August [85; 96].

Average winter temperatures are around +13°C in El Arish, with an average low of +7°C in the early morning and generally rising to +11°C in the afternoon with an average high of around +18°C.

In summer the temperature rises to +26°C (average value in El Arish). The average summer maximum temperature ranges between +29.9°C and +31.1°C.

On summer nights the air temperature drops to an average minimum temperature of +22°C.

Spring is characterized by moderate temperatures around +20°C with hot periods of Khamsin, when the air temperature sometimes rises above +40°C. The average minimum temperature during this season is around +13ºC, while the average maximum temperature is +26ºC.

Autumn is characterized by moderate temperatures, similar to spring and slightly lower than summer. Temperatures during September usually range from +15°C at midnight and +28°C at midday.

Precipitation has always been a serious problem in northern Sinai. The highest average annual rainfall of up to 300 mm/year is observed only in a very limited area, in the Rafah region, in the northeastern part of the study area [72]. On more than 80% of the territory of North Sinai, the average annual precipitation is less than 60 mm/year, that is, most of the study area is in an arid climate [31].

At the same time, an extremely important problem of the arid zone under consideration is that precipitation during flood periods falls extremely unevenly in different years (Fig. 2.5). For this reason, the northern areas of Sinai are periodically subject to either severe drought or flooding, especially near wadis.

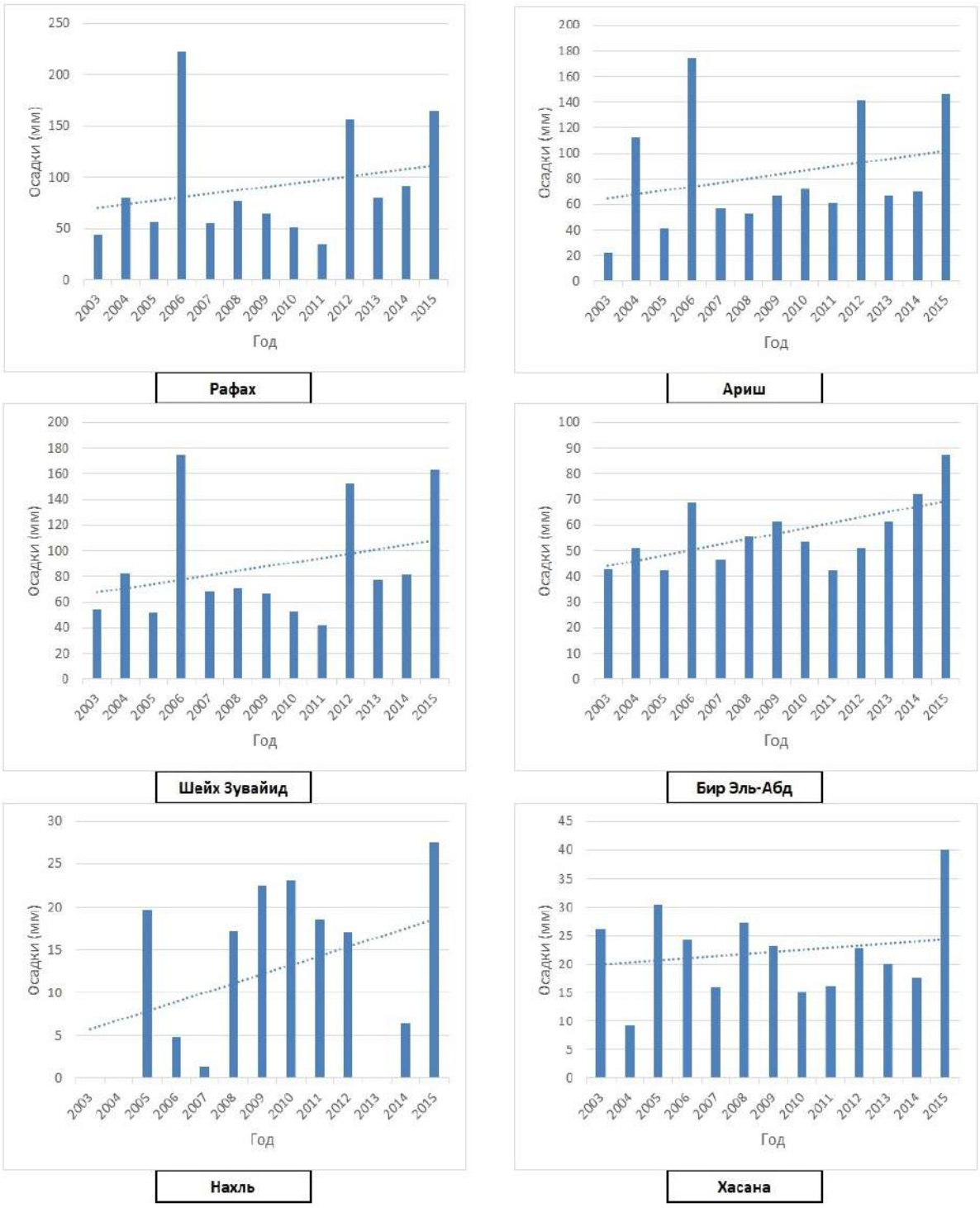

Fig. 2.5.Changes in average annual precipitation in different areas of North Sinai during 2003-2015

In general, the climate in the North Sinai study area is very dry and groundwater recharge is very limited, but in recent years there has been a trend towards an increase in the amount and intensity of precipitation in North Sinai.

Thus, there are great opportunities to collect, store and use this water for agriculture or industrial development of North Sinai.

2.3. Geological structure

Geologically, the Sinai Peninsula is part of the Arab-Nubian massif, gradually plunging north towards the Mediterranean Sea. The geological section contains rocks of the Precambrian basement, overlain by Cambro-Ordovician, Carboniferous, Permian, Triassic, Jurassic, Cretaceous and Paleogene deposits. The section is completed by Quaternary deposits (Fig. 2.6, 2.7, 2.8).

In northern Sinai, the studied part of the section is limited to Triassic limestones; underlying rocks were exposed only in central Sinai. The coastal plain of North Sinai is a large amplitude fault, and the base of the Triassic sediments is exposed at a depth of more than 2000 m [8].

The characteristics of the geological structure of the Sinai Peninsula presented below are compiled from the totality of the results of all geological studies previously carried out in this territory, including those carried out in recent years [9; 12; 20; 23; 38; 47; 48; 67; 68; 77; and etc.].

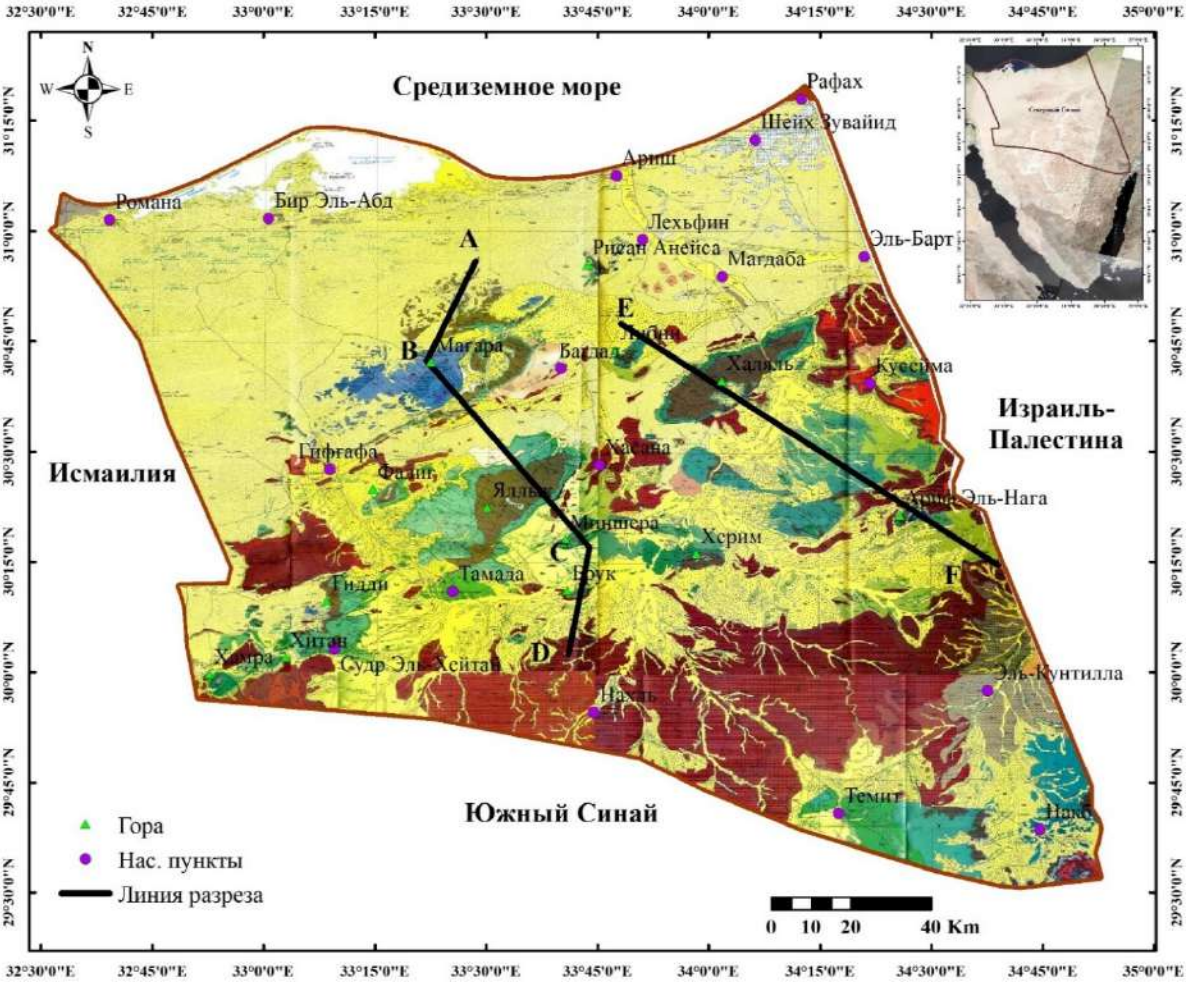

Легенда

ЧЕТВЕРТИЧНЫЕ ОТЛОЖЕНИЯ

- Qsd — Песчаные дюны и покровы
- Qw — Отложения вади
- Qp — Пляжные отложения
- Qfs — Фангломераты
- Qhc — Алювиальные отложения Хамада

ТРЕТИЧНЫЕ ОТЛОЖЕНИЯ

- Tplba, Tplkn — Нижний плиоцен
- Temaj — Средний эоцен (Мокаттамия)
- Telqd, Telm — Иперсиан (нижнеэоценовые-верхнеливийские)
- Telm — Палеоцен-нижний эоцен (нижнеливийские)

МЕЛОВЫЕ ОТЛОЖЕНИЯ

- Ksd — Маастрихт
- Kdu, Kmt — Кампан
- Kwt — Турон
- Khl — Сеноман
- Krz — Альб
- Kml — Альб-апт

ЮРСКИЕ ОТЛОЖЕНИЯ

- Jbjh — Байос
- Jlh — Лейас (верхний лейас)
- Jr — Формация Райабия (средний лейас)
- Jmsh — Формация Машабба (нижний лейас)

ТРИАСОВЫЕ ОТЛОЖЕНИЯ

- Trns — Нижний карн-ладин
- Trnj — Анизий

ГЕОЛОГИЧЕСКИЕ СИМВОЛЫ

- Геологический контакт
- Нормальный разлом
- Антиклиналь, стрелкой показано направление погружения оси
- Синклиналь
- 10 — Простирание и падение слоев

Fig. 2.6. Geological schematic map of North Sinai

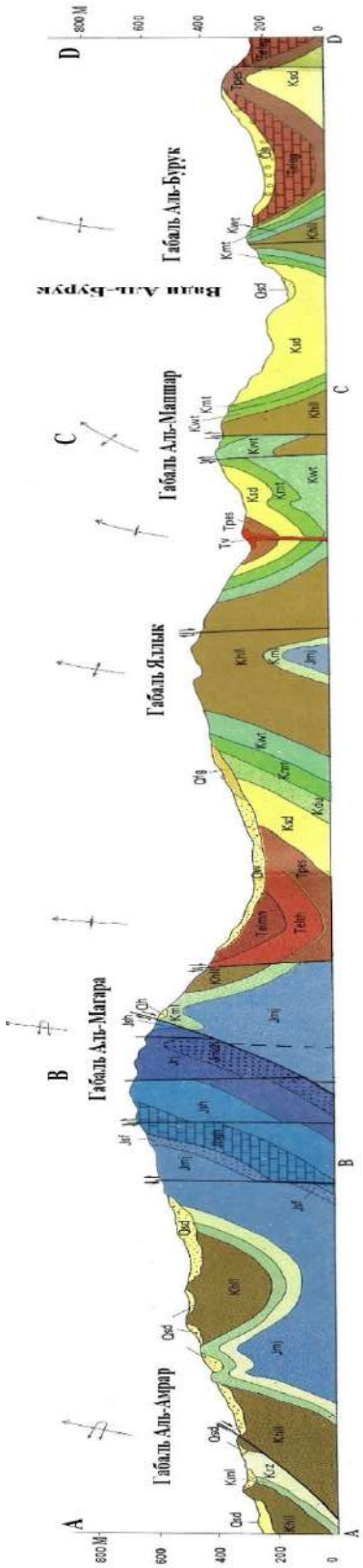

Fig. 2.7. Geological schematic section of North Sinai along line ABCD (see Fig. 2.6)

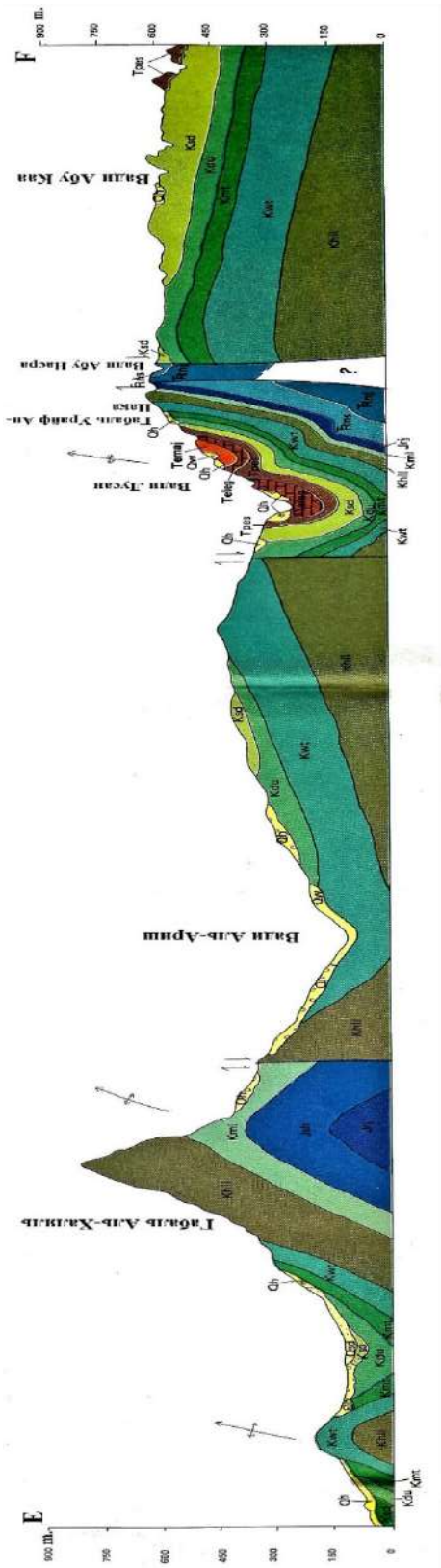

Fig.2.8. Geological schematic section of North Sinai along line EF (see Fig. 2.6)

Mesozoic era

Triassic

Triassic rock deposits were found only in the dome area of Gebel Arif El Naga, on the southeastern border of North Sinai (Figs. 2.6 and 2.7) [34]. Triassic deposits are mainly represented by shales, limestones, sandstones, dolomites, dolomitic shales and conglomerates with interlayers of mudstones and anhydrites up to a few tens of meters thick.

Jurassic

Sediments of Jurassic formations come to the surface only in the dome structures of the northern part of North Sinai: Gebel Magara, Gebel Yalqa, Gebel Arif El-Naga and Gebel El-Giddi (Fig. 2.6 and 2.8) [34]. A complete section of Jurassic deposits within the Sinai Peninsula, that is, from the Lower to the Upper Jurassic, was discovered only at Gebel Magara. The total thickness of these layers reaches approximately 2000 m. The northern flank of this dome is relatively flat, and on the southern flank there is a vertical structure cut by a thrust fault.

The Jurassic formation is represented by sandstones and shales with rare intercalations of siltstone and sandy marl, as well as limestone and coal seams [34].

Cretaceous

Lower cretaceous

Lower Cretaceous rocks in North Sinai vary from sandstones to limestones (north of Gebel Magara - Risan Aneiza Formation) (Fig. 2.6) [34; 60]. Most sections are dominated by medium- to coarse-grained porous sandstones [34; 60]; Sometimes layers of waterproof shale are observed [34]. There are areas where there are outcrops of Lower Cretaceous rocks - Gebel Magara, Gebel Halal, Gebel Falig, Gebel Minshera, Gebel Herim, Gebel Giddi, and Gebel Arif El-Naga. Typically, inclined formations are observed (Fig. 2.7 and 2.8) [34]. Power - in the range of 200-300 m [53].

Upper cretaceous

The Upper Cretaceous on the Sinai Peninsula is represented by the Cenomanian and Turonian stages and the Senonian over stage [34; 60]. Cenomanian deposits are conformably overlain by Lower Cretaceous deposits and are also conformably overlain by rocks of the Turonian stage. Sometimes part or all of the Upper Turonian-Coniacian section is missing due to erosion, and most often the Senonian deposits unconformably overlie the Turonian deposits.

The deposits of the Cenomanian stage in the lowermost part are represented by limestones and calcareous sandstones, passing higher into limestones, dolomitic limestones and dolomites. Quite thick Cenomanian rocks are found mainly in the following areas: Gebel Minshera (thickness 575 m), Gebel Magara (550 m), Gebel Hamra (550 m), Wadi el-Giddi (545 m) and Gebel Halal (535 m). The Cenomanian thickness is low in the areas of Gebel Jelleke, Falige, Kherime and Arif El-Nage. Here the Cenomanian is represented by a predominance of dolomites and dolomitic limestones and various facies consisting of calcareous sandstones, shales and limestones [100].

Turonian deposits consist predominantly of limestones, dolomitic limestones and chalk limestones. Loose sandstone deposits usually appear at the base of the formation. In the Gebel Halal area, the Turonian deposits consist mainly of foraminiferal limestones, but also contain some inclusions of grey-green shale. Turonian rocks are either partially or completely eroded in many areas: Gebel Magar, Gebel Arif El-Naga and Nakba. The average thickness of Turonian deposits is noted in the areas of Gebel Falig, Yellek and Kherim, where it ranges from 70 to 85 m. The thickest Turonian layers are present in the areas of Gebel Halal, Gebel Libni, Gebel Minshera, El Bruk, and Gebel Giddi. The thickness of the Turonian in these areas is from 100 m to 270 m, the maximum thickness is observed in the Gebel Libni and Gebel Giddi areas.

The Senonian deposits in North Sinai generally consist of a homogeneous chalk sequence. The maximum thickness of the Senonian is observed in the Gebel Minshera region (270 m). Here the base of the Senonian is represented by shales 90 m thick; shales up to 20 m thick also appear at the base of the Upper Senonian section and are overlain by a 180 m thick layer of chalk and cretaceous limestone.

Cenozoic era

Paleogene

Paleocene

Paleocene rocks in North Sinai are represented by the Esna formation, consisting of shales and marls [34; 60]. A relatively deep sea covered the Sinai as a result of transgression at the end of the Upper Cretaceous - beginning of the Paleocene. Therefore, the Esna Formation was deposited in depressions between the main structural maxima in the Upper Cretaceous sediments. The Esna Formation is overlain by Eocene limestones. Typically, the thickness of Eocene deposits in North Sinai varies from 30 m to 65 m, but, for example, in the Gebel Magara region their thickness is only about one meter, and often Eocene rocks are completely absent. The Esna Formation is exposed on steep slopes or cliffs. This is often observed in areas west of the Halal, Quseima, Arif El Naga and El Quntilla areas. The Esna Formation consists of shales or marls, as well as alternating shales and marls (in the Ain Gudeirat area in eastern Kuseim). Although the Esna Formation is cut by a large number of faults, the strata in this area are generally subhorizontal and there is little folding. It is assumed that no intense tectonic movements occurred after the formation was deposited.

Eocene

The Eocene sediments conformably overlie the Esna Formation and generally form a single sequence. Eocene rocks are represented by the Egma formation, which consists mainly of limestones and dolomitic limestones [34; 60]. Eocene limestones are divided into two groups - lower Eocene and middle-upper

Eocene. Lower Eocene limestones in northern Sinai are distributed in wide synclines. They have almost the same lithological composition. Their thickness varies from very small (meters) to complete absence. The middle-upper Eocene section in northern and central Sinai is characterized by major unconformities; parts of this section are missing in some areas.

Quaternary

The thickness of Quaternary deposits is usually from 80 to 100 m. The stratigraphy of Quaternary deposits in the study area is schematic (Fig. 2.6) [34; 60]. Quaternary formations are mainly represented by the following groups of sediments: "sand dunes", "ancient beach sands", "gravels" and "kurkar".

"Kurkar" is a local name for calcareous sandstone that was compacted after deposition. Kurkar was deposited in a shallow marine environment and is therefore distributed within the coastal plain.

"Ancient Beach Sands" They are primarily composed of fine- to coarse-grained sand (poorly cemented sandstone) with inclusions of gravel and clay layers. This layer has a thickness of approximately 20 m to 60 m. In some areas, they conformably overlap the kurkar deposits, forming a single groundwater aquifer with them. Contact with overlying sand dune deposits is often difficult to discern.

"Sand Dunes" wide spread in the coastal plain, usually overlying ancient beach sands, with local inclusions of clay and gravel layers. In some cases, sand dunes overlie low-permeability clayey sediments, which serve as aquifers for locally developed aquifers in the dunes. The thickness of sand dunes is in most cases from 20 m to 30 m.

"Gravel" found only in the lower reaches of Wadi El-Arish, contains local inclusions of sandy and clayey layers. The thickness of the layer is from 20 m to 60 m. These deposits cover the kurkar (in local areas), forming a single ground aquifer with it.

CHAPTER 3. HYDROGEOLOGICAL CONDITIONS AND ZONING OF THE TERRITORY OF NORTH SINAI ACCORDING TO THE VALUES OF FILTRATION PARAMETERS OF ROCKS

3.1. Hydrogeological conditions of North Sinai

The hydrogeological conditions of North Sinai are characterized by the totality of the results of all hydrogeological studies previously carried out in this territory, including those carried out in recent years [14; 24; 25; 42; 43; 45; 52; 55; 63; 89; and etc.]. The basis of the factual basis for the research was information on hydrogeological wells contained in the summary report “North Sinai Groundwater Resources Study in the Arab Republic of Egypt” [60], as well as additionally provided by the Water Research Institute (WRRI) under the Ministry of Irrigation and Water Resources of the Arab Republic of Egypt. Republic of Egypt [7]. As part of this work, information on all existing hydrogeological wells in the North Sinai region was updated. The result of this systematization was a corresponding database, which collectively included materials from 180 wells [31; 34; 71; 72; 73; 101; and etc.].

In hydrogeological terms, the study area is distinguished by a zone of distribution of bedrock sedimentary rocks and a coastal zone, where water-bearing Quaternary sediments of large thickness are developed [56].

Quaternary aquifers

Quaternary sediments are widespread in the study area. However, the distribution of aquifers of significant thickness in them is limited only to the coastal plain along the Mediterranean Sea. Relatively thick Quaternary sediments extend along the coastal plain in a strip 10 to 15 km wide from the mouth of Wadi El Arish to the Rafah area (Fig. 3.1), and from Bir El Abd to Roman in a strip about 10 km wide.

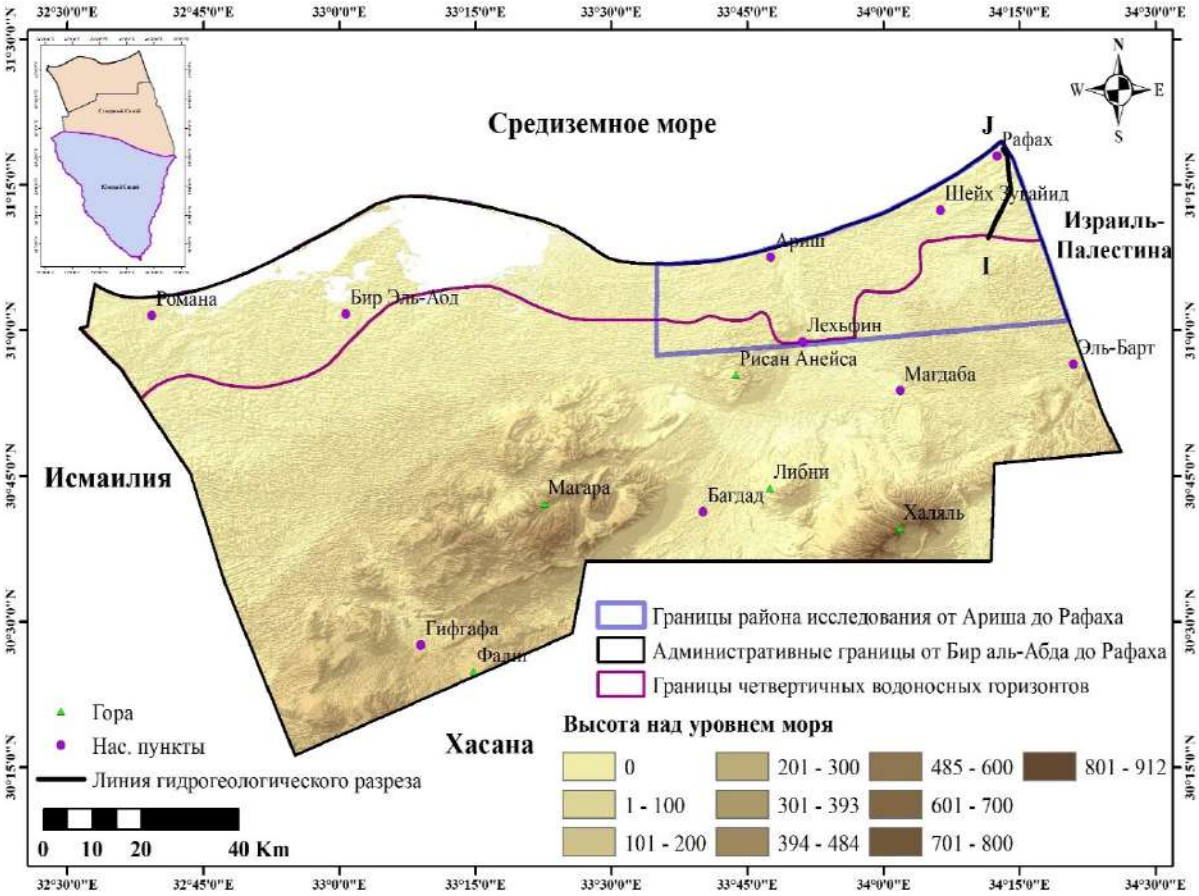

Fig. 3.1. Northern zone of North Sinai within the development of Quaternary deposits

North Sinai is divided into a zone of bedrock sedimentary rocks and a coastal zone, where Quaternary sediments of great thickness are developed. The main water-bearing rocks in the Quaternary aquifer are sand, gravel and kurkar sediments (Fig. 3.2).

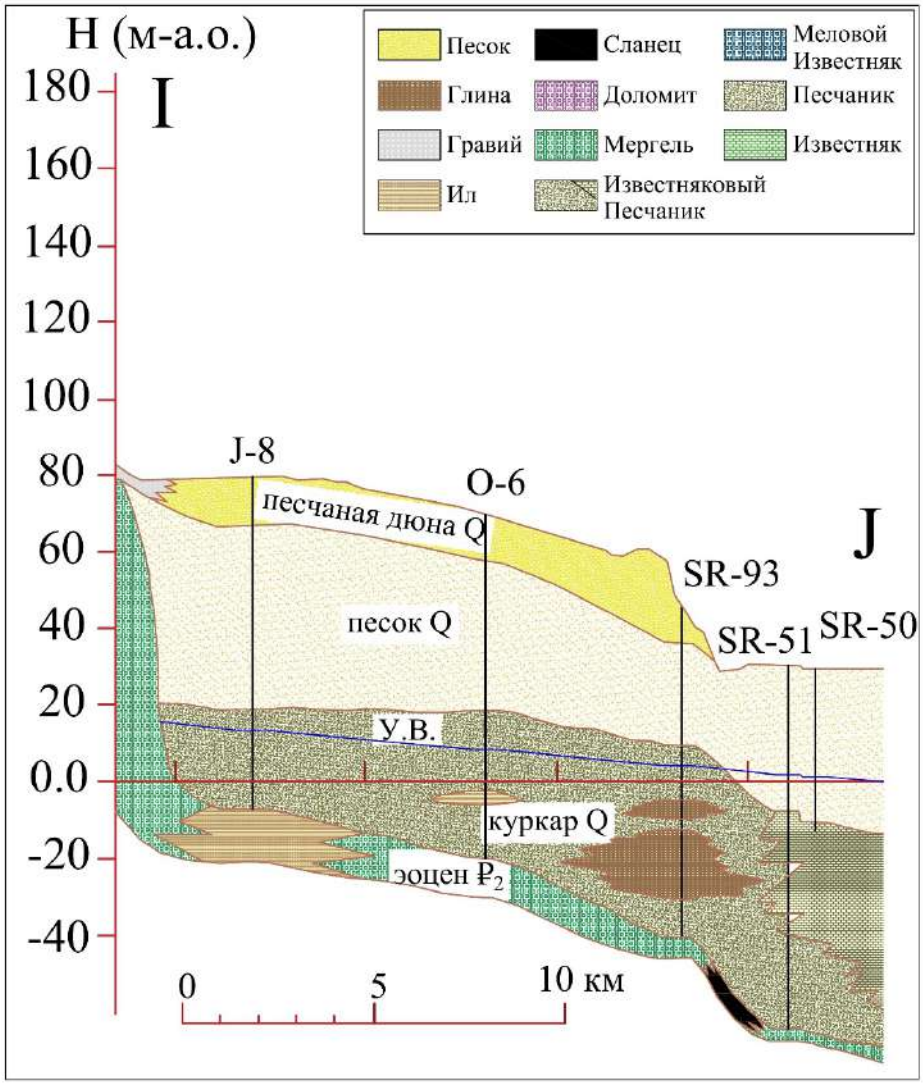

Fig. 3.2. Hydrogeological section within the development of Quaternary deposits

As seen in Figure 3.3, within the specified strip, the total thickness of Quaternary deposits varies over a fairly wide range, increasing from the first meters on the southern border of the specified strip to 80−100 meters in the north. In general, the following trend is observed: the thickness of the Quaternary cover west of Wadi El-Arish is smaller compared to that east of Wadi El-Arish.

The main water-bearing rocks of Quaternary sediments in the area under consideration are sand, gravel and deposits of kurkar - calcareous sand, almost ubiquitous in the coastal plain.

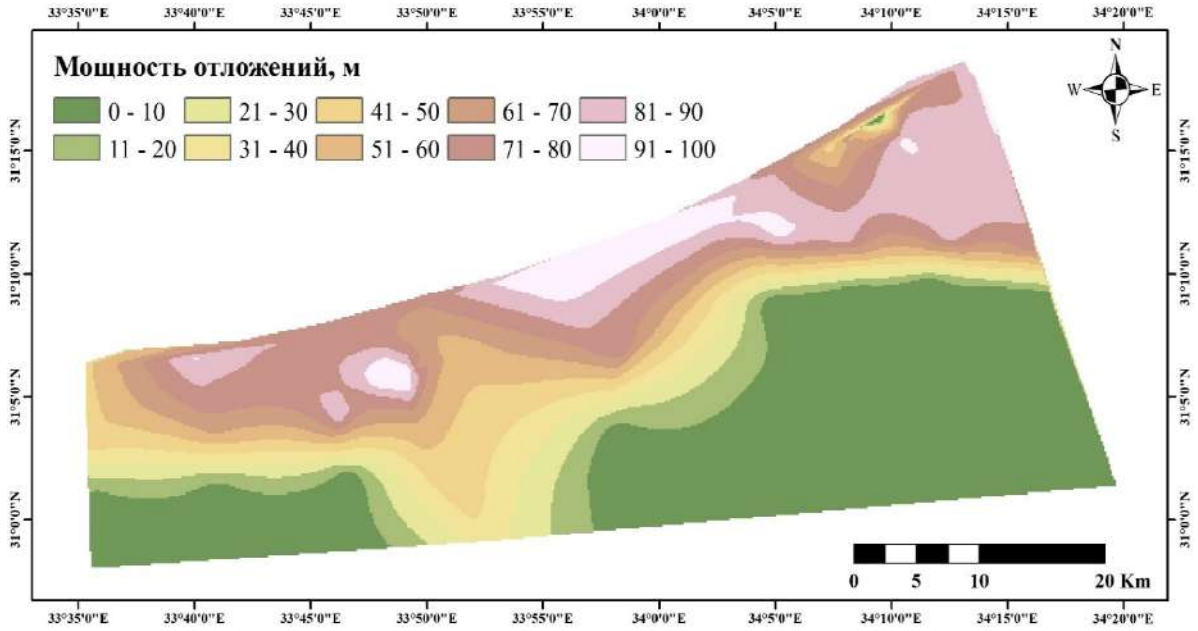

Fig. 3.3. Map of thickness isolines (total thickness) of Quaternary deposits

Typically, in the coastal zone, the top layer is sand 20 to 40 m thick, consisting of sand dune deposits and ancient beach sands. Differentiation of these formations in the lithological profile of wells is quite difficult. However, ancient beach sands overlain by dune sands are usually considered one of the promising aquifers. The sand layer is underlain by gravel or kurkar deposits. The distribution of sand thickness in the Wadi El Arish valley and the coastal plain as a whole from Sheikh Zuwayid to Rafah is shown in Figure 3.4.

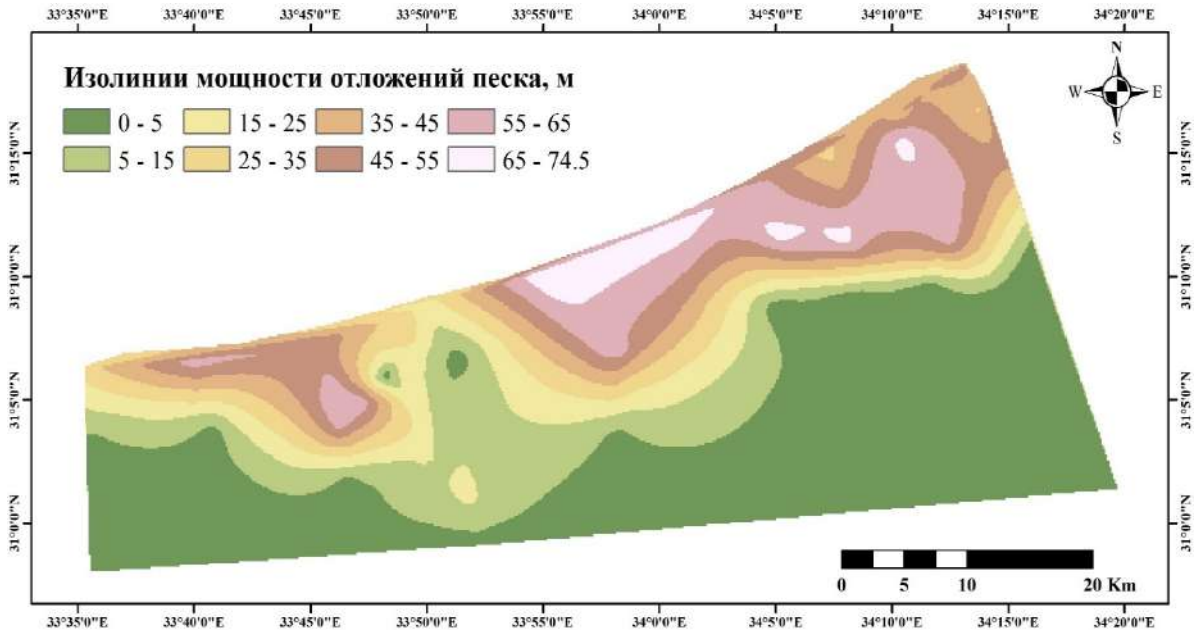

Fig. 3.4. Map of isoline thickness of sediments represented by sands

Gravel deposits occur in many parts of the area under consideration, but as an independent aquifer, this formation is concentrated mainly in the alluvial valley in the area of Wadi El-Arish: it extends approximately 10 km along the bed of Wadi El-Arish. The origin of this gravel is debatable. However, it is clear that it extends beyond the modern alluvial valley of Wadi El Arish. The thickness distribution of the gravel aquifer is shown in Figure 3.5.

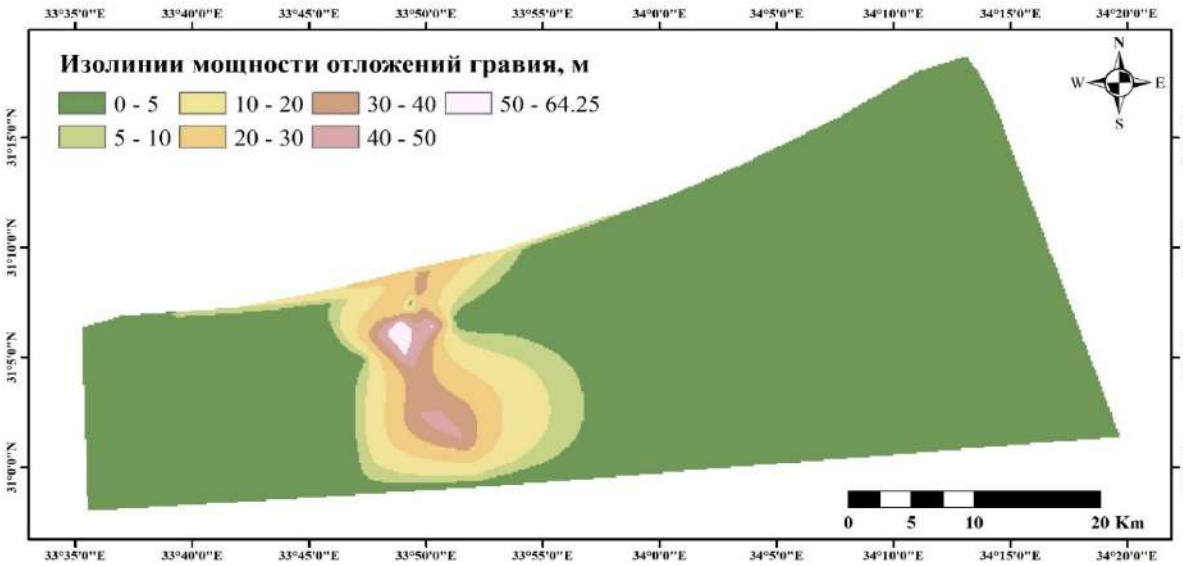

Fig. 3.5. Map isolines of the thickness of sediments represented by gravel

In the coastal plain as a whole, from Sheikh Zuwayid to Rafah, gravel layers are observed only in local areas. Appearently these are local sediments accumulated in ancient wadis. In most cases, it is noted here that groundwater levels in wells are set below the base of the gravel. For this reason, the water availability of gravel here is considered low.

Kurkar deposits are widely developed within the coastal plain, in the area from Sheikh Zuwayid to Rafah, under sand dune deposits. The absolute elevation of the base of the Kurkar deposits ranges from -60 to -20 m. Its thickness varies from 10 to 40 m. In some parts of the coastal zone of the Kurkar sand dunes, wedges out. The thickness distribution of these deposits is shown in Figure 3.6.

In the wells of the alluvial valley of Wadi El-Arish, the Kurkar can be traced for 10 km along the wadi bed and is covered with gravel. In this zone, the filters of most wells are installed specifically on kurkar deposits.

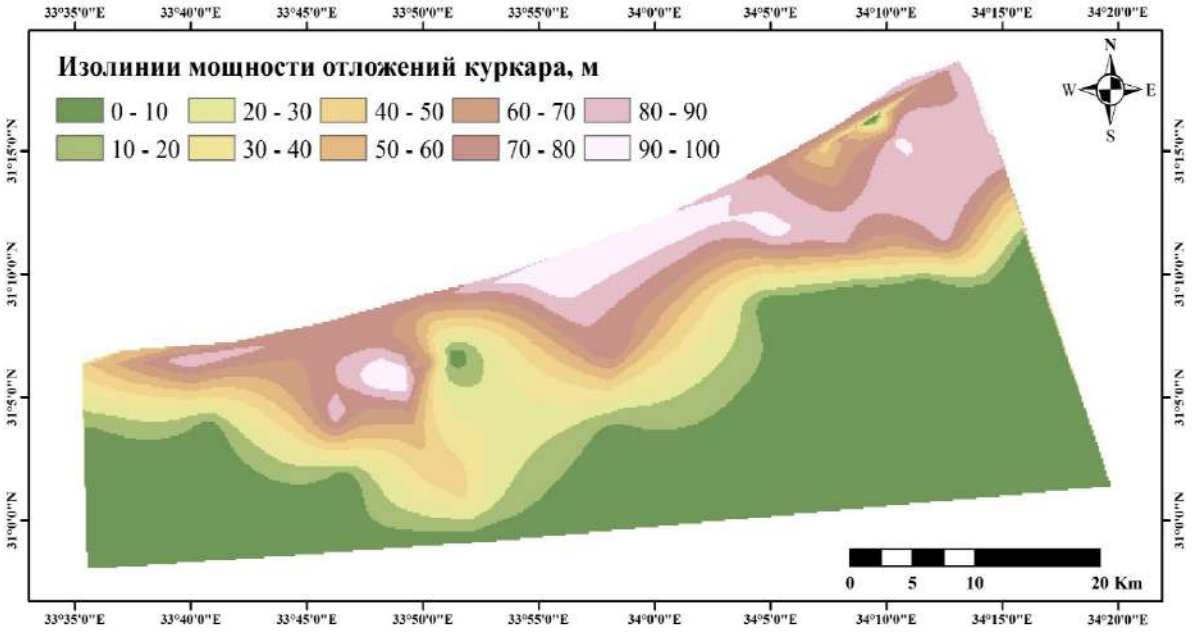

Fig. 3.6. Map of isoline thickness of sediments represented by Kurkar

Pre-Quaternary aquifers

The lithological composition, distribution area and conditions of occurrence of pre-Quaternary sediments are described in Chapter 2. Pre-Quaternary sediments are widespread in the study area, but the distribution of aquifers of significant thickness in them is limited to the area shown in Fig. 3.7.

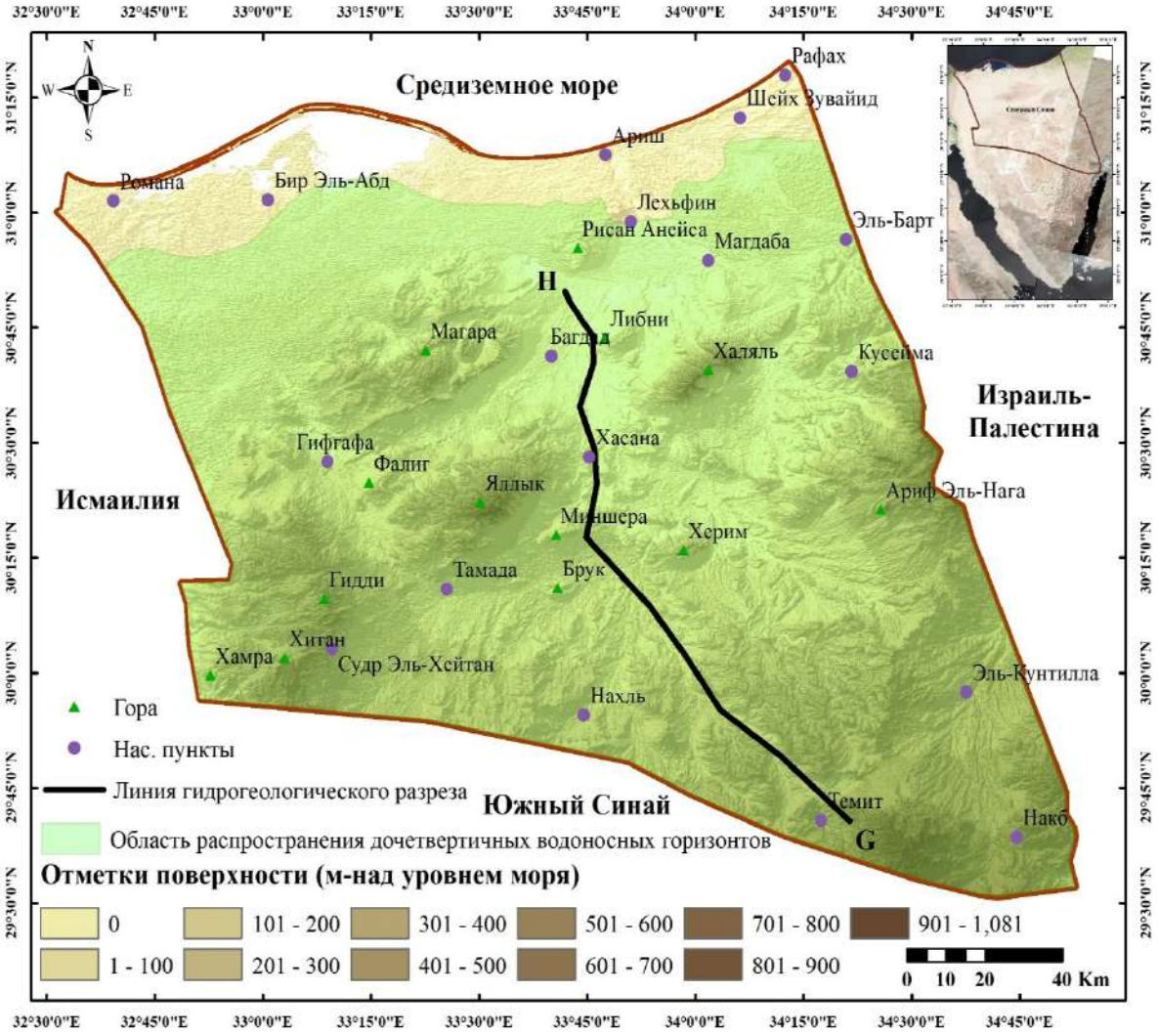

Fig. 3.7. Development of pre-Quaternary aquifers within northern Sinai

In pre-Quaternary deposits, the main aquifers are confined mainly to Paleogene-Upper Cretaceous limestones and Lower Cretaceous sandstones (Fig. 3.8).

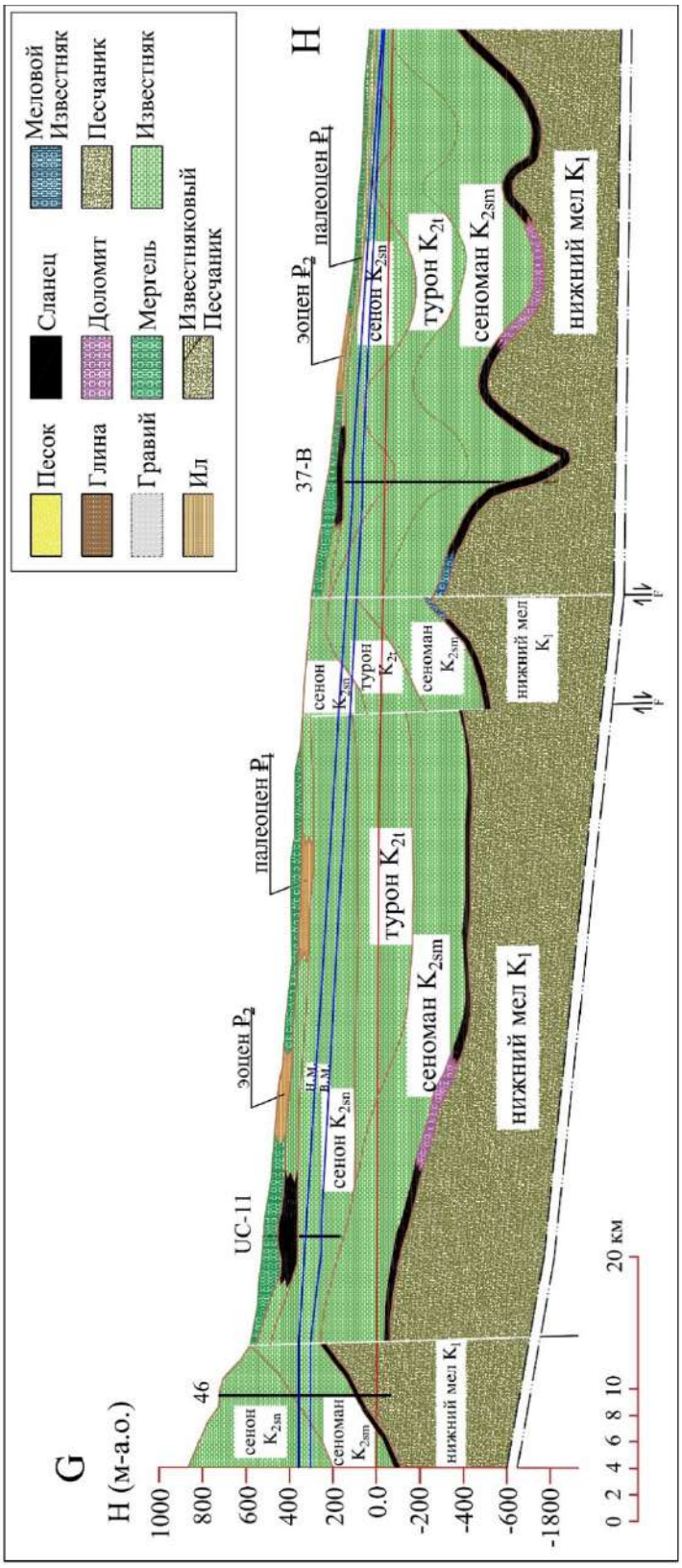

Fig. 3.8. Hydrogeological section within the development of pre-Quaternary deposits

Paleogene
Eocene

Aquifers in the Eocene developed mainly in limestones. The water conductivity of the marl layers present in the Eocene is very low, and they should be considered as impermeable. A characteristic feature of the occurrence of groundwater in the limestone aquifer is that it is contained in the basal part of the limestone underlying the rocks of the Paleocene Esna Formation. Apparently, therefore, despite the fact that the Eocene is not covered by any other sediments except wadi deposits, the groundwater is confined. Probably, the upper part of the uncracked limestone, together with the layers of marl, plays the role of an aquifer, creating pressure conditions. The porosity of limestone itself is not very high, and the main reserves of groundwater are located in cracks developed in the limestone. The thickness of the Eocene aquifer of limestone reaches 100 meters or more; the depths are shown in figure 3.9.

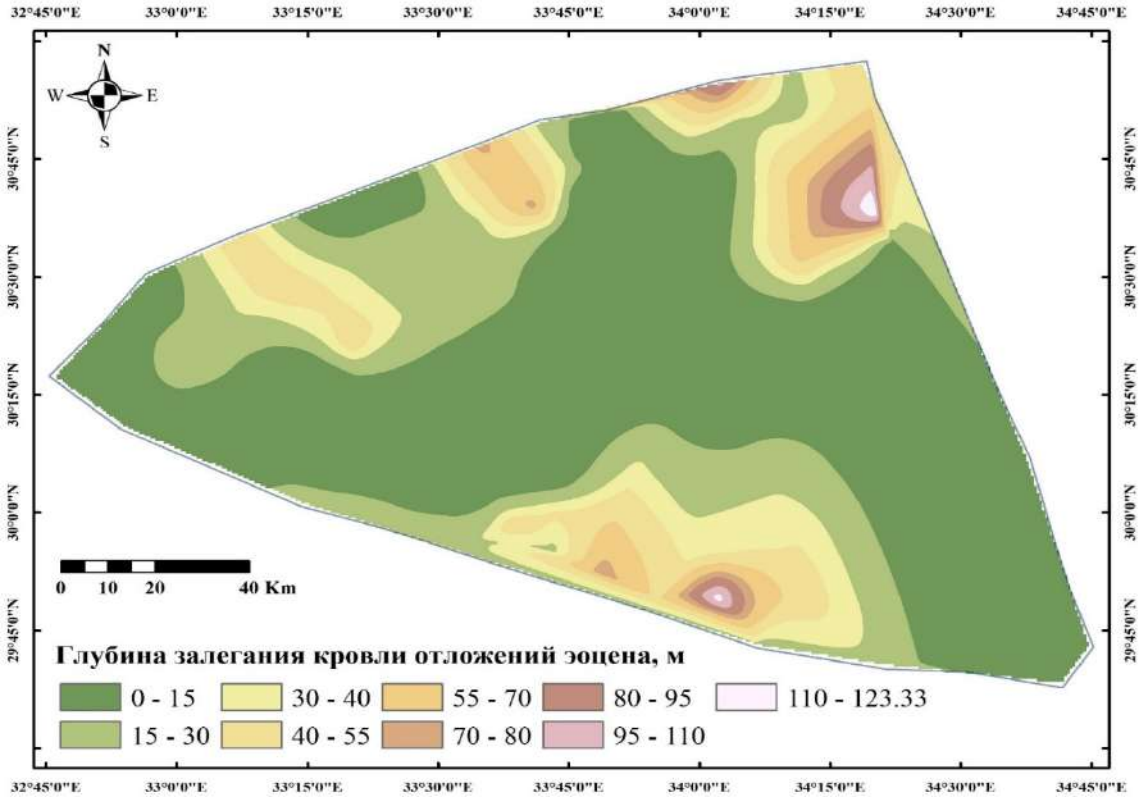

Fig. 3.9. Map depths of Eocene sediments

Paleocene

Paleocene deposits in North Sinai, as already indicated in Chapter 2, are represented by the Esna Formation and consist mainly of shales with rare marls, which allows us to define this horizon as relatively water-resistant. The total thickness of these shales and marls varies from a few meters to tens and even hundreds of meters. The burial depths are shown in Fig. 3.10. Shale often acts as a waterproof base for aquifer Eocene limestone.

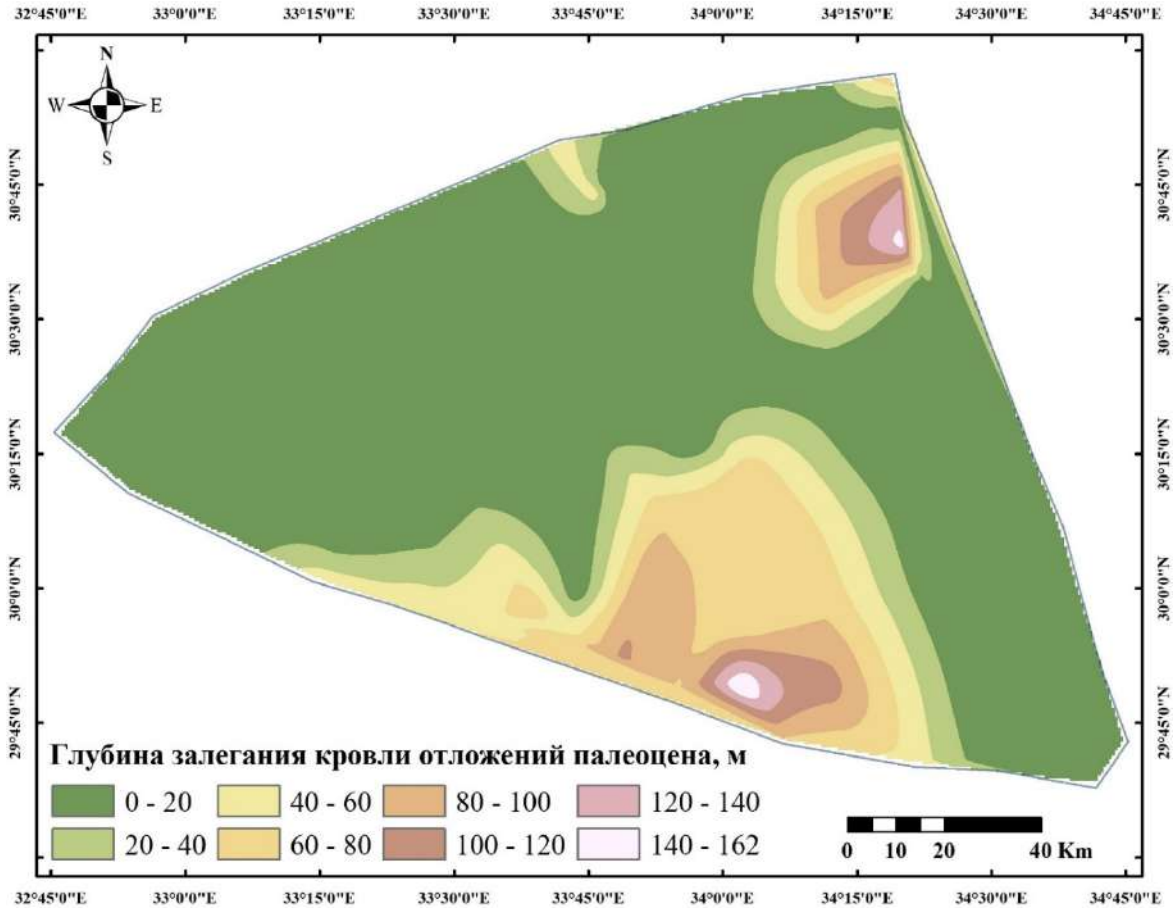

Fig. 3.10. Map depths of Paleocene deposits

Upper Cretaceous

Senon

Senon is widespread in the study area. The upper part of the Senonian is represented by chalk with limestones, and the lower part by limestones and shales. Aquifers are developed in the limestones of both the upper and lower Senonian. Groundwater occurs in both predominantly porous and predominantly fractured

parts of the limestone. Marl and shale are weakly permeable and form relatively water-resistant layers. Several layers of limestone, separated by layers of shale or marl, apparently form an aquifer complex. The depth map of the Senonian aquifer complex is presented in Figure 3.11.

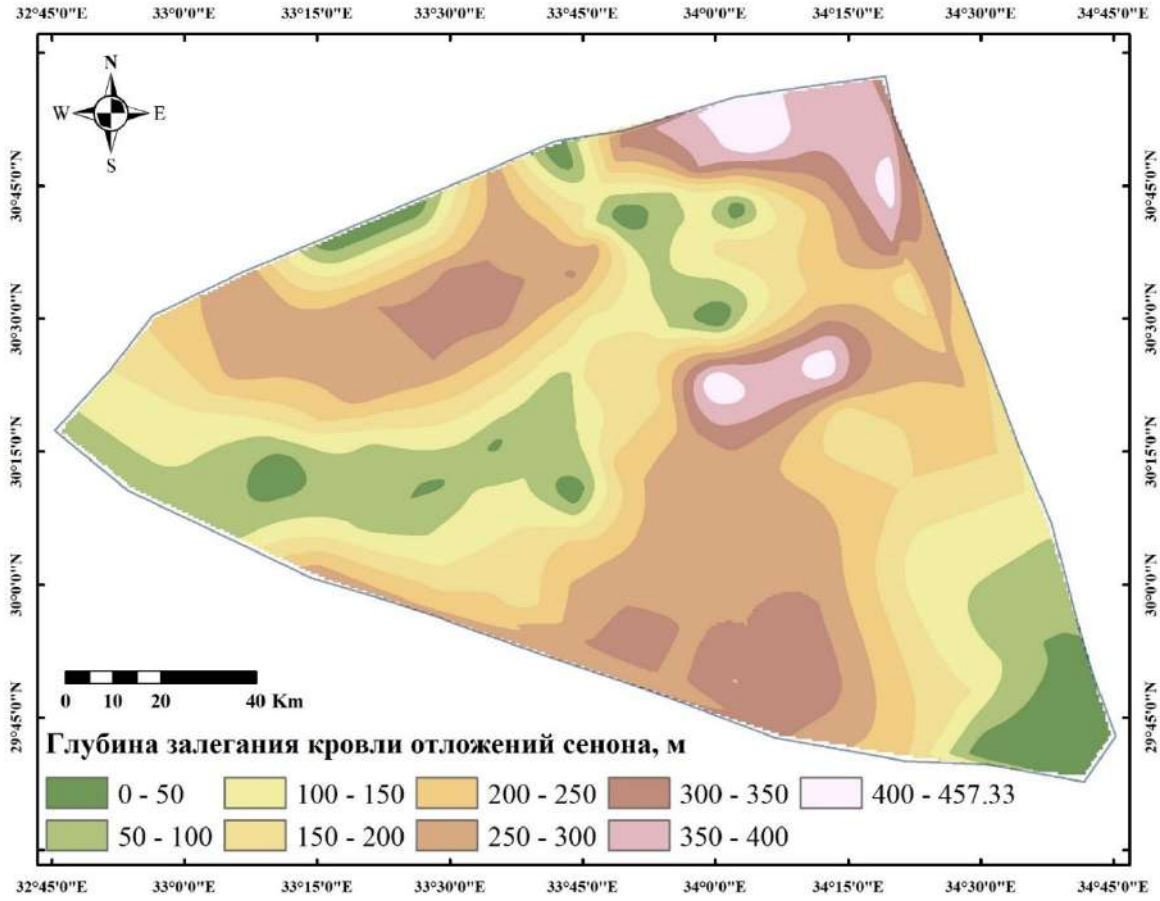

Fig. 3.11. Map depths of Senonian deposits

Turon

Turonian is represented predominantly by limestone with shales at the base. Aquifers are developed, as in previous cases, mainly in limestone - most actively in the Hassan and Naqab regions. A map of the depths of Turonian deposits is presented in figure 3.12.

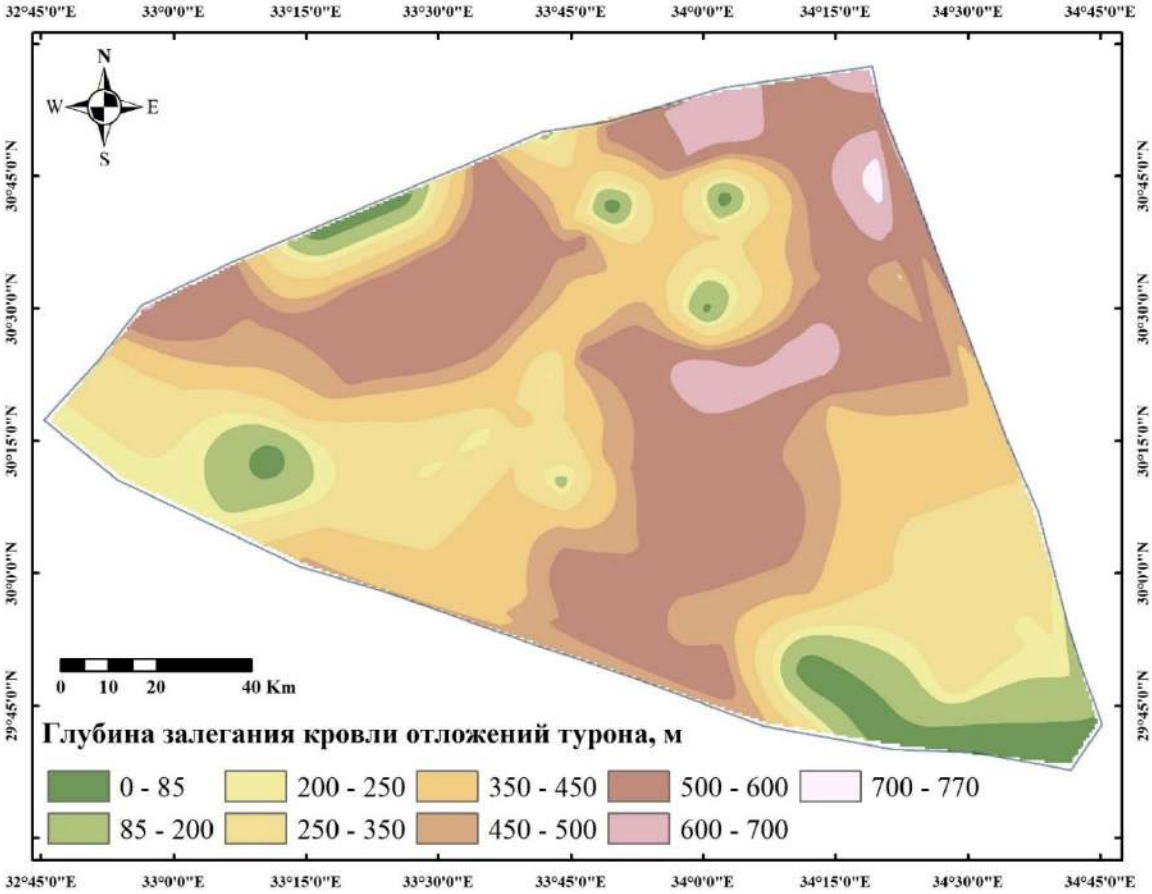

Fig. 3.12. Map depths of Turonian deposits

Cenomanian

The basement rocks of the Cenomanian, overlying the Lower Cretaceous, are represented by aquifer calcareous sandstone. The upper part of the Cenomanian is also represented by aquifer limestones and dolomitic limestones, and in addition, dolomites. Cenomanian rocks are exposed only on the domes; in the rest of the distribution area, they are covered by other rocks.

Locally, karst caves are recorded in the Cenomanian limestones, which by definition means their extremely high permeability in these narrow local zones. Calcareous deposits in the lower part contain interlayers of shale. These shales, usually included in dolomite facies, have a continuous distribution and thickness of about 20 m, and are relatively aquitard. A map of the depths of Cenomanian sediments is presented in Figure 3.13.

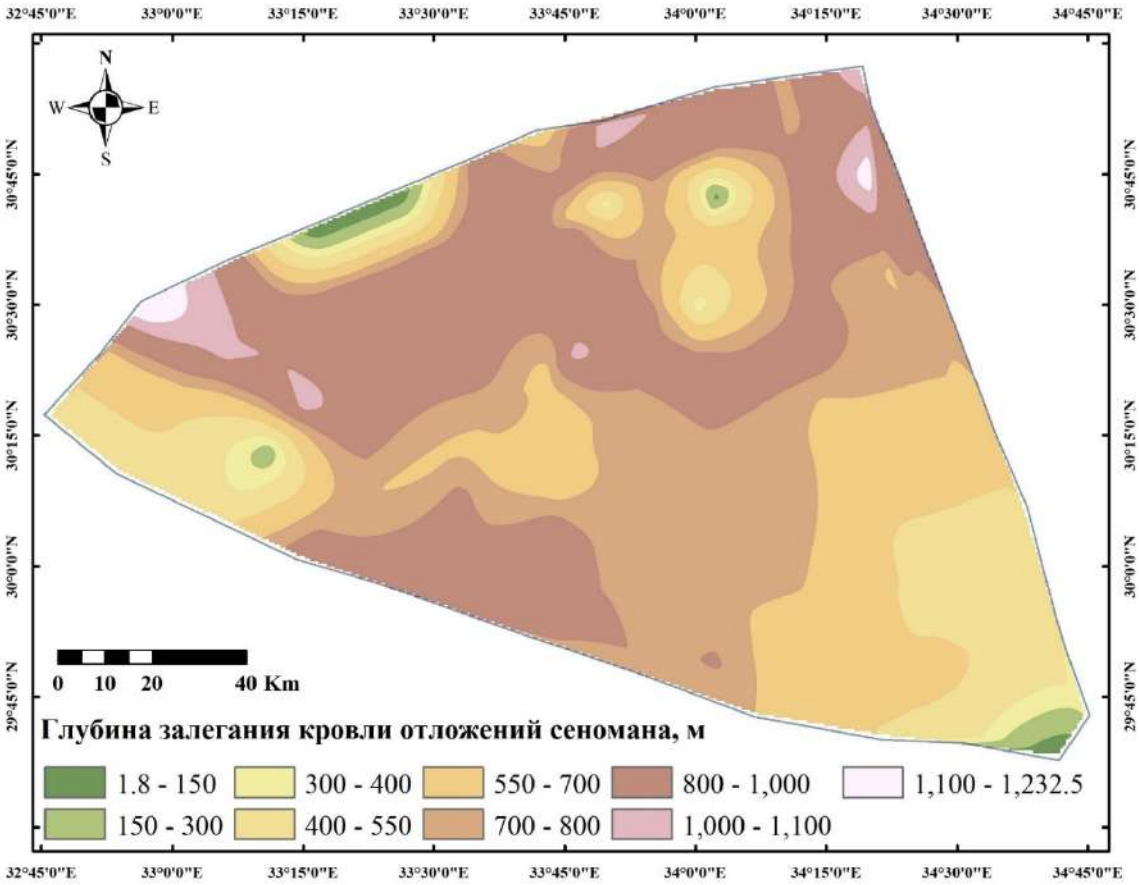

Fig. 3.13. Map depths of Cenomanian sediments

Lower Cretaceous

Lower Cretaceous deposits are common throughout much of northern Sinai. The Lower Cretaceous rocks are represented by permeable quartz (Nubian) sandstones or limestones replacing them in the littoral zone to the north. The sandstone section contains interbeds of shale of varying thickness in different areas of North Sinai (mainly in the northern). The depth to the Lower Cretaceous varies in area and exceeds 1000 m at most points (Fig. 3.14).

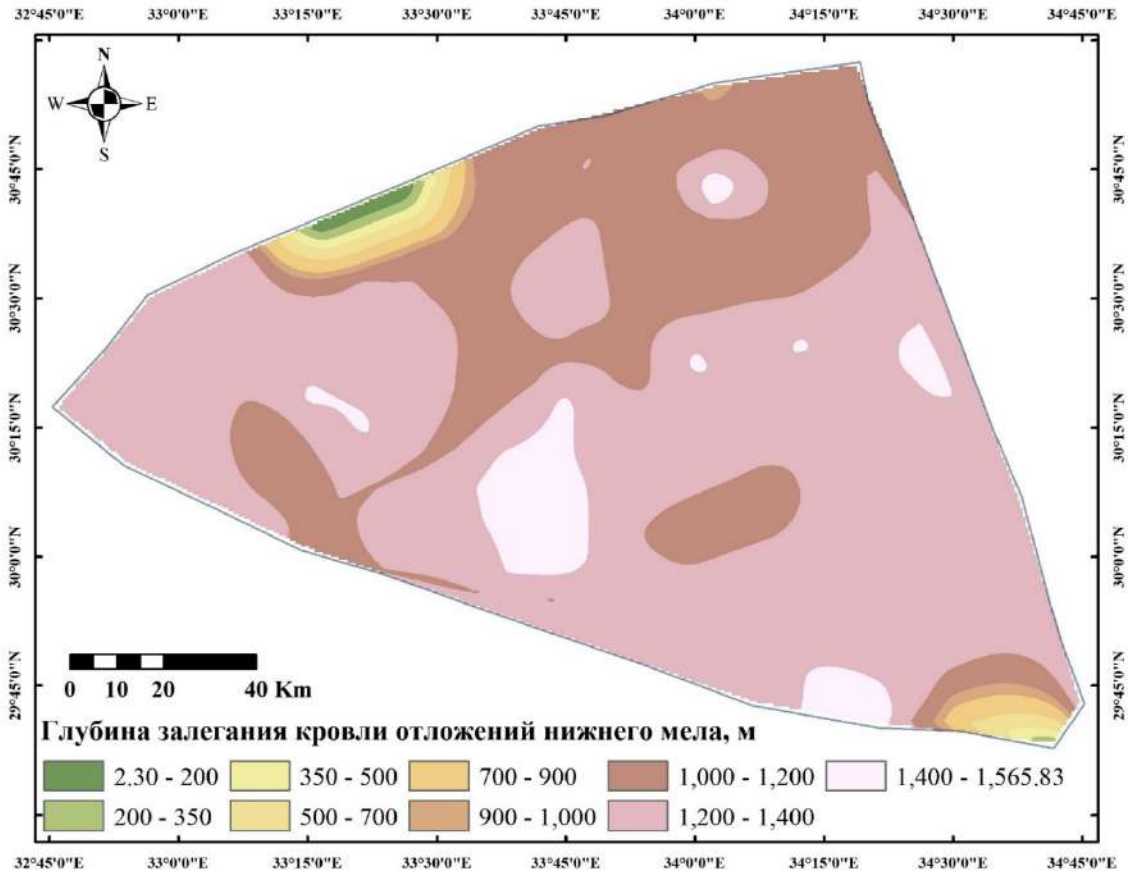

Fig. 3.14. Map depths of Lower Cretaceous deposits

In areas where Lower Cretaceous sandstones unconformably overlie Jurassic sandstones, there is no aquifer hydrogeological boundary between the two formations.

Jurassic

The Middle and Lower Jurassic formations are represented by aquifer sandstones and relatively water-resistant shales with intercalations of thin coal seams. Rock salt was found in one of the coal mines. Upper Jurassic formations are represented mainly by limestones, usually developed in dome structures.

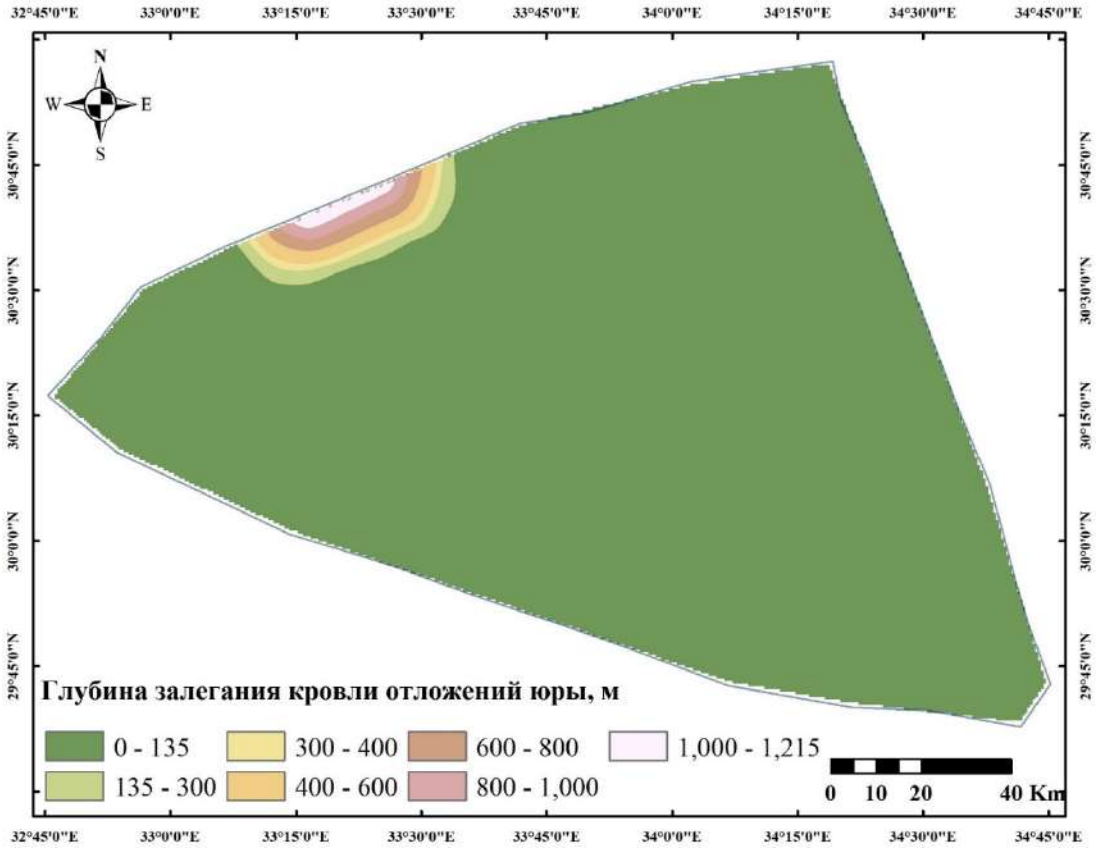

Fig. 3.15. Map depths of Jurassic deposits

Wells tapping Jurassic aquifers are present only in the Gebel Maghara area (Figure 3.15), distributed along the northern margin of the Maghara dome. The flow rate of these wells ranges from 5 to 35 m^3/h (120-840 m^3/day). It is assumed that the area of groundwater recharge of the Upper Jurassic formation is located on the northern edge of the dome. Wells that have penetrated the Middle-Lower Jurassic sandstone aquifer have yields ranging between 3.8 and 5.8 m^3/h (91.2 – 139.2 m^3/day), but the aquifer is not currently considered to be promising neither in terms of quantity nor quality of groundwater, therefore it is not considered in the work.

3.2. Zoning of North Sinai according to the filtration properties of water-bearing rocks

This chapter presents GIS maps of the development of various aquifers compiled by the author, discusses the results of a statistical analysis of the values of filtration parameters of rocks, as well as the results of zoning the territory of

North Sinai in accordance with the values of the filtration coefficient. All these assessments and constructions were carried out in accordance with the age and lithological composition of the water-bearing rocks (for Quaternary sediments, Upper Cretaceous-Paleogene limestones and Lower Cretaceous sandstones).

In this study, statistical estimates were made using SPSS to determine the distribution of filtration coefficient values K (m/day) obtained from field testing of wells.

Quaternary deposits

For Quaternary deposits, various data samples were considered depending on the sampled aquifers and sampling areas: 1) the general population for all Quaternary deposits (All); 2) joint sampling (single filter) of gravel and kurkar deposits - in the valley of Wadi El-Arish (kurkar + gravel_A); 3) kurkar deposits on the northeastern coast of the study area, in the areas of El Arish, Sheikh Zuwayid and Rafah (kurkar_ASR); 4) sand deposits on the northeastern coast of the study area in the same areas of El Arish, Sheikh Zuwayid and Rafah (sand_ASR); 5) sandy deposits in the northwestern region of Bir El-Abd (sand_BR). The results of calculating statistical parameters are given in Table 3.1.

Table 3.1- Statistical parameters of the distribution of filtration coefficient values (K, m/day) in various aquifers of Quaternary sediments

Parameters	All	kurkar+gravel _A	kurkar_ASR	sand_ASR	sand_BR
N - number of measurements	52	31	eleven	6	4
Mean	118	120	75	45	327
Median	92	102	77	37	361
Std. Dev.	106	91	54	19	149
Minimum	2.7	21	2.7	29	131
Maximum	457	360	177	77	457

As shown in Table 3.1, according to the results of sampling 52 wells, all Quaternary sediments are characterized by very high values of filtration

coefficients, averaging tens and even hundreds of m/day with an absolute single minimum of 2.7 m/day (kurkar).

At the same time, kurkar and gravel deposits are characterized by a very large scatter in the filtration coefficient: the minimum and maximum values differ by tens (almost hundreds) of times. Most likely, this is due to different degrees of cementation of these rocks at different sampling sites.

On the contrary, sand deposits seem to be more homogeneous from a filtration point of view: the minimum filtration coefficients differ from the maximum by only 2.5−3.5 times. But at the same time, the average value of the filtration coefficient of sands west of Wadi El-Arish (in the Bir El-Abd area) is generally the highest of all the tested facies of Quaternary sediments (327 m/day) and approximately 7 times higher than in the sands eastern zone, in the areas of El Arish, Sheikh Zuwayid and Rafah. The conclusions made regarding sands today should be considered conditional, requiring further clarification, due to the very small number of their samples.

Figures 3.16−3.20 show graphs of correlations between the filtration coefficient (K) and the depth of the tested well (ds) both for all wells equipped for Quaternary sediments, and for the above various data samples, depending on the tested aquifers and sampling areas.

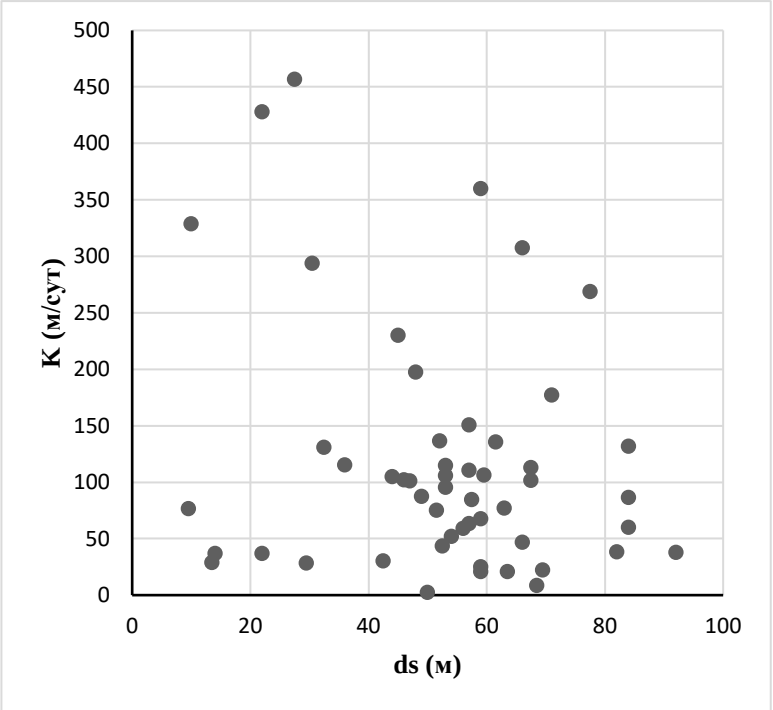

Fig. 3.16. Correlation between the filtration coefficient (K) and well depth (ds) for all wells equipped for Quaternary sediments

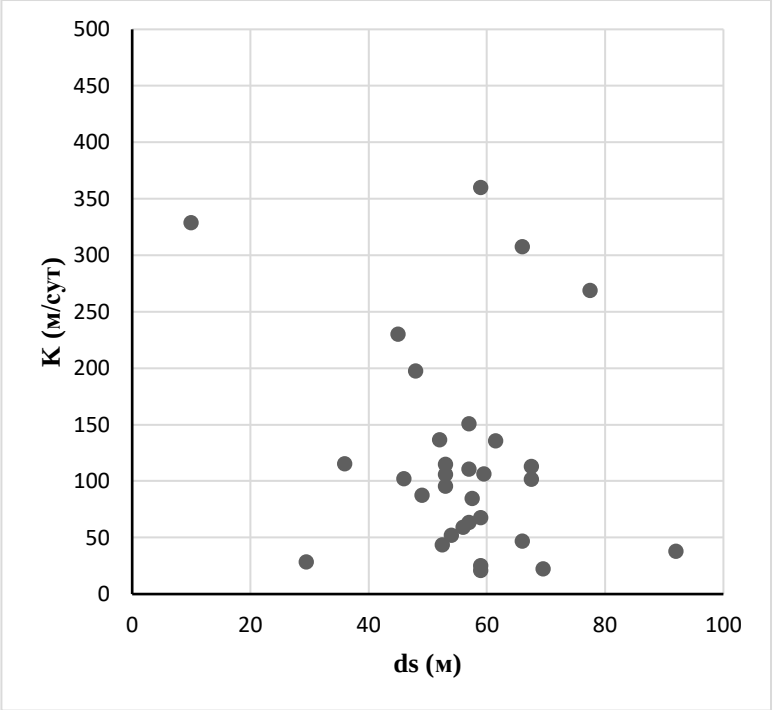

Fig. 3.17. Correlation between filtration coefficient (K) and well depth (ds) for wells equipped with a single filter for Kurkar and gravel deposits in the Wadi El Arish

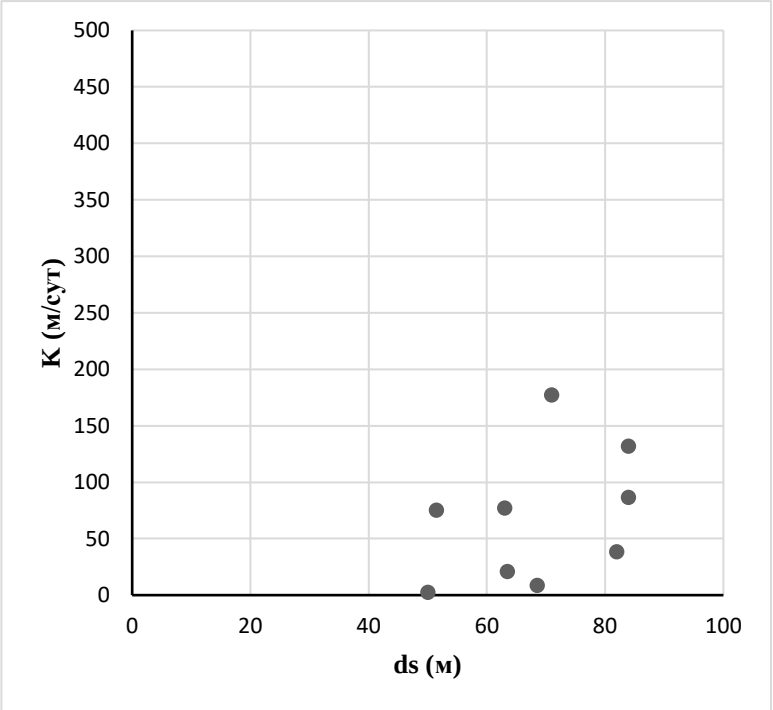

Fig. 3.18. Correlation between filtration coefficient (K) and well depth (ds) in the kurkar deposits on the northeast coast, in the areas of Al Arish, Sheikh Zuwayid and Rafah

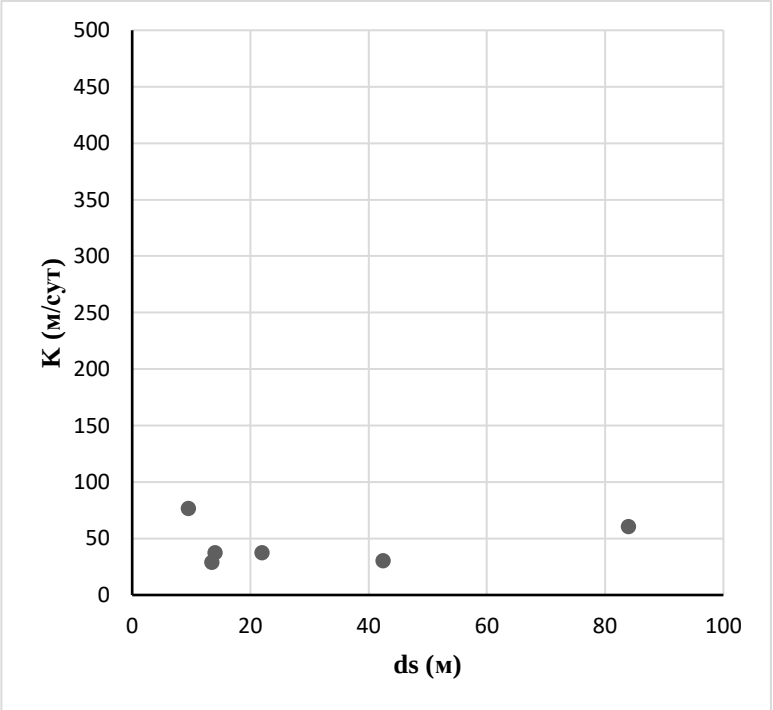

Fig. 3.19. Correlation between filtration coefficient (K) and well depth (ds) in sand deposits on the northeast coast, in the areas of Al Arish, Sheikh Zuwayid and Rafah

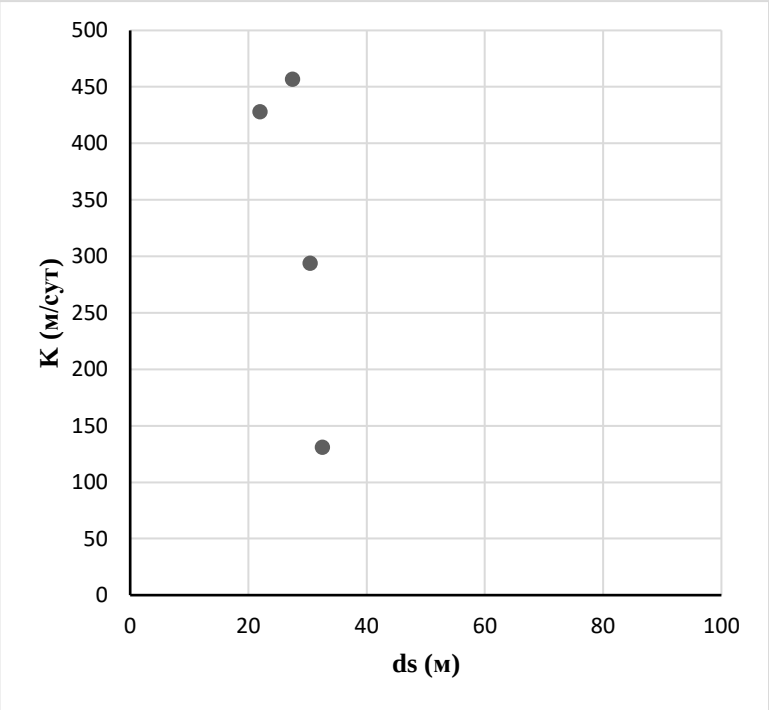

Fig. 3.20. Correlation between filtration coefficient (K) and well depth (ds) in sandy sediments in the northwestern region of Bir El-Abd

As can be seen in these figures, an unambiguous relationship (trend) is not observed either for all Quaternary deposits as a whole, or for each of the individual samples. Thus, it should be accepted that within the limits of the development of Quaternary rocks to actually recorded depths not exceeding 100 meters, there is no change in the filtration properties of rocks with depth. And, consequently, the ranges of changes in the values of the filtration coefficients of various Quaternary deposits recorded above are determined not by geostatic pressure, but by the packing density of loose rocks and the degree of their secondary cementation, formed both directly during sedimentation and during the course of subsequent secondary processes, obviously associated with groundwater filtration.

In accordance with the above, an areal (in plan) zoning of the territory of development of Quaternary deposits was carried out according to the values of filtration coefficients of rocks within the coastal plain up to 15 km wide, which is extremely important from the point of view of assessing the prospects for water supply of the area under consideration. In arid regions like North Sinai, groundwater is virtually the only source of water used by local residents. It is

obvious that the extraction of groundwater from aquifers in areas with higher filtration coefficient values will be easier and cheaper, and, therefore, the development of these areas will be faster and more comprehensive. Thus, the zoning carried out creates the basis for more effective planning and management of groundwater resources, since in fact it is the basis for further zoning according to the size of groundwater resources:

$$\frac{V}{t} = \frac{K*h*A}{l} \qquad (1)$$

Where V – volume of water, t – time (V / t – flow rate of natural groundwater resources at the point in question); K – filtration coefficient; h/l – hydraulic slope of groundwater, A – cross-sectional area of groundwater flow.

The indicated zoning of the coastal plain by permeability was carried out, as well as statistical estimates, separately for the areas of development of various types of rocks (Figs. 3.21 and 3.22): 1) for the combined aquifer represented by Kurkar deposits and gravel (single filter) in the El-Arish area and aquifer of Kurkar deposits on the northeastern coast of the study area (these sediments were not sampled in the western part of the coastal plain) and 2) for the aquifer composed of sands and developed both on the northeast coast of the study area, in the areas of El Arish, Rafah and Sheikh Zuwayid, and in the northwest, in the area of Bir El-Abd.

As shown in Figure 3.21, in the very northeastern part of the area under consideration, near the border of the Republic of Egypt with the Gaza Strip and Israel, the values of the filtration coefficient in the aquifer represented by the Kurkar deposits will be less than 100 m/day (K <100 m/day) , and in the rest of the area, in the area of Wadi El Arish and in the interior parts of the study area, where the gravel aquifer is additionally developed, filtration coefficients will generally be greater than 100 m/day (K > 100 m/day). Thus, the development of

water supply through kurkar deposits and gravels is more promising in the area of Wadi El Arish than in the northeastern areas of North Sinai.

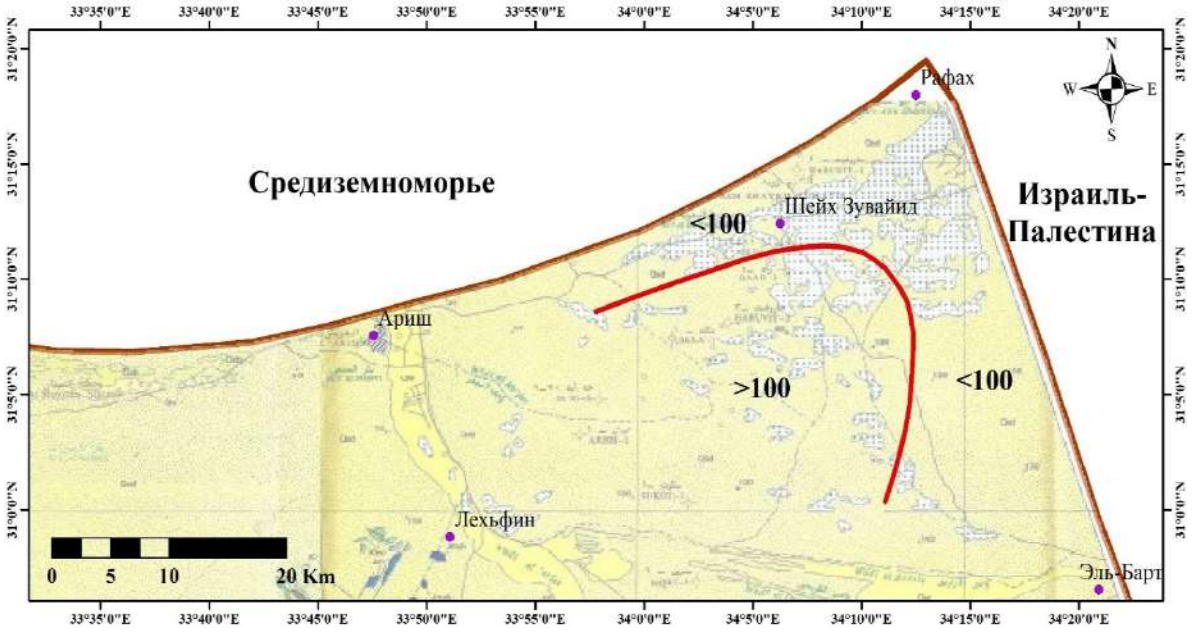

Fig. 3.21. Map of zoning the area of kurkar deposits and gravel, according to the value of the filtration coefficient K, m/day

Fig. 3.22. Map of zoning the area of sand, according to the value of the filtration coefficient K, m/day

As shown in Figure 3.22, in the sand aquifer, in general, in all northeastern regions of North Sinai (El-Arish, Rafah, and Sheikh Zuwayid), the values of filtration coefficients are less than 100 m/day (K < 100 m /day), and in the north-

west of North Sinai, in the area of Bir El-Abd, filtration coefficients are more than 100 m/day (K > 100 m/day). Thus, the development of water supply due to the horizon represented by sands in the areas of the northwestern part of North Sinai will be more promising than in its northeastern part.

Pre-Quaternary deposits

As for Quaternary aquifers, for aquifers developed in pre-Quaternary sediments, statistical estimates were made using the SPSS program for the distribution of filtration coefficient values K (m/day) obtained as a result of field testing of wells.

As samples for statistical assessments, two types of water-bearing rocks were identified, developed almost throughout the entire territory of Northern Sinai: 1) Upper Cretaceous and Paleogene limestones and 2) Lower Cretaceous sandstones. A more detailed division by age of the water-bearing rocks turned out to be impossible due to the similarity of the lithological and hydrodynamic features of the Upper Cretaceous and Paleogene aquifers. The results of calculating statistical parameters for these samples in comparison with statistical characteristics for the general population for all pre-Quaternary aquifers are shown in Table 3.2.

Table 3.2- Statistical parameters for the distribution of filtration coefficient values (K, m/day) in various rocks of pre-Quaternary deposits

Parameters	All	Limestone K_2	Sandstone K_1
N	128	68	60
Mean	13	19	7
Median	4	4	4
Std. Dev.	24	29	13
Minimum	0.01	0.01	0.13
Maximum	113	113	87

As can be seen from Table 3.2, the mean and median values of filtration coefficients in both limestone and sandstone of pre-Quaternary deposits are values

of the same order, but several times and even tens of times less than in Quaternary aquifers (see Table 3.1). At the same time, there is a very large scatter in the values of the filtration coefficient within each of the considered samples: in limestones - from 0.10 to 113 m/day, in sandstones - from 0.13 to 87 m/day. Thus, it is obvious that the permeability of all pre-Quaternary sediments is determined not by the filtration properties in porous blocks, but by the intensity of fracturing of both limestone and sandstone. This is especially noticeable in the sample for limestones - the median is only 4 m/day with an average of 19 m/day, which indicates the local development of fracturing in certain areas, where the filtration coefficient is significantly higher than the mean.

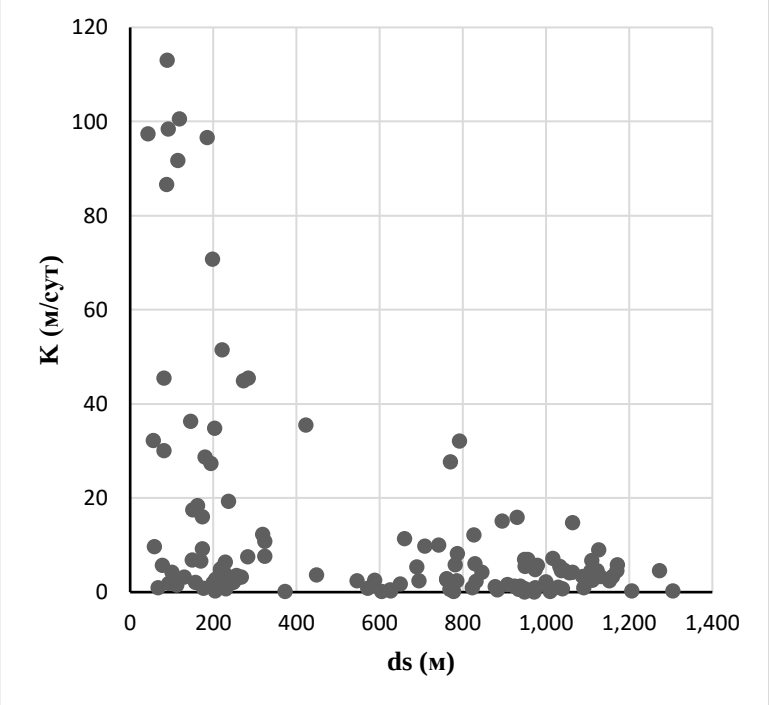

Fig. 3.23. Correlation relationship between the filtration coefficient (K) and well depth (ds) for all wells equipped for pre-Quaternary sediments

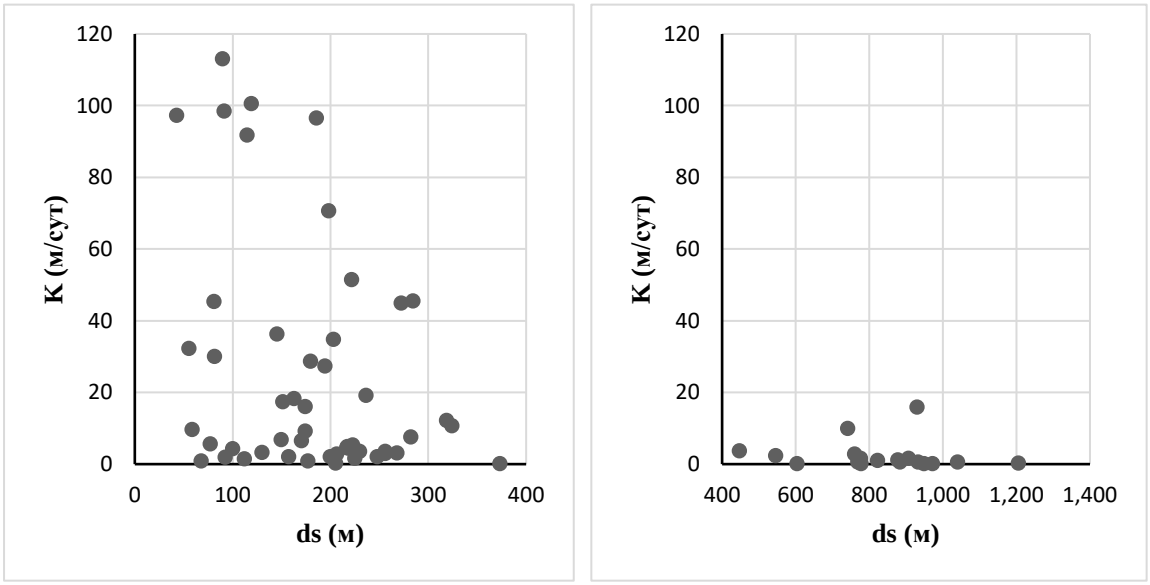

a b

Fig. 3.24 a, b. Correlation between filtration coefficient (K) and well depth (ds) for all wells penetrating limestone

Figures 3.23−3.25 show graphs of correlations between the filtration coefficient (K) and the depth of the tested well (ds) both for all wells equipped for pre-Quaternary sediments, and for the above two samples corresponding to Upper Cretaceous-Paleogene limestone and Lower Cretaceous sandstone.

As shown in these figures, the highest values of filtration coefficients (more than 60 m/day) in both limestones and sandstones are observed only to a depth of less than 200 meters. The most indicative in this regard are the graphs for limestone (Fig. 3.24 a, b). Up to a depth of about 400 m, an unambiguous relationship (trend) is, in principle, not observed, and the values of filtration coefficients vary from hundredths of m/day to more than 100 m/day. But at depths of more than 400 meters, these values do not exceed 20 m/day at all, being in the vast majority no more than 5 m/day. In sandstones at depths of more than 400 m, filtration coefficients in the vast majority of cases also do not exceed 20 m/day, tending to values less than 10 m/day (Fig. 3.25).

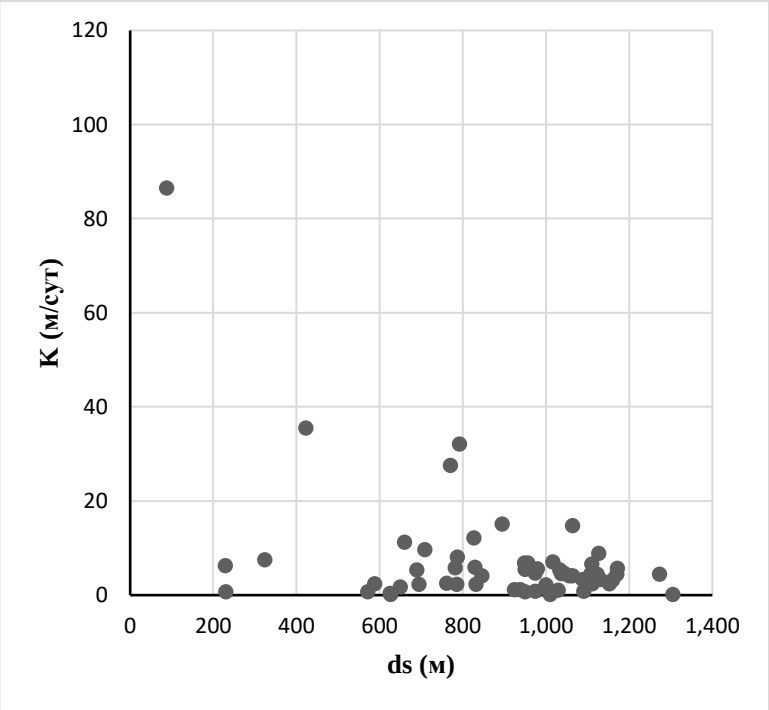

Fig. 3.25. Correlation between filtration coefficient (K) and well depth (ds) for all wells penetrating sandstones

These facts, in the author's opinion, confirm the above assumption that the filtration permeability of all pre-Quaternary sediments is determined primarily by the intensity of fracturing of both limestone and sandstone. In this case, the decrease in the values of the filtration coefficient with depth is logical, since it is caused by geostatic pressure: the mass of the overlying sediments increases, which leads to a significant decrease in the fracturing of the water-bearing rocks (compression of fractures), while the porosity in cemented sediments (limestone and sandstone) changes few.

At the same time, at shallow depths, the increased permeability of bedrock is probably determined by the location of the sampled point to some fault within which increased permeability naturally occurs. This is precisely what can explain the large scatter in the values of filtration coefficients at shallow depths.

In accordance with the above, an areal (in plan) zoning of the territory of development of pre-Quaternary deposits was carried out according to the values of filtration coefficients of rocks within North Sinai, which is extremely important

from the point of view of assessing the prospects for water supply of the area under consideration.

Zoning, as well as statistical assessments, was carried out separately for water-bearing rocks, represented by limestone, and sediments, represented by sandstone. In both samples, the entire set of filter coefficient values was divided into three main gradations (small, medium and high values), presented in Tables 3.3 and 3.4, respectively.

Table 3.3- Gradations of filtration coefficient values in limestone (K_2+P_g) during zoning

No.	Zone	K (m/day)	Gradation
1	A	<10	small
2	B	10 - 40	average
3	C	> 40	high

Table 3.4- Gradations of filtration coefficient values in sandstone (K_1) during zoning

No.	Zone	K (m/day)	Gradation
1	A	<3	small
2	B	3 - 10	average
3	C	> 10	high

Maps compiled based on the results of zoning the territory of North Sinai according to the specified gradations of filtration coefficient values are presented in Figures 3.26 (for limestone) and 3.27 (for sandstone).

As can be seen in these figures, in the vast majority of the territory of Northern Sinai, water-bearing pre-Quaternary rocks (both limestone and sandstone) with medium and low values of filtration coefficients are developed. Areas with high values of filtration coefficients are noted only in certain local zones.

From a practical point of view, it can be stated that the most promising areas for the extraction of groundwater from aquifers (without taking into account

their chemical composition) are the following areas: in the vicinity of Al-Qusaim, Gebel El-Magara, Baghdad, Gebel Libni for horizons represented by limestones, and around Al-Qusaim, Gebel Arif Al-Naga, and in Rafah and Sheikh Zuwayid for sandstone aquifer.

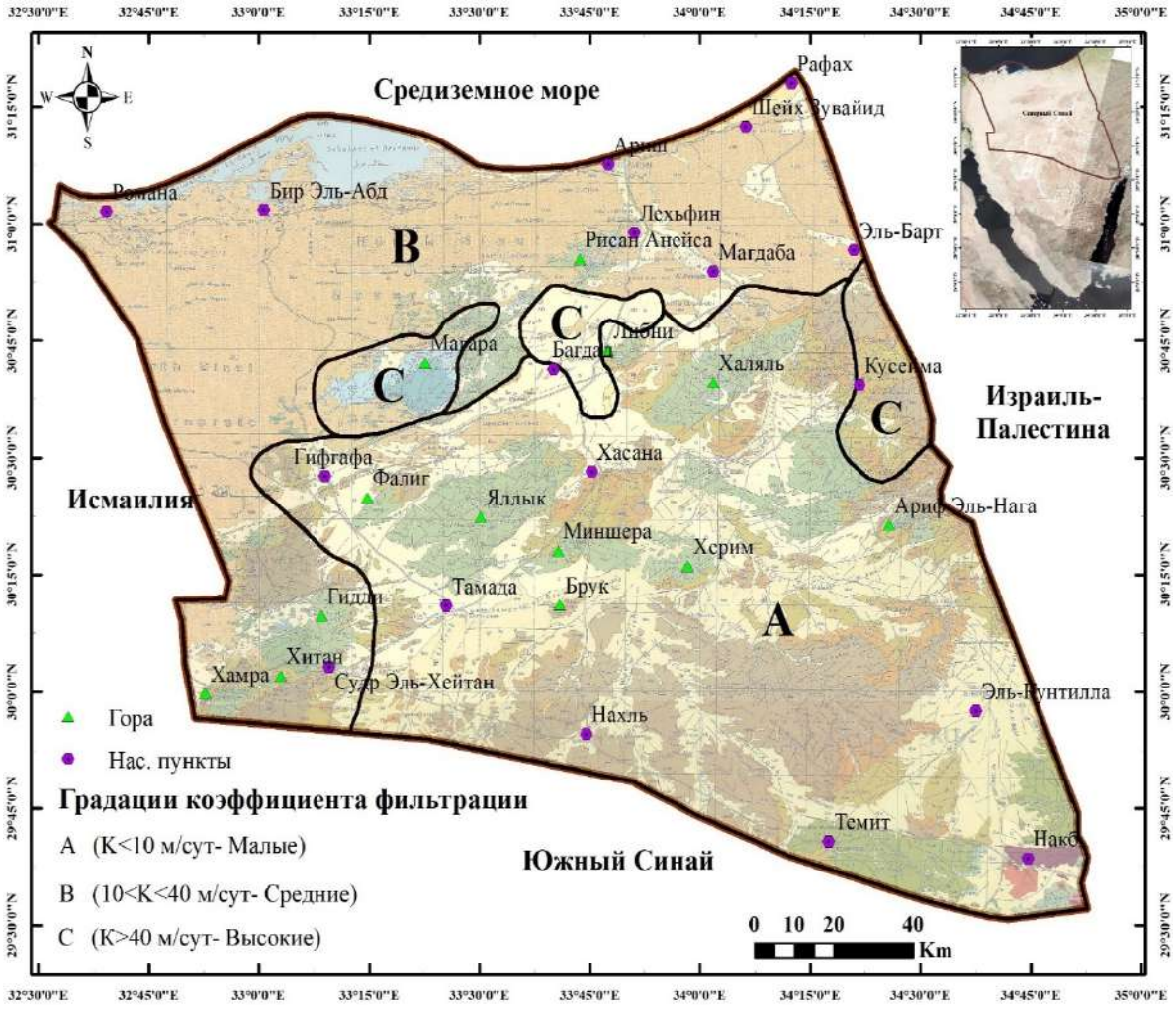

Fig. 3.26. Map of zoning the aquifer of limestone according to the value of the filtration coefficient K, m/day

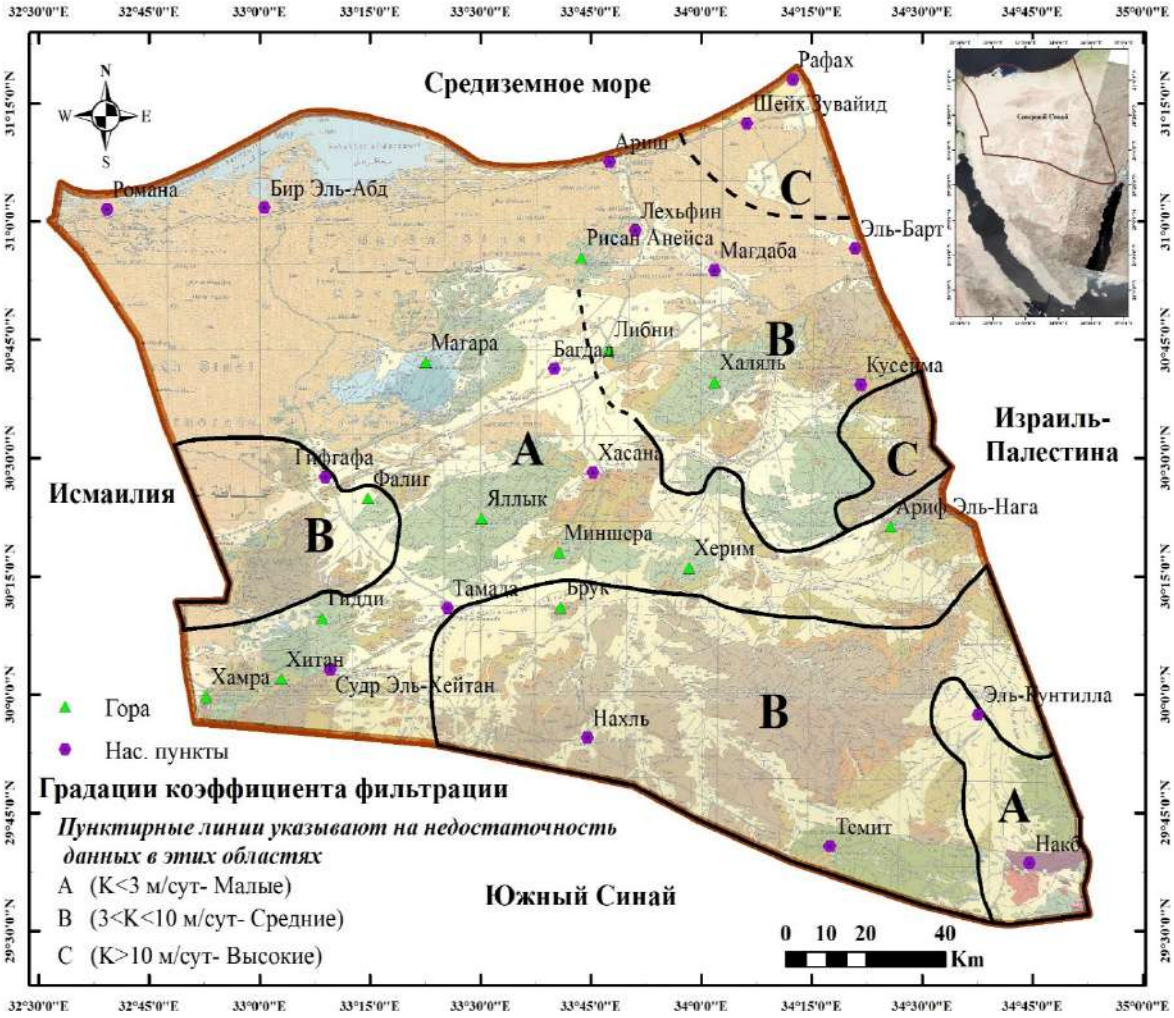

Fig. 3.27. Map of zoning the aquifer of sandstone according to the value of the filtration coefficient K, m/day

CHAPTER 4. CHARACTERISTICS OF THE CHEMICAL COMPOSITION OF GROUNDWATER IN NORTH SINAI

The chemical composition of groundwater in northern Sinai is the main factor in assessing the possibility of its use for drinking water supply and irrigation of agricultural land. The characteristics of the chemical composition of groundwater in North Sinai presented below are based on the totality of the results of hydrogeological studies previously carried out in this territory, including those carried out in recent years [16; 17; 26; 27; 33; 37; 39; 40; 43; 46; 50; 63; 66; 70; 74; 83; 88; 90; 98; 104; 105; and etc.]. As in the case of assessing the filtration properties of rocks discussed in Chapter 3, the basis of the factual basis for the chemical composition of groundwater was also information on hydrogeological wells contained in the summary report “North Sinai Groundwater Resources Study in the Arab Republic of Egypt” [60], and additionally provided by the Water Research Institute (WRRI) under the Ministry of Irrigation and Water Resources of the Arab Republic of Egypt [7]. The result of the systematization was a database on the chemical composition of groundwater, which collectively included materials from 200 wells [31; 34; 71; 72; 73; 101; and etc.].

This chapter provides an overview of the various hydrochemical characteristics of groundwater in North Sinai: total salinity (TDS); concentrations of macrocomponents - main anions (HCO_3^-, Cl^-, SO_4^{2-} and CO_3^{2-}) and cations (Mg^{2+}, Na^+, Ca^{2+} and K^+) and pH values. The author carried out a statistical analysis of existing hydrochemical data, calculated some genetic coefficients, and also assessed the saturation indices (SI) of groundwater in relation to the main rock-forming minerals using the PHREEQC program. All these estimates are made in accordance with the age of the water-bearing rocks (separately for Quaternary and pre-Quaternary deposits), as well as in accordance with the type of water-bearing rocks. Finally, the territory of North Sinai was zoned according to total mineralization (TDS) values.

4.1. Quaternary aquifer

The conditions for the development of aquifers in Quaternary sediments are described in detail in Chapter 3. Let us note the main thing here: the distribution of Quaternary aquifers of significant thickness is limited to a coastal plain 10 to 15 km wide in the northernmost part of North Sinai, along the Mediterranean Sea; The main water-bearing rocks of the Quaternary sediments are sand, gravel and kurkar sediments.

The main problem with the use of groundwater from Quaternary aquifers in the area under consideration is its high salinity. There are three main factors that may determine this increased salinity: salinization by groundwater from underlying pre-Quaternary aquifers, evaporative concentration, or intrusion of modern seawater from the Mediterranean Sea.

Analyzing the hydrogeochemical situation in Quaternary deposits by rock type as a whole, we can state the following.

The salinity of groundwater in sandy aquifers or coastal sand dunes developed in the upper part of the section is low and ranges from 300 to 800 mg/dm^3, especially in the sand dunes in the Sheikh Zuwayid and Rafah areas, where it is the least. Wells in coastal sand dune deposits are typically shallow, 20 to 40 meters, and the sands there often rest on a clay aquiclude. That is, this horizon is locally isolated from the underlying ones and is fed in accordance with the current hydrometeorological cycle of precipitation.

The gravel aquifers are exploited only within the alluvial valley of Wadi El Arish. In wells located in the lower reaches of the wadi, at the northern end of the alluvial valley, mineralization is less than 2000 mg/dm^3; and in the rest of the valley, it ranges from 3000 to 5100 mg/dm^3. Fresh water with a salinity of less than 1000 mg/dm3 in individual wells drilled into gravel deposits clearly indicates

the replenishment of fresh water reserves in these layers due to modern infiltration feeding by atmospheric precipitation, just as in coastal sand dunes.

Groundwater salinity in kurkar ranges from 2500 to 3800 mg/dm^3 in the alluvial valley of Wadi El Arish and from 2200 to 5600 mg/dm^3 in Sheikh Zuwayid and Rafah areas. When combined with wells testing horizons composed of gravel and kurkar, between which there is a hydraulic connection in natural conditions, mineralization varies in the range from 2200 to 3700 mg/dm^3. It is possible that the high salinity of groundwater in the kurkar deposits is primordial – syngenetic. However, there is also the possibility of their salinization by saline groundwater from underlying aquifers of pre-Quaternary age, represented by limestone or sandstone. In addition, it should be taken into account that the aquifer in the kurkar deposits in the El Arish area is inevitably recharged by periodic large floods that occur during the flood period with an intensity of once every ten to fifteen years.

In this study, using the SPSS program, statistical estimates were made for the distribution of the values of the above hydrochemical indicators of groundwater obtained as a result of field testing of wells, and various correlations were constructed. Various data samples were considered depending on the sampling areas (see Chapter 3): 1) the general population for all Quaternary deposits (“Quaternary as a whole”); 2) “zone_A” – the El-Arish region, where aquifers are represented by sands, gravels and kurkar deposits (74 wells); 3) “zone_SR” – the Rafah and Sheikh Zuwayid areas, where aquifers composed of sands and kurkara sediments are developed (25 wells); 4) “zone_BR” – the Bir El-Abd area, where only a sandy aquifer occurs (65 wells).

The following variables were considered (“selected” values): mineralization (TDS) in the dimension mg/dm^3 (ppm), concentrations of all the above dissolved macrocomponents in % eq (% epm), pH value in units. pH, as well as the depth of the tested well (ds) in meters. Table 4.1 presents the results

of statistical processing of the various above-mentioned samples according to the mineralization of groundwater in the dimension mg/dm3; Table 4.2 shows the results of statistical processing for the pH value in units. pH; and in tables 4.3-4.8 - the results of statistical processing of the same samples for the concentrations of macrocomponents HCO_3^-, SO_4^{2-}, Cl^-, Mg^{2+}, Ca^{2+} and Na^+ in %-eq, respectively.

There are no fundamental differences in the statistical parameters of the distribution of various indicators of the chemical composition of groundwater for the indicated three territorial samples: zone_A, zone_SR and zone_BR. In all three zones, both fresh and brackish, near-neutral or slightly alkaline groundwater is developed, on average sulfate-chloride calcium-magnesium-sodium (or magnesium-sodium). Some deviation is noted for the waters of the eastern BR zone, where, with relatively increased mineralization, minimum values of HCO_3 concentration are recorded: 0.1-2.5% equivalent.

Table 4.1- Statistical parameters for the distribution of salinity values (TDS, mg/l) in different zones of aquifer development in Quaternary sediments

Statistics	All	Zone_A	Zone_SR	Zone_BR
N	164	74	25	65
Mean	3304	2868	1668	4431
Median	3174	2800	1339	4100
Std. Dev.	1909	1118	1519	2105
Minimum	248	526	248	329
Maximum	13400	6500	5600	13400

Table 4.2- Statistical parameters for the distribution of pH values (pH units) in various zones of aquifer development in Quaternary sediments

Statistics	All	Zone_A	Zone_SR	Zone_BR
N	101	41	19	41
Mean	7.5	7.9	7.5	7.3
Median	7.4	7.9	7.4	7.3
Std. Dev.	0.4	0.3	0.35	0.25
Minimum	7.1	7.1	7.1	7.1
Maximum	8.7	8.3	8.3	8.7

Table 4.3- Statistical parameters for the distribution of HCO_3 concentration (%-eq) in different zones of aquifer development in Quaternary sediments

Statistics	All	Zone_A	Zone_SR	Zone_BR
N	101	41	19	41
Mean	6.5	8	15.5	1
Median	3.5	7.5	6	1
Std. Dev.	10	4	18	0.5
Minimum	0.11	1.8	1.8	0.11
Maximum	54.0	20.5	54.0	2.5

Table 4.4- Statistical parameters for the distribution of SO_4 concentration (%-eq) in different zones of aquifer development in Quaternary sediments

Statistics	All	Zone_A	Zone_SR	Zone_BR
N	101	41	19	41
Mean	31	28.5	33	32.5
Median	31.5	28	33.5	35.5
Std. Dev.	11.5	9	16.5	10.5
Minimum	6.8	9.1	6.8	7.7
Maximum	66.0	45.9	66.0	51.2

Table 4.5- Statistical parameters for the distribution of Cl concentration (%-eq) in different zones of aquifer development in Quaternary sediments

Statistics	All	Zone_A	Zone_SR	Zone_BR
N	101	41	19	41
Mean	62	63	50.5	66.5
Median	63	64.5	50.5	64
Std. Dev.	12.5	9.5	15.5	10.5
Minimum	22.5	45.3	22.5	47.9
Maximum	92.2	87.9	75.2	92.2

Table 4.6- Statistical parameters for the distribution of Mg concentration (%-eq) in different zones of aquifer development in Quaternary sediments

Statistics	All	Zone_A	Zone_SR	Zone_BR
N	101	41	19	41
Mean	26.5	27.5	23	26.5
Median	27	27.5	17.5	27
Std. Dev.	7	6	12	5
Minimum	6.5	14.0	6.5	15.6
Maximum	56.3	39.8	56.3	37.6

Table 4.7- Statistical parameters for the distribution of Ca concentration (%-eq) in different zones of aquifer development in Quaternary sediments

Statistics	All	Zone_A	Zone_SR	Zone_BR
N	101	41	19	41
Mean	14	24.5	7.5	6
Median	9.5	25	5	6.5
Std. Dev.	10	5	8	3
Minimum	0.63	14.2	1.8	0.63
Maximum	37.9	37.9	32.2	12.9

Table 4.8- Statistical parameters for the distribution of Na concentration (%-eq) in different zones of aquifer development in Quaternary sediments

Statistics	All	Zone_A	Zone_SR	Zone_BR
N	101	41	19	41
Mean	59	47	68.5	66.5
Median	61	45.5	75.5	64.5
Std. Dev.	13	7	16	5.5
Minimum	32.2	35.3	32.2	60.0
Maximum	90,	61.8	90.4	79.2

Figures 4.1–4.2 show graphs of correlations between groundwater salinity (TDS) and the depth of the tested well (ds) for two samples depending on the sampling areas: zone_A and zone_SR, respectively. As can be seen in these figures, there is no clear dependence in these coordinates for any of these zones.

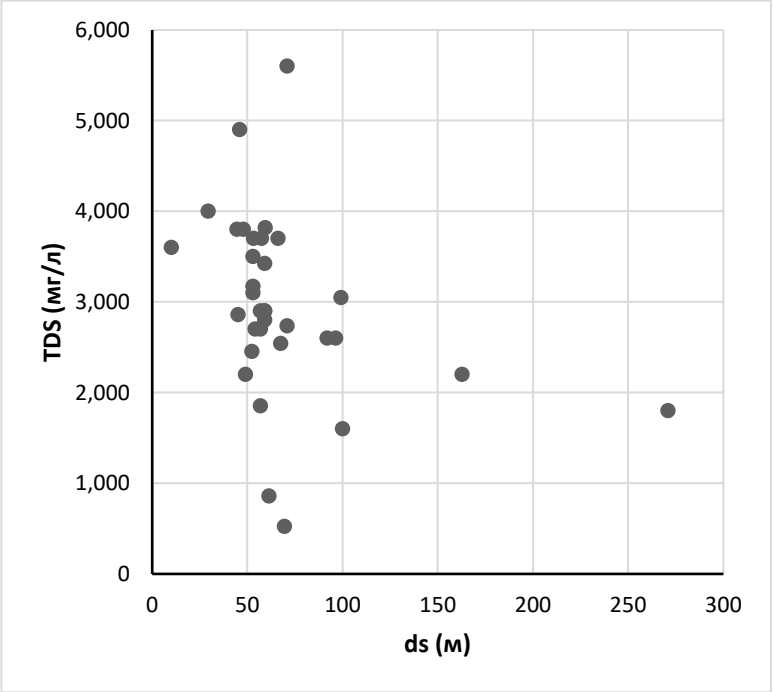

Fig. 4.1. Correlation between mineralization (TDS, mg/l) and well depth (ds, m) for wells in zone_A

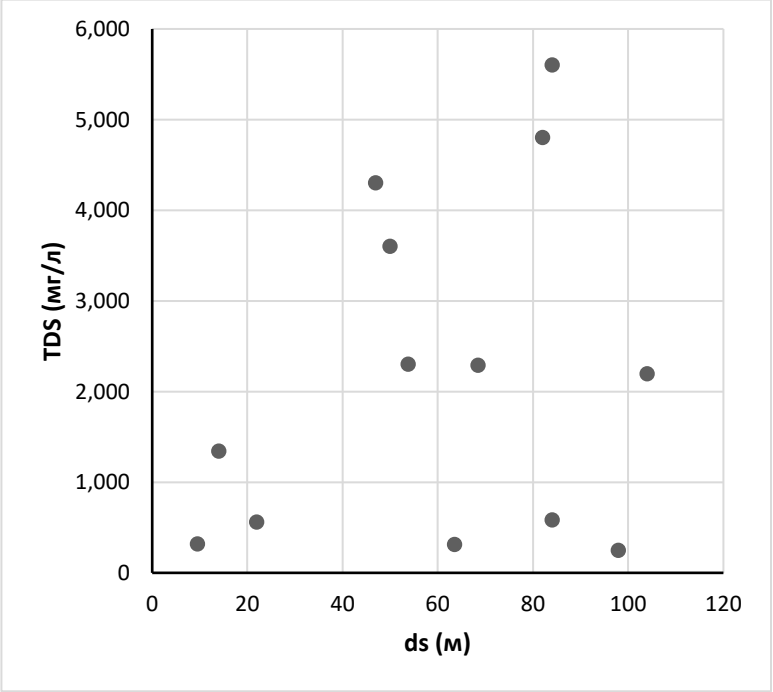

Fig. 4.2. Correlation between mineralization (TDS, mg/l) and well depth (ds, m) for wells in zone_SR

For all three sampling zones A, SR and BR, correlations were also constructed between mineralization (TDS) and the concentrations of all macrocomponents in mg-eq/l. Figures 4.3 a, b, c for zone_A, 4.4 a, b, c for zone_SR and 4.5 a, b, c for zone_ BR present the corresponding graphs for Cl, SO_4 and Na, where a direct linear dependence of mineralization on the concentrations of Cl and Na and, less clearly, on the SO_4 content. For the remaining macrocomponents: HCO_3, Mg and Ca, no significant dependence is observed in any of the three zones.

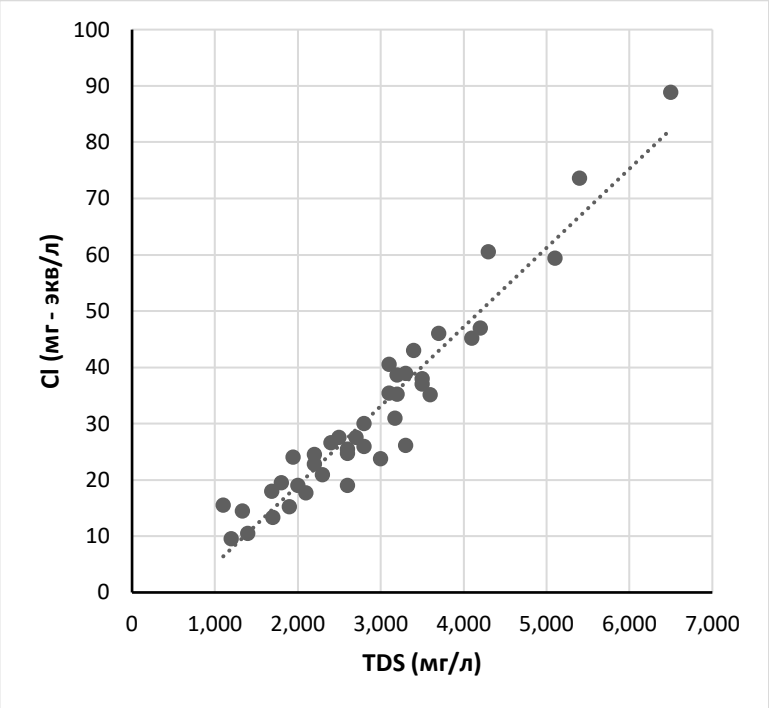

Fig. 4.3, a. Correlation between mineralization (TDS, mg/dm^3) and Cl concentration (mg-eq/dm^3) for wells in zone_A

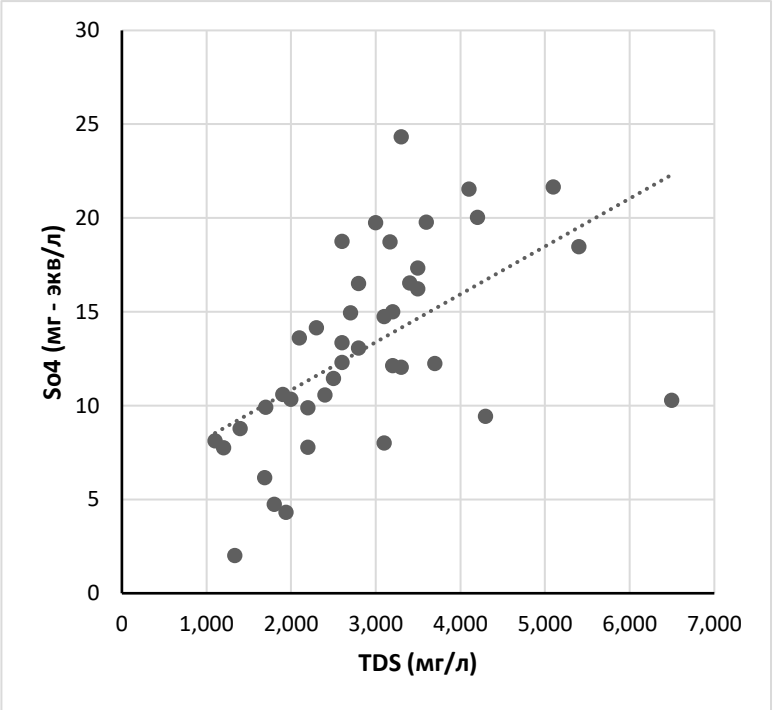

Fig. 4.3, b. Correlation between mineralization (TDS, mg/dm^3) and SO_4 concentration (mg-eq/dm^3) for wells in zone_A

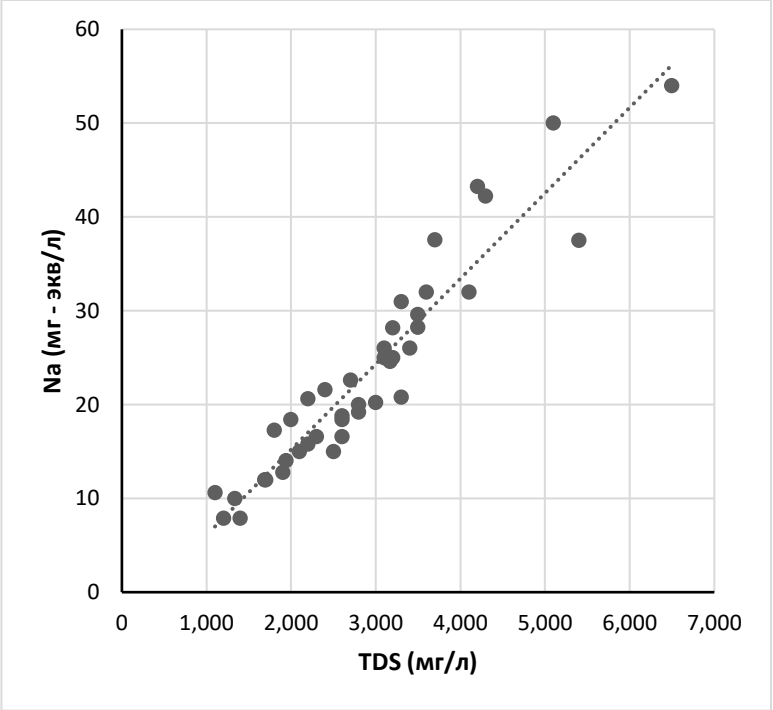

Fig. 4.3, c. Correlation between mineralization (TDS, mg/dm^3) and Na concentration (mg-eq/dm^3) for wells in zone_A

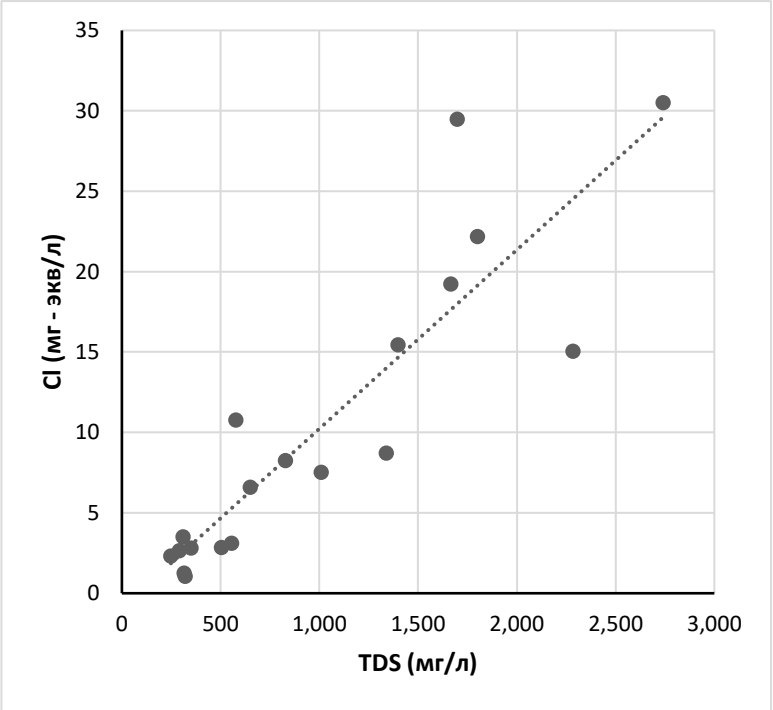

Fig. 4.4, a. Correlation between mineralization (TDS, mg/dm^3) and Cl concentration (mg-eq/dm^3) for wells in zone_SR

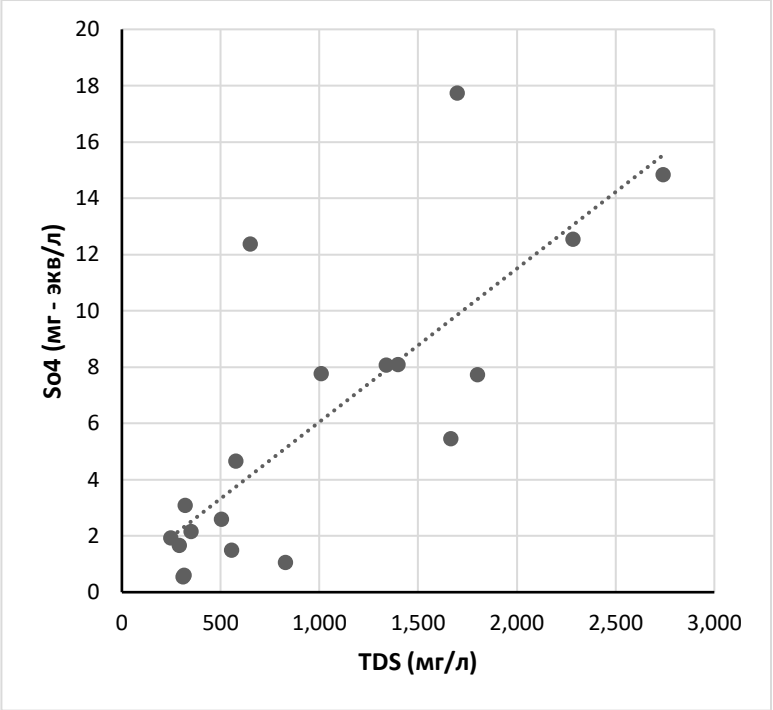

Fig. 4.4, b. Correlation between mineralization (TDS, mg/dm^3) and SO_4 concentration (mg-eq/dm^3) for wells in zone_SR

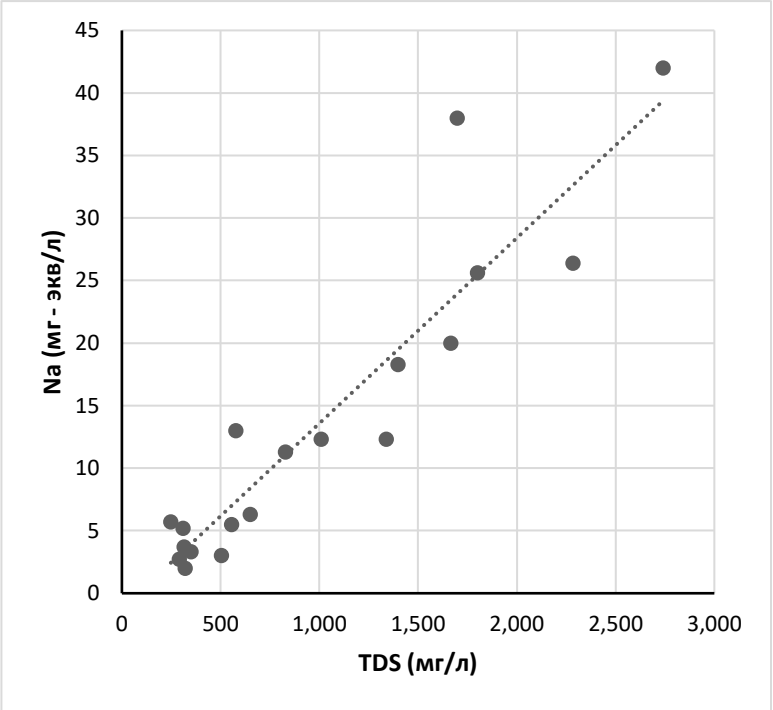

Fig. 4.4, c. Correlation between mineralization (TDS, mg/dm^3) and Na concentration (mg-eq/dm^3) for wells in zone_SR

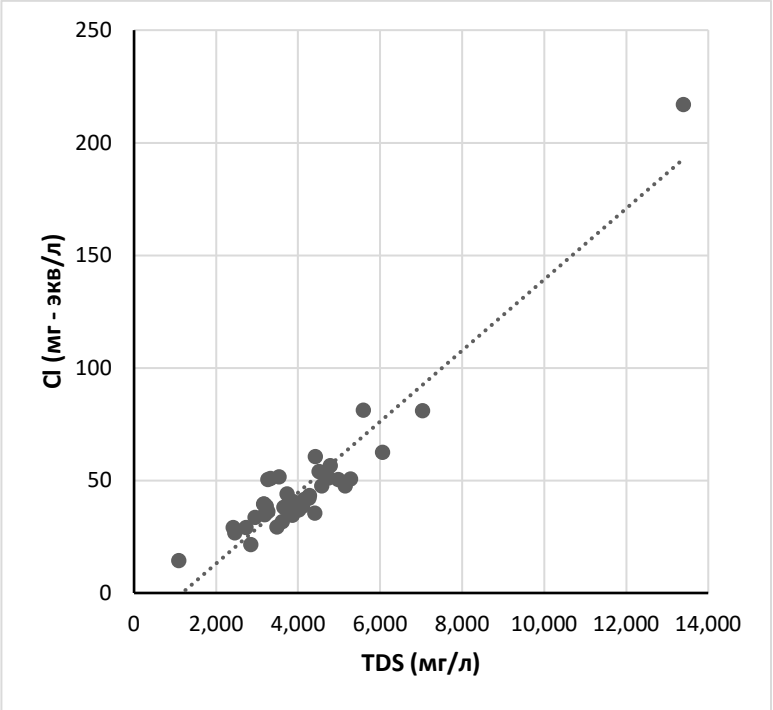

Fig. 4.5, a. Correlation between mineralization (TDS, mg/dm^3) and Cl concentration (mg-eq/dm^3) for wells in zone_BR

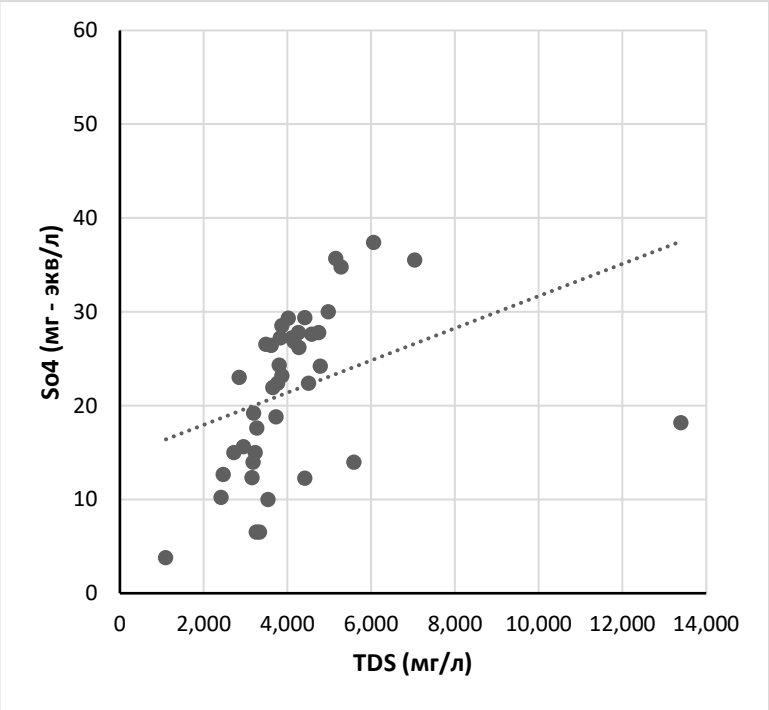

Fig. 4.5, b. Correlation between mineralization (TDS, mg/dm^3) and SO_4 concentration (mg-eq/dm^3) for wells in zone_BR

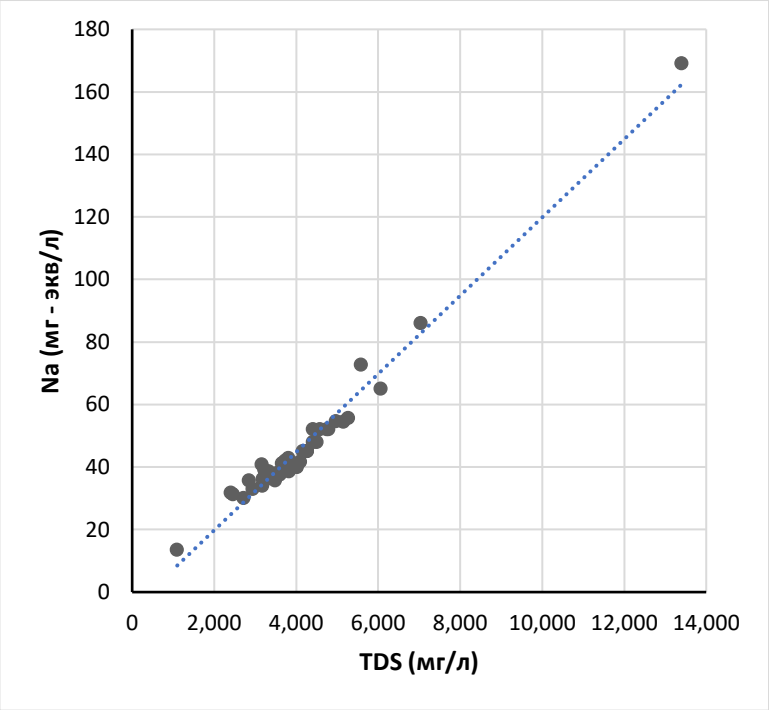

Fig. 4.5, c. Correlation between mineralization (TDS, mg/dm^3) and Na concentration (mg-eq/dm^3) for wells in zone_BR

Thus, in accordance with the above average ratios of %-equivalent concentrations of macrocomponents (Table 4.3-4.8), the main anion determining the mineralization of groundwater in aquifers in Quaternary sediments for all three

zones under consideration (at least in brackish waters with mineralization above 1 g/dm^3) is Cl^- (with the additional influence of SO_4^{2-}), and the main cation is Na^+.

Figures 4.6, 4.7 and 4.8 show the correlations between mineralization (TDS) and the concentrations of all macrocomponents in % equivalent. for each of the three sampling zones A, SR and BR, respectively. These figures clearly show that as the mineralization of groundwater increases in each of the three zones, there is an increase in the % contents of Cl and Na and, conversely, a decrease in the % contents of Ca, Mg, SO_4 and HCO_3. And this also indicates that the main macrocomponent ions that determine the mineralization of brackish groundwater in aquifers in Quaternary sediments are Cl^- and Na^+.

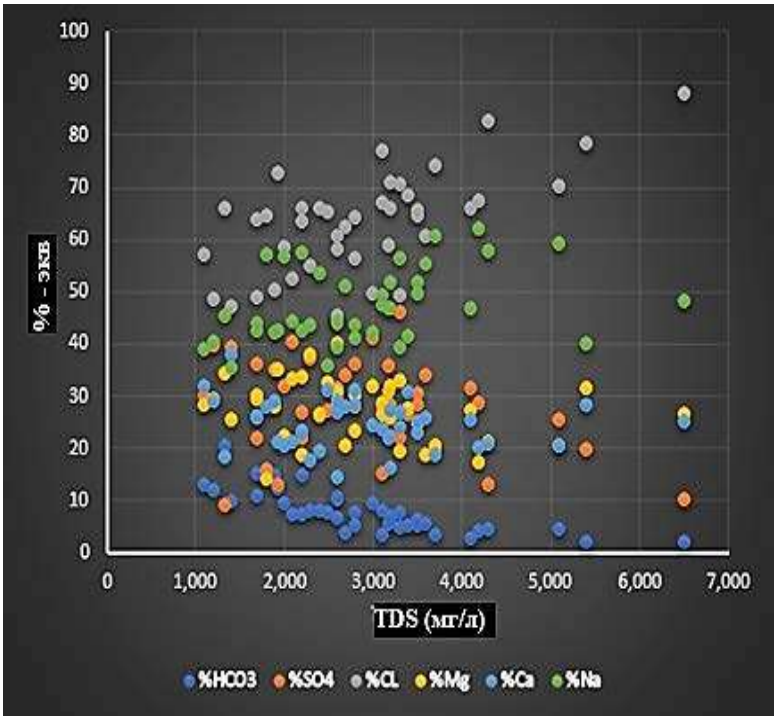

Fig. 4.6. Correlation between mineralization (TDS, mg/dm^3) and concentrations of macrocomponents (%-eq) for wells in zone_A

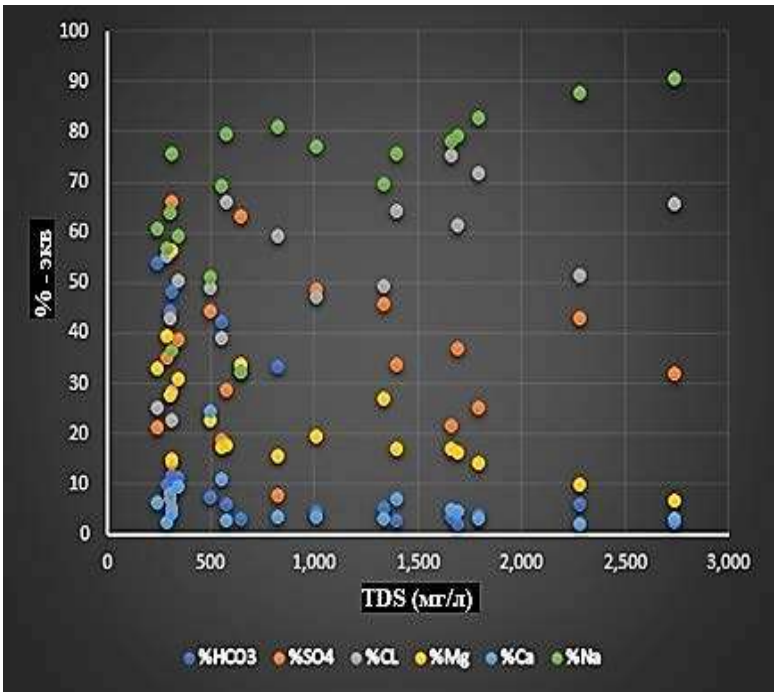

Fig. 4.7. Correlation between mineralization (TDS, mg/dm^3) and concentrations of macrocomponents (%-eq) for wells in zone_SR

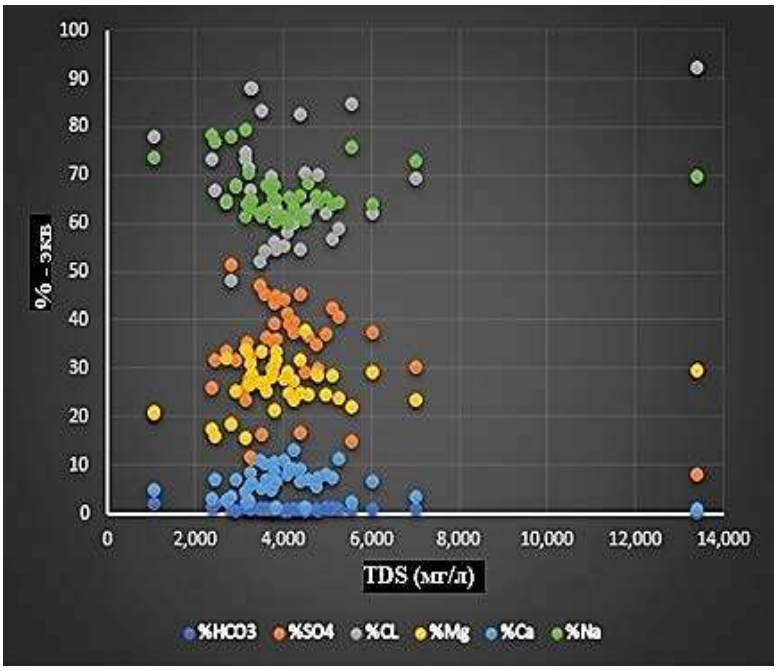

Fig. 4.8. Correlation between mineralization (TDS, mg/dm^3) and concentrations of macrocomponents (%-eq) for wells in zone_BR

Correlation dependencies between mineralization values (TDS) and pH values for the indicated zones A, SR and BR are presented in Figures 4.9, 4.10 and 4.11. As can be seen in these figures, there is no clear correlation in these coordinates. And, therefore, the formation of the acidity of the groundwater

environment in Quaternary sediments is a multifactorial process and, obviously, depends both on the amount of infiltration or other nutrition of the horizons, and on the intensity of interactions in the water-rock system in each of the individual areas.

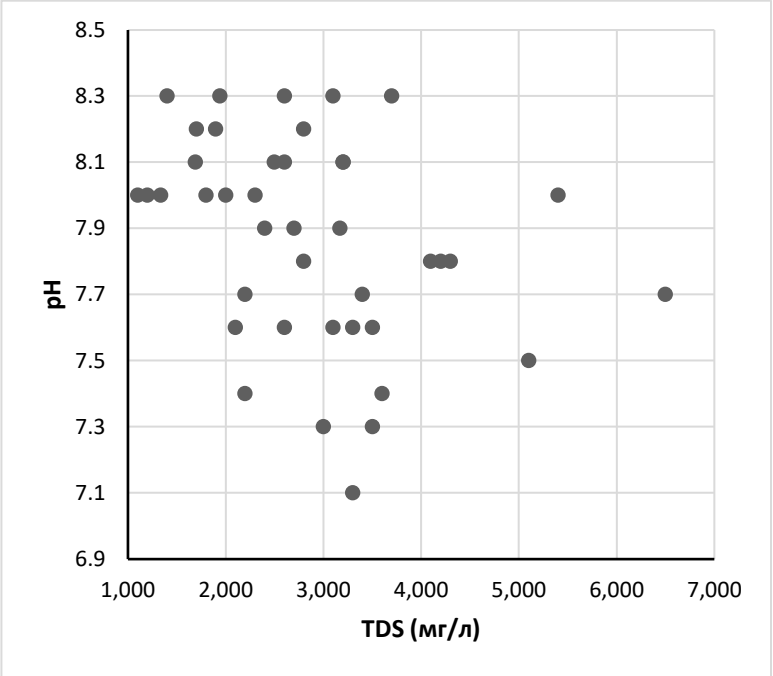

Fig. 4.9. Correlation between mineralization (TDS, mg/dm^3) and pH value for wells in zone_A

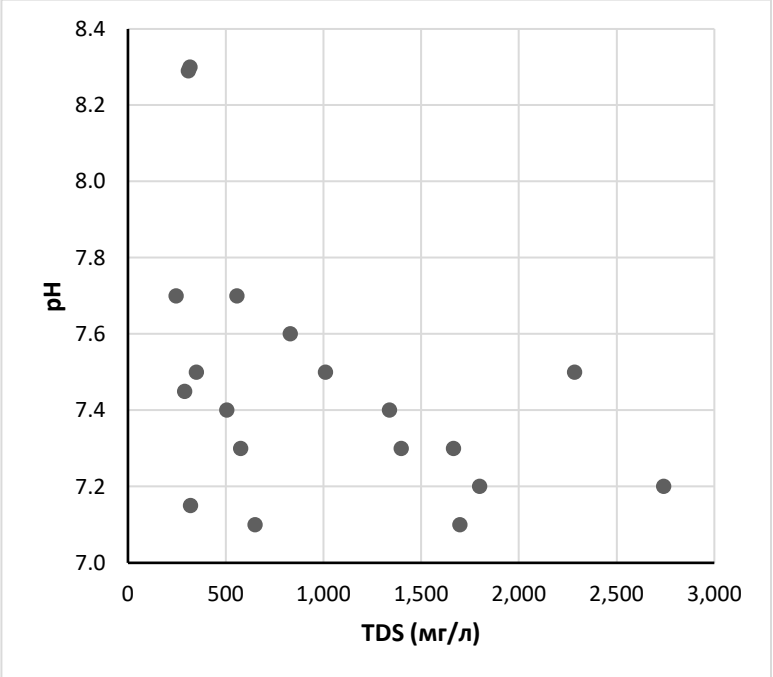

Fig. 4.10. Correlation between mineralization (TDS, mg/dm^3) and pH value for wells in zone_SR

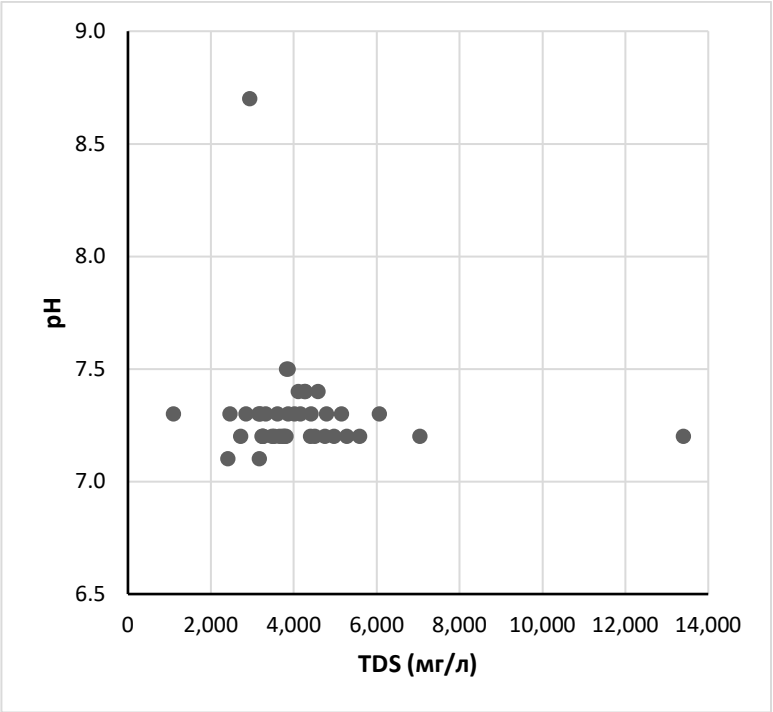

Fig. 4.11. Correlation between mineralization (TDS, mg/dm^3) and pH value for wells in zone_BR

Additionally, also for all three sampling zones A, SR and BR correlations were built between mineralization values (TDS) and various genetic hydrogeochemical coefficients, determined by the ratios of the concentrations of different macrocomponents: Requ=$(Na^+ + K^+)/(Ca^{2+} + Mg^{2+})$; Na^+/Cl^-; SO_4^{2-}/Cl^-; Ca^{2+}/SO_4^{2-}. For almost all of these coefficients for all three sampling zones, no unambiguous correlation is observed. For the most characteristic sampling points within each zone, the absolute values of metamorphization coefficients (rNa/rCl) were calculated [6] and genetic types according to V.A. Sulina [6] (Table 4.9).

Table 4.9- Values of genetic coefficients for some wells that penetrated Quaternary deposits

Item no.	Zone	Well number	Well depth, m	pH	rNa/rCl	Sulin type	TDS, mg/dm^3
1	A	5-5	300	8.00	0.88	Cl-Mg	1,800
2	A	1-64	101	7.6	0.65	Cl-Mg	2,600
3	A	1-136	60	7.5	0.84	Cl-Mg	5,100
4	SR	SR T10	103	7.7	1.50	HCO_3-Na	248
5	SR	SR T1	24	7.7	1.77	HCO_3-Na	557
6	SR	SR T8	64	7.2	1.15	SO_4-Na	2,740
7	BR	No.73		7.3	0.93	Cl-Mg	1,099
8	BR	No.45		7.5	1.10	SO_4-Na	3,827
9	BR	No.28		7.3	1.08	SO_4-Na	4,164
10	BR	No.64		7.2	1.06	SO_4-Na	7,040

In the area of Wadi El Arish (zone_A), magnesium chloride waters along the Sulin are distributed mainly with metamorphization coefficients close to sea waters, which gives reason to believe that the waters are most likely of mixed genesis - surface, underlying aquifer complexes or modern marine intrusions from the Mediterranean seas. The waters of the Bir El-Abd zone are characterized by metamorphization coefficients generally greater than 1 and the sodium sulfate type according to Sulin, which most likely indicates their infiltration origin, and increased mineralization is the result of evaporation of atmospheric precipitation in an arid climate. The waters of the Rafah and Sheikh Zuwayid zones are sodium bicarbonate according to Sulin, the metamorphization coefficients are greater than 1, which indicates their infiltration origin.

Thus, the results obtained do not provide prerequisites for an unambiguous determination of the genesis of groundwater in Quaternary deposits; all types of water are most likely of mixed genesis with the predominance of certain

processes: intra-ground evaporation, the introduction of modern marine intrusions from the Mediterranean Sea, overflow from underlying aquifers. In addition, the waters under consideration are the result of a deep transformation of source waters of one or another genesis, including processes of sedimentation-dissolution of rocks and processes of ion (cation) exchange.

For the majority of wells for which there was a full set of hydrochemical parameters, using the PHREEQC program version 3.5.0.14000 (developed by the US Geological Survey - freely available on the Internet), the physical and chemical equilibrium in the groundwater - rock-forming minerals system was calculated. As a result of these calculations, taking into account the formation of dissolved associated ions and neutral associates based on the constants of the corresponding reactions in a homogeneous aqueous medium, saturation indices (SI) were estimated, that is, the degree of saturation of a particular aqueous solution (groundwater) in relation to various rock-forming minerals.

$$SI = Lg\ (PA) / Lg\ (PR) \quad (2)$$

where PA is the product of the activities (molal concentrations) of ions dissolved in water participating in the equilibrium process of dissolution-precipitation of a particular mineral; PR - solubility product: an empirically established constant for the equilibrium state of a given mineral in an aqueous solution. Moreover, if the SI value is close to 0, then the system (aqueous solution) is close to saturation with this mineral. If the SI value > 0, then the groundwater is supersaturated with respect to the mineral, and this mineral must form as a solid phase (precipitate). If the SI value < 0, then the groundwater is undersaturated with respect to the mineral, and this mineral should dissolve.

In this study, for aquifers in Quaternary sediments, the equilibrium state in the carbonate and sulfate systems was considered, that is, saturation indices were assessed in relation to the main rock-forming carbonate and sulfate minerals: aragonite, calcite, dolomite, magnesite, gypsum and anhydrite for each of the

three tested zones A, SR and BR separately. An assessment of the equilibrium state could only be made with a complete set of analyzed hydrochemical parameters. In accordance with this, material from 40 wells was analyzed in zone_A, from 19 wells in zone_SR, and from 41 wells in zone_BR.

Figures 4.12-4.14 show the correlations between mineralization (TDS, mg/dm^3) and saturation index (SI) in relation to calcite for all three zones A, SR and BR. For the remaining carbonate minerals: aragonite, dolomite and magnesite, the picture is approximately the same.

As can be seen in these figures, the saturation index of groundwater in Quaternary sediments with respect to carbonate minerals outside Wadi El Arish is in the vast majority of cases significantly less than zero (see SR and BR zones - Figures 4.13 and 4.14). And at the same time, there is practically no dependence of saturation on the mineralization of groundwater.

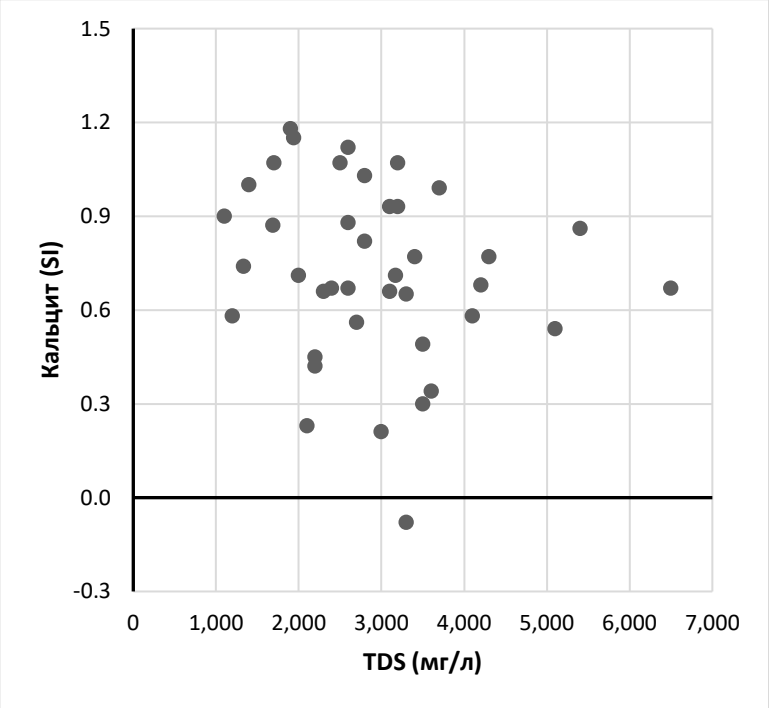

Fig. 4.12. Correlation between mineralization (TDS, mg/dm^3) and saturation index (SI) in relation to calcite for wells in zone_A

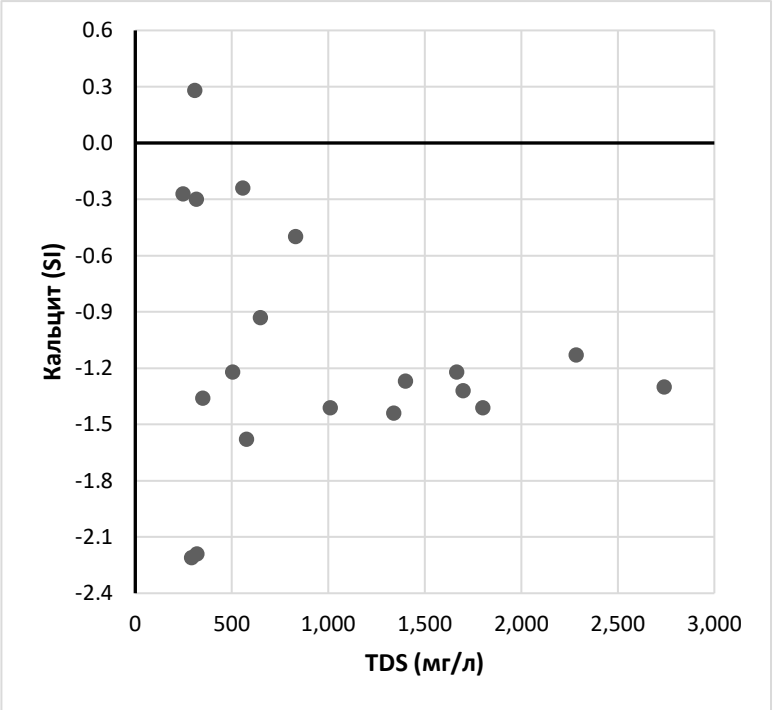

Fig. 4.13. Correlation between mineralization (TDS, mg/dm^3) and saturation index (SI) in relation to calcite for wells in zone_SR

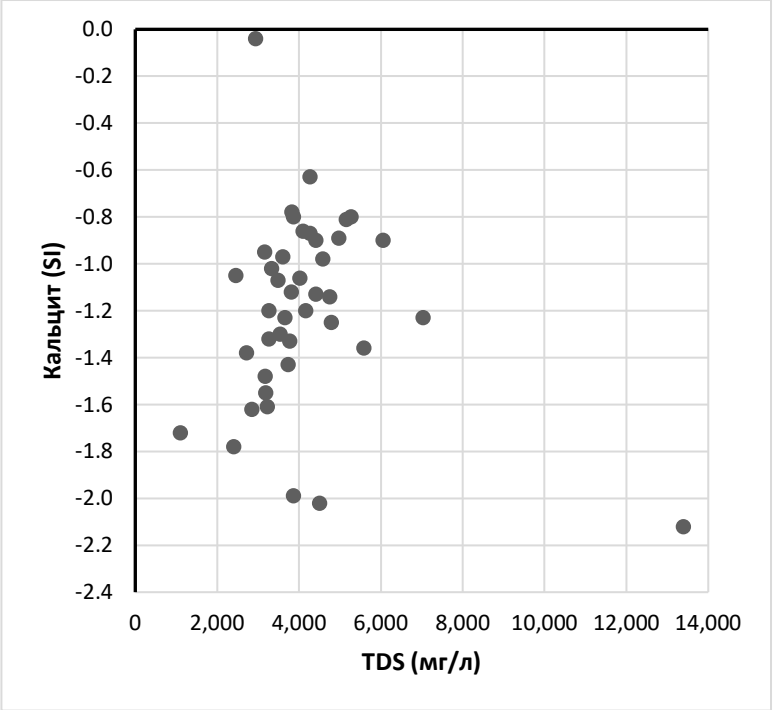

Fig. 4.14. Correlation between mineralization (TDS, mg/dm^3) and saturation index (SI) in relation to calcite for wells in zone_BR

Obviously, in the main part of the coastal (towards the Mediterranean Sea) zone of development of Quaternary sediments, represented mainly by sands and only partly by kurkar deposits, in principle, the possible interaction of

groundwater with carbonate minerals is practically not manifested in the chemical equilibrium composition. And thus, in the formation of the chemical composition of waters, the predominant influence is exerted by infiltration feeding by atmospheric precipitation and/or intrusion of sea water from the Mediterranean Sea. Moreover, even a relatively high average evaporation rate in an arid climate does not lead to the saturation of groundwater with respect to carbonate minerals. Most likely, this is explained by the fact that during short-term flood periods, the intensity of infiltration of atmospheric precipitation into aquifers significantly exceeds the intensity of evaporation of this atmospheric precipitation.

In the El-Arish area (zone_A), on the contrary, the vast majority of groundwater is supersaturated with respect to all carbonate minerals up to an SI of even 1 or more (Fig. 4.12), which should inevitably lead to secondary precipitation of these minerals in Quaternary sediments. The dependence of saturation on the mineralization of groundwater is also practically absent. It is obvious that the formation of these waters is determined, first of all, not by the infiltration of atmospheric precipitation during flood periods and not by the intrusions of salty waters from the Mediterranean Sea, but by the inversion feeding of Quaternary aquifers directly from the El-Arish wadi during periods of floods, when the water line mark in the watercourse significantly exceeds groundwater levels in adjacent areas, up to the flooding of these territories (noted above). At the same time, the chemical composition of the water flowing through the wadi during these periods is obviously formed much higher upstream - within the development of pre-Quaternary sediments. This is confirmed by both the values of metamorphization coefficients and the genetic type of water according to Sulin.

Any obvious relationship between the index of groundwater saturation in relation to carbonate minerals and the sampling depth (within about 120 meters)

is not observed either in general in the coastal strip, in the SR and BR zones, or in the area of Wadi El Arish (zone_A).

But, quite naturally, there is a direct dependence of the degree of saturation of groundwater in relation to all carbonate minerals on the pH value for all three considered zones A, SR and BR. Figures 4.15-4.17, for example, present these correlations for SI in relation to calcite. It is well known that with an increase in pH values (with a decrease in the acidity of an aqueous solution), the equilibrium between soluble carbonate associated ions and neutral associates in the series CO_2 – H_2CO_3 – HCO_3^- – CO_3^{2-} (“carbonate system”) shifts towards the formation of the latter. And this is precisely what leads to an increase in the degree of saturation of aqueous solutions in relation to all carbonate minerals.

Figures 4.18-4.20 show the correlations between mineralization (TDS, mg/l) and saturation index (SI) in relation to gypsum for all three zones A, SR and BR. For another sulfate mineral - anhydrite - the graph is similar. As can be seen in these figures, in all three zones under consideration, the saturation index of groundwater in Quaternary sediments in relation to sulfate minerals in all samples is significantly less than zero. But at the same time, in contrast to the situation with carbonate minerals, there is a certain tendency to increase the degree of saturation as the mineralization of groundwater increases, which is in agreement with the fact noted above that the content of sulfates in groundwater increases with increasing salinity (Fig. 4.3b, 4.4 b and 4.5b).

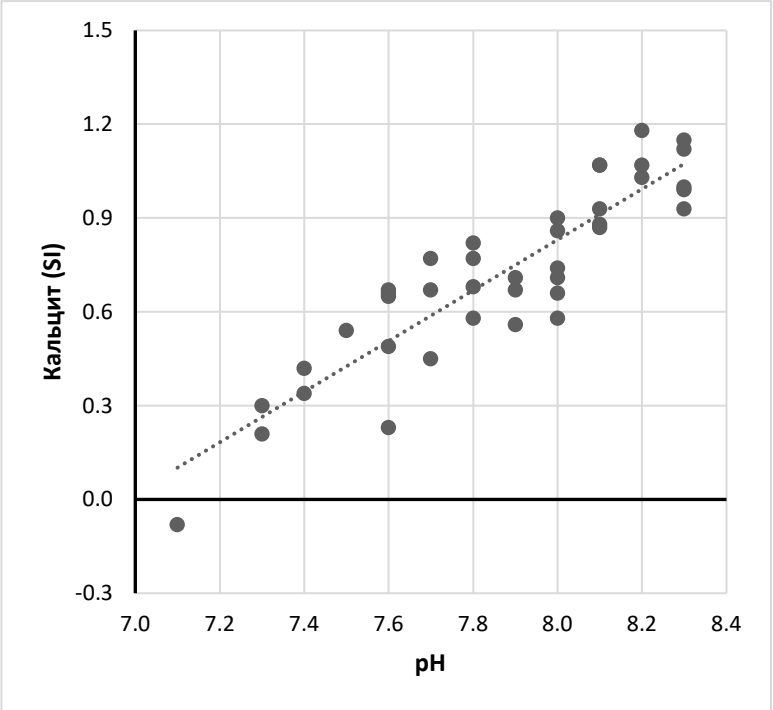

Fig. 4.15. Correlation between the pH value and the saturation index (SI) in relation to calcite for wells in zone_A

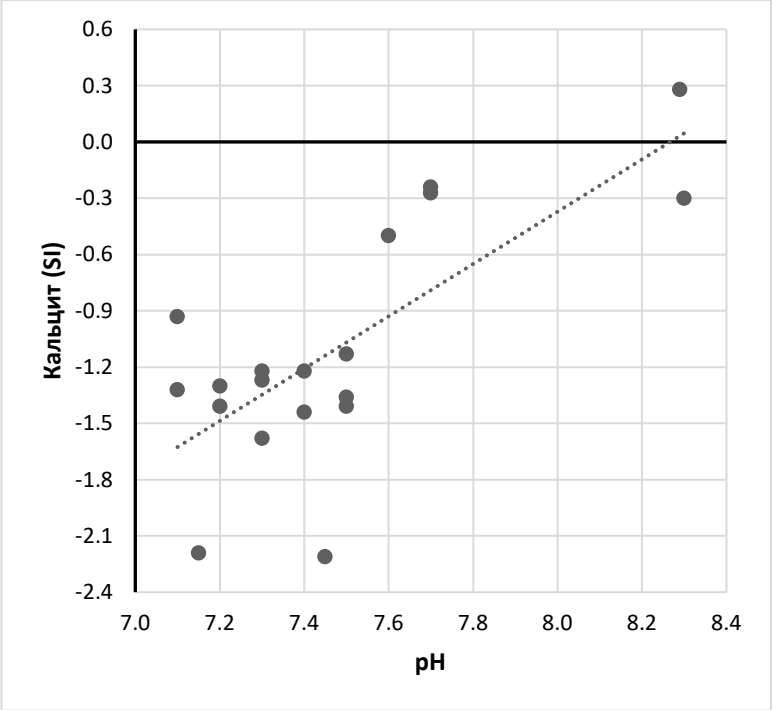

Fig. 4.16. Correlation between the pH value and the saturation index (SI) in relation to calcite for wells in zone_SR

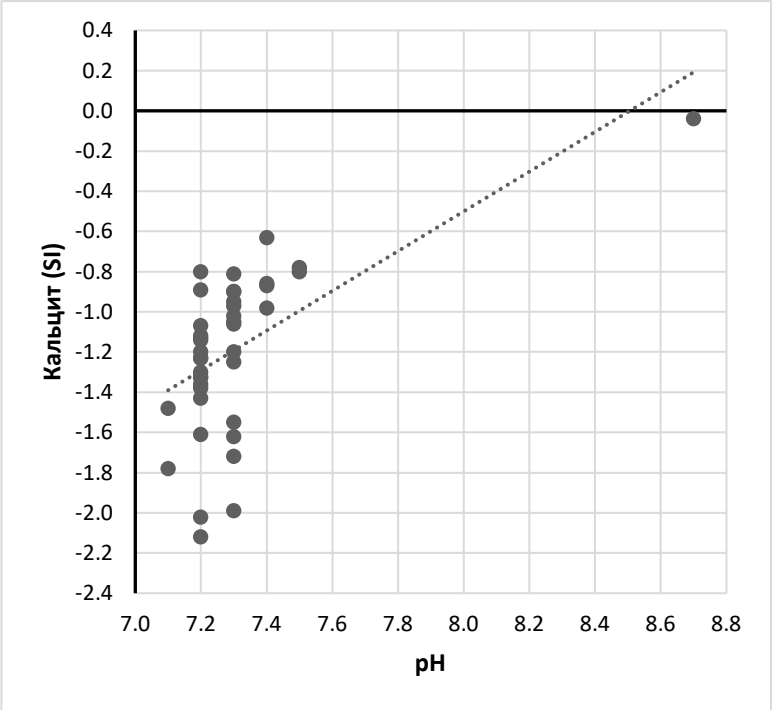

Fig. 4.17. Correlation between the pH value and the saturation index (SI) in relation to calcite for wells in zone_BR

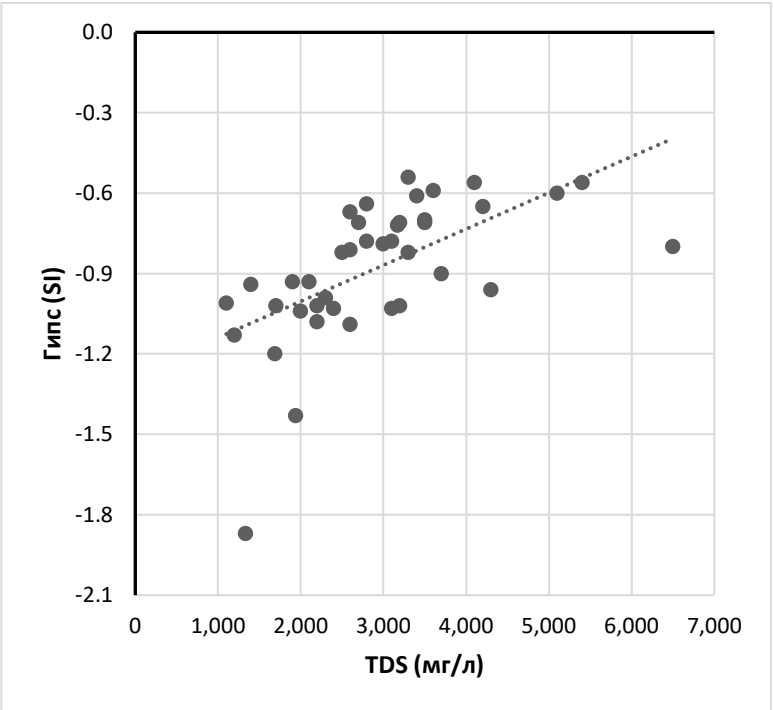

Fig. 4.18. Correlation between mineralization (TDS, mg/dm^3) and saturation index (SI) in relation to gypsum for wells in zone_A

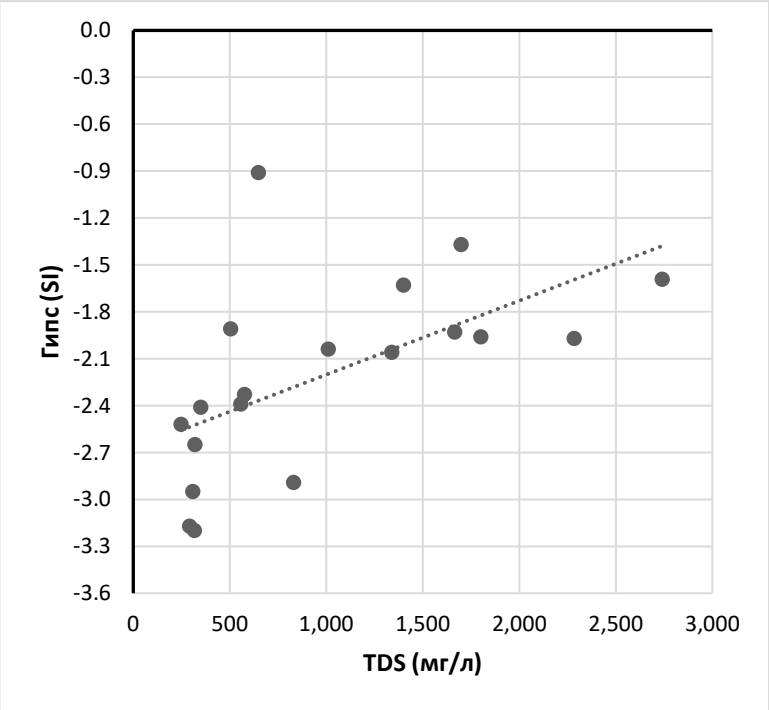

Fig. 4.19. Correlation between mineralization (TDS, mg/dm^3) and saturation index (SI) in relation to gypsum for wells in zone_SR

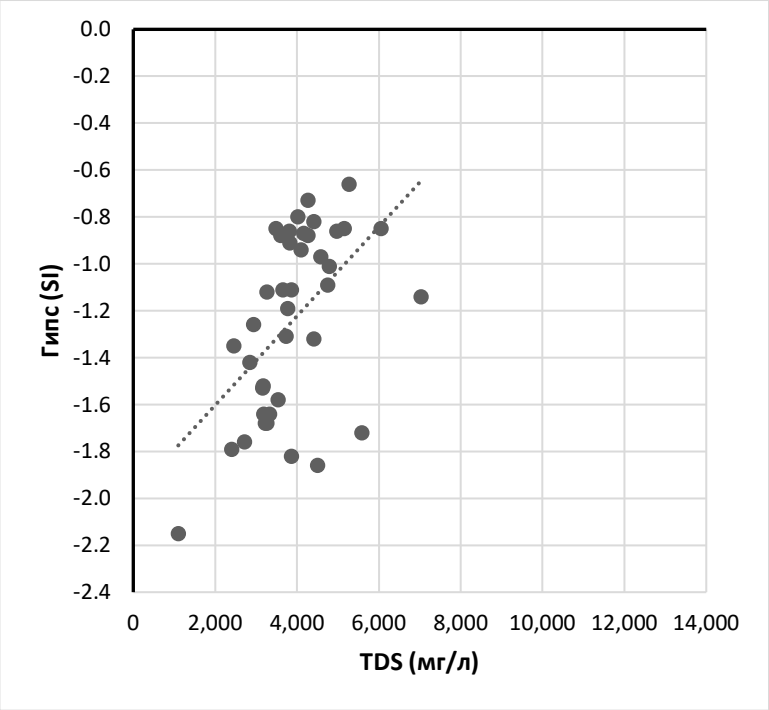

Fig. 4.20. Correlation between mineralization (TDS, mg/dm^3) and saturation index (SI) in relation to gypsum for wells in zone_BR

In Quaternary sediments, represented either by purely terrigenous sands and gravels or carbonated sediments of the Kurkar, there are no sulfate minerals in the rock-forming composition, the dissolution of which could lead to an

increase in the concentration of sulfates and, accordingly, to high values of the underground saturation index in relation to gypsum and anhydrite. Therefore, the described situation is quite natural. It should be noted that the degree of metamorphization of natural waters during the evaporation of atmospheric precipitation does not reach the level at which water becomes saturated with respect to sulfate minerals. This should also be considered natural, since, as indicated above, the degree of evaporation of atmospheric precipitation in the north of Sinai does not even reach the level of saturation in relation to much less soluble carbonate minerals.

It is likely that the source of increased concentrations of sulfates in groundwater in Quaternary sediments is either the evaporation of infiltrating atmospheric precipitation, or water developed in pre-Quaternary rocks, which enters Quaternary sediments due to subvertical flow from bottom to top or during the above-described process of outflow of water from the wadi into aquifers during flood periods.

4.2. Pre-Quaternary aquifers

The conditions for the development of aquifers in pre-Quaternary sediments are described in detail in the previous Chapter 2. Predominant development in the composition of bedrock was obtained by limestones and sandstones of different ages (mainly Paleogene, Late Cretaceous, Early Cretaceous and Jurassic).

The main problem with the use of groundwater from pre-Quaternary aquifers, as well as aquifers in the Quaternary sediments, in North Sinai is their high salinity.

The quality of groundwater, occurring even in the uppermost horizons, is quite low: its mineralization ranges from 1400-5500 mg/l. Rock formation occurred mainly in coastal continental and shelf conditions. It is assumed that the

salt water that originally entered the host rocks was diluted by infiltrating precipitation during the Pliocene and naturally continues to be diluted at the present time.

To clarify the genesis of waters of pre-Quaternary sediments, metamorphization coefficients (rNa/rCl) were determined in some water analyzes [6] and water type according to V.A. Sulin [6] (Table 4.10).

Table 4.10- Values of genetic coefficients for some wells that penetrated pre-Quaternary deposits

Item no.	Name	Well depth, m	aquifer	pH	rNa/rCl	according to Sulin	TDS, mg/dm^3
1	Sudr El-Heitan	1025	K_1	7.00	1.19	SO_4-Na	1,246
2	Sheira-1	804	K_1	7.50	0.91	Cl-Mg	1,575
3	J No.16 El Bruk-1	799	K_1	7.00	1.05	HCO_3-Na	2,318
4	J No.19 Arif El Naga	900	K_1	7.10	1.05	HCO_3-Na	3,008
5	No. 5 mine	215	K_1	7.00	0.62	Cl-Mg	4,700
6	Nekhl-1	1,020	K_1	8.10	1.00	Cl-Mg	1,344
7	Nekhl-2	1.095	K_1	8.00	0.82	Cl-Mg	1,280
8	Nekhl-5	1,150	K_1	7.90	0.79	Cl-Mg	1,408
9	Hassana-2	1.241	K_1	8.00	0.65	Cl-Ca	2,989
10	Hassana-4	1.045	K_1	7.40	0.61	Cl-Ca	3,078
11	Arif El Naga	902	K_1	7.70	0.70	Cl-Mg	356
12	El-Halal deep	800	K_1	7.80	0.79	Cl-Mg	2,739
13	El-Halal medium	170	K_1	7.70	0.58	Cl-Mg	3,180
14	No.53B EL-Arish-18	180	K_2+P_g	7.00	1.99	HCO_3-Na	950
15	No.54A EL-Fath-4	249	K_2+P_g	7.00	1.67	SO_4-Na	2,200
16	No.53A EL-Arish-18	158	K_2+P_g	7.00	1.09	SO_4-Na	3,810
17	No.63A Libni-1	300	K_2+P_g	7.30	0.78	Cl-Ca	4,500
18	No.50 El-ArishNo.15	295	K_2+P_g	7.30	0.97	Cl-Mg	7,000

In aquifers of the Upper Cretaceous-Paleogene, mineralization values fluctuate in a slightly larger range: 1100-7000 mg/dm^3. Many authors assume that salt water was initially buried in rocks during the period of sedimentation (sedimentogenic waters), and then it was diluted or replaced by relatively fresh

waters of infiltration genesis. This origin of the underground waters of the Upper Cretaceous limestones is confirmed by the presence, and at some sampling points, of hydrocarbonate-sodium and sulfate-sodium waters according to Sulin with metamorphization coefficients greater than 1. The most intensive replacement processes probably occurred in those areas where cracks associated with faults are well developed.

The mineralization of groundwater in the Lower Cretaceous (Nubian) sandstone aquifer varies approximately in the same range as in the Upper Cretaceous groundwater: 1200-5700 mg/l. Some researchers assume that in cases where Lower Cretaceous deposits do not lie first from the surface, the initially sedimentogenic waters contained in them are in a “stagnant” state (a zone of very difficult water exchange). Although the absence of recorded mineralizations above 6000 mg/l allows us to unequivocally state that infiltration dilution by atmospheric precipitation also takes place under these conditions. This is confirmed by isotope data [8], according to which the waters of some sampling points of Nubian sandstones are slightly “depleted” of deuterium and O-18 isotopes, that is, in cold geological epochs there was a dilution of the original water, while according to Sulin’s classification, most waters are magnesium chloride and calcium chloride, and the metamorphization coefficients close to those for sea waters or lower.

The mineralization of water samples from wells tapping a fairly locally developed aquifer in Jurassic limestones, which has no practical significance, again fluctuates within approximately the same limits: from 950 to 4700 mg/l.

It has been noted that in wells equipped with Upper Cretaceous limestones and Nubian sandstones and characterized by the highest flow rates, mineralization is lower, but increases rapidly after pumping begins. This fact indicates that in local zones of development of bedrock with increased permeability (increased fracturing within and near faults), that is, in the most “washed” by precipitation,

mineralization is reduced. But in the undisturbed rock blocks adjacent to these local zones, the intensity of infiltration dilution is much lower.

As samples for statistical assessments, two main aquifers were identified, developed almost throughout the entire territory of Northern Sinai: 1) Upper Cretaceous-Paleogene limestones - from 63 wells and 2) Lower Cretaceous (Nubian) sandstones - from 61 wells. Statistical assessments of the distribution of the values indicated at the beginning of this chapter of the hydrochemical indicators of groundwater were also made using the SPSS program; Various correlations were constructed. As in the case of groundwater in Quaternary deposits, the following variables ("sample" values) were considered: mineralization (TDS) in the dimension mg/dm3 (ppm), concentrations of all the above dissolved macrocomponents in mg-eq/dm3 (epm) and in %-eq (% epm), pH value in units. pH, as well as the depth of the tested wells (ds) in meters.

Table 4.11 presents the results of statistical processing for both of the above samples based on the mineralization of groundwater in the dimension mg/dm3; Table 4.12 shows the results of statistical processing for the pH value in units. pH; and in tables 4.13-4.18 - the results of statistical processing of the same samples for the concentrations of macrocomponents HCO_3^-, SO_4^{2-}, Cl^-, Mg^{2+}, Ca^{2+} and Na^+ in %-eq, respectively. In addition to the two indicated samples for limestones and sandstones, all these tables also present characteristics for the general population for all groundwater in pre-Quaternary deposits ("Pre-Quaternary as a whole").

Table 4.11- Statistical parameters for the distribution of salinity values (TDS, mg/dm^3) in various zones of development of aquifers in pre-Quaternary sediments

Parameters	All	Limestone K_2+P_g	Sandstone K_1
N	124	63	61
Mean	3353	3658	3037
median	3255	4000	2973
std. Dev.	1367	1335	1338
minimum	892	892	1200
maximum	7000	7000	5768

Table 4.12- Statistical parameters for the distribution of pH values (pH units) in various zones of development of aquifers in pre-Quaternary sediments

Parameter	All	Limestone K_2+P_g	Sandstone K_1
N	92	33	55
Mean	7.2	7.2	7.1
median	7.1	7.1	7.1
std. Dev.	0.4	0.4	0.4
minimum	6.1	6.2	6.1
maximum	8.2	7.9	8.2

Table 4.13- Statistical parameters for the distribution of HCO_3 concentration (%-eq) in different zones of aquifer development in pre-Quaternary sediments

Parameter	All	Limestone K_2+P_g	Sandstone K_1
N	21	15	6
Mean	9	8	10.5
median	5.5	5.5	9
std. Dev.	9	9	9
minimum	0	0.94	0
maximum	29.3	29.3	24.5

Table 4.14- Statistical parameters for the distribution of SO_4 concentration (%-eq) in different zones of aquifer development in pre-Quaternary sediments

Parameter	All	Limestone K_2+P_g	Sandstone K_1
N	21	15	6
Mean	24	24	24
median	22	21.5	28.5
std. Dev.	15.5	15	17.5
minimum	1.3	1.3	2.0
maximum	56.6	56.6	43.1

Table 4.15- Statistical parameters for the distribution of Cl concentration (%-eq) in various zones of aquifer development in pre-Quaternary sediments

Parameter	All	Limestone K_2+P_g	Sandstone K_1
N	21	15	6
Mean	67.5	68	65.5
median	69	75	64
std. Dev.	17	18	15.5
minimum	37.2	37.2	46.6
maximum	93.2	93.2	85.6

Table 4.16- Statistical parameters for the distribution of Mg concentration (%-eq) in various zones of aquifer development in pre-Quaternary sediments

Parameter	All	Limestone K_2+P_g	Sandstone K_1
N	21	15	6
Mean	16.5	14.5	23.5
median	15.5	14	27.5
std. Dev.	9.5	8.5	10
minimum	0.4	0.4	10.6
maximum	32.3	31.5	32.3

Table 4.17- Statistical parameters for the distribution of Ca concentration (%-eq) in different zones of aquifer development in pre-Quaternary sediments

Parameter	All	Limestone K_2+P_g	Sandstone K_1
N	21	15	6
Mean	19.5	21.5	16
median	19.5	19.5	16.5
std. Dev.	11.5	12	11.5
minimum	0.78	0.78	3.9
maximum	45.7	45.7	27.7

Table 4.18- Statistical parameters for the distribution of Na concentration (%-eq) in various zones of aquifer development in pre-Quaternary sediments

Parameter	All	Limestone K_2+P_g	Sandstone K_1
N	21	15	6
Mean	63	64	60.5
median	60.5	60.5	55.0
std. Dev.	15.5	13.5	21
minimum	39.8	39.8	41.1
maximum	97.4	97.4	85.5

There are no fundamental differences in the statistical parameters of the distribution of various indicators of the chemical composition of groundwater for the indicated two samples: limestones and sandstones. Both limestones and sandstones contain both practically fresh (about 1 g/dm^3) and brackish, near-neutral or slightly alkaline groundwater, on average sulfate-chloride, predominantly sodium (or calcium-sodium). That is, in terms of chemical composition, groundwater in pre-Quaternary deposits differs little from groundwater developed in Quaternary deposits.

Noteworthy is the fact that even the minimum mineralization values in both limestones and sandstones are at least 0.9 g/dm^3. This clearly indicates that even in those points where the genetic formation of groundwater in pre-Quaternary sediments is due only to the infiltration of atmospheric precipitation (and these

are, apparently, points with metamorphization coefficients greater than 1 and hydrocarbon and sulfate sodium waters according to Sulin), these sediments have undergone physicochemical transformation due to evaporation either on the surface of the earth, or within the aeration zone or in the upper watered layers (perch).

Figures 4.21–4.22 present graphs of the correlation relationships between groundwater salinity (TDS) and the depth of the tested well (ds) for both samples of limestone and sandstone, respectively. As can be seen in these figures, an unambiguous dependence in these coordinates, as for groundwater in Quaternary deposits, is not observed in any of the samples.

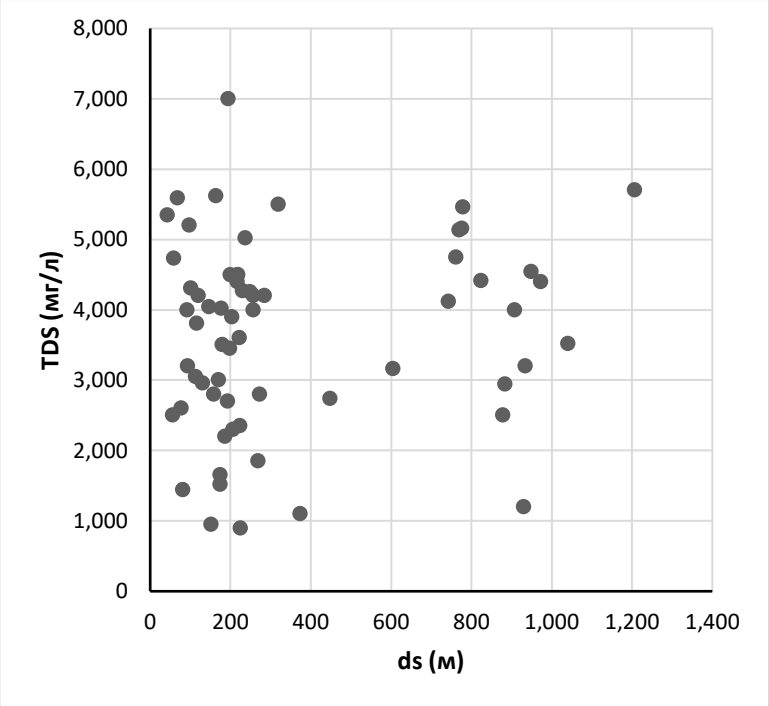

Fig. 4.21. Correlation between mineralization (TDS, mg/dm^3) and well depth (ds, m) for wells drilled on limestone

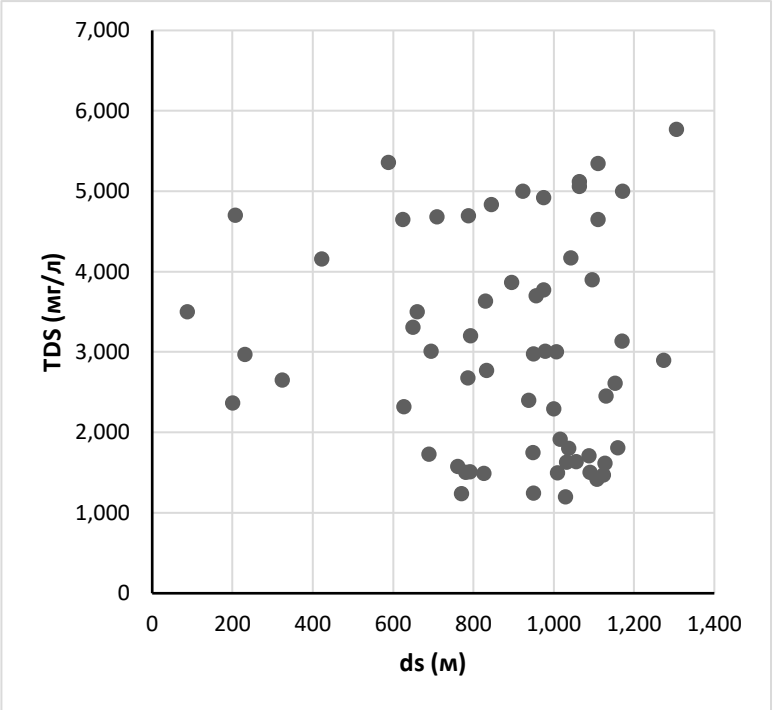

Fig. 4.22. Correlation between mineralization (TDS, mg/dm^3) and well depth (ds, m) for wells drilled on sandstones

For both samples of limestone and sandstone, correlations were also constructed between mineralization (TDS) and the concentrations of all macrocomponents in mg-eq/dm^3. Figures 4.23 a, b, c for limestones and 4.24 a, b, c for sandstones show the corresponding graphs for Cl, SO_4 and Na, where, as for groundwater in Quaternary deposits, a direct linear relationship between mineralization and Cl concentrations is clearly evident and Na and, less clearly, SO4 contents. For the remaining macrocomponents - HCO_3, Mg and Ca, no significant relationship is observed in either of the two aquifers.

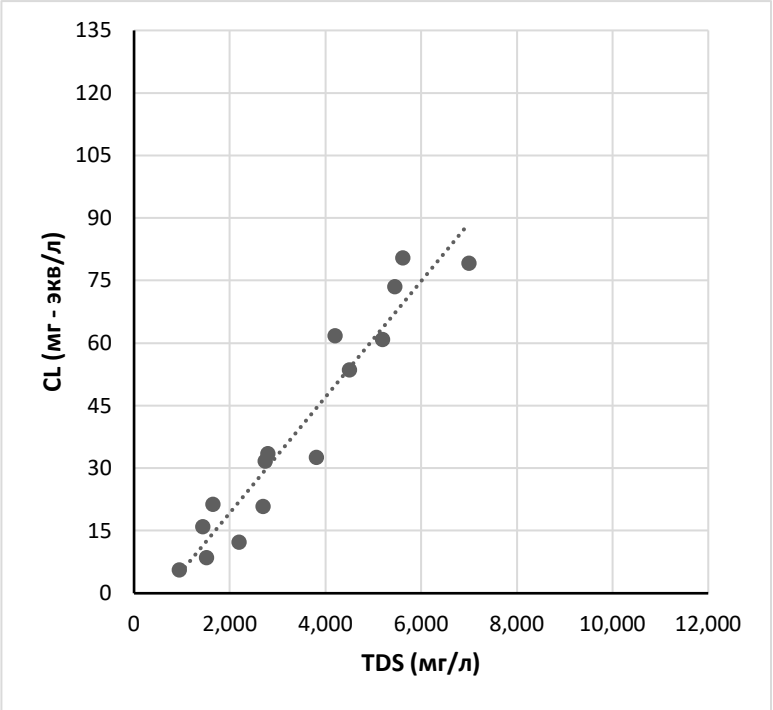

Fig. 4.23, a. Correlation between mineralization (TDS, mg/dm^3) and Cl^- concentration (mg-eq/dm^3) for wells equipped with limestone

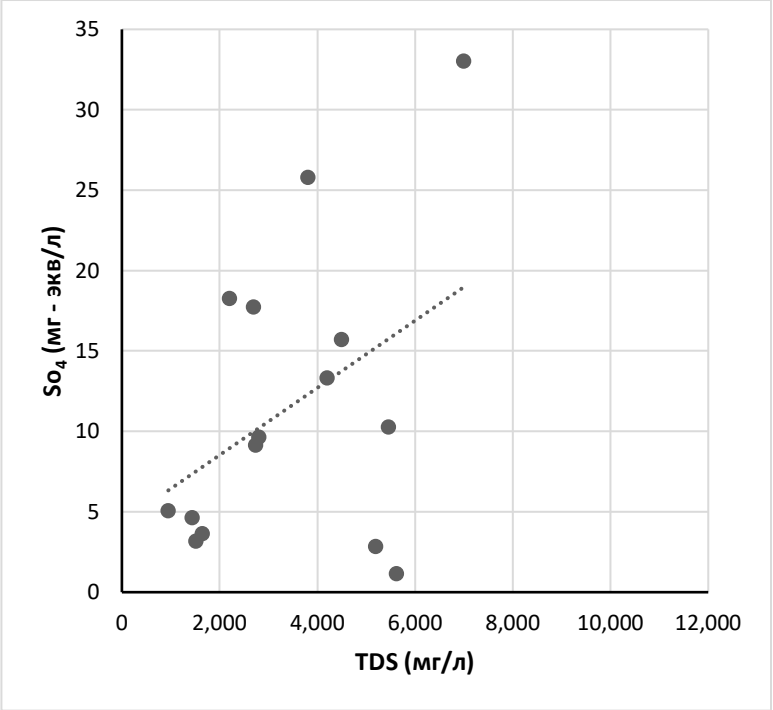

Fig. 4.23, b. Correlation between mineralization (TDS, mg/dm^3) and SO_4^{2-} concentration (mg-eq/dm^3) for wells equipped with limestone

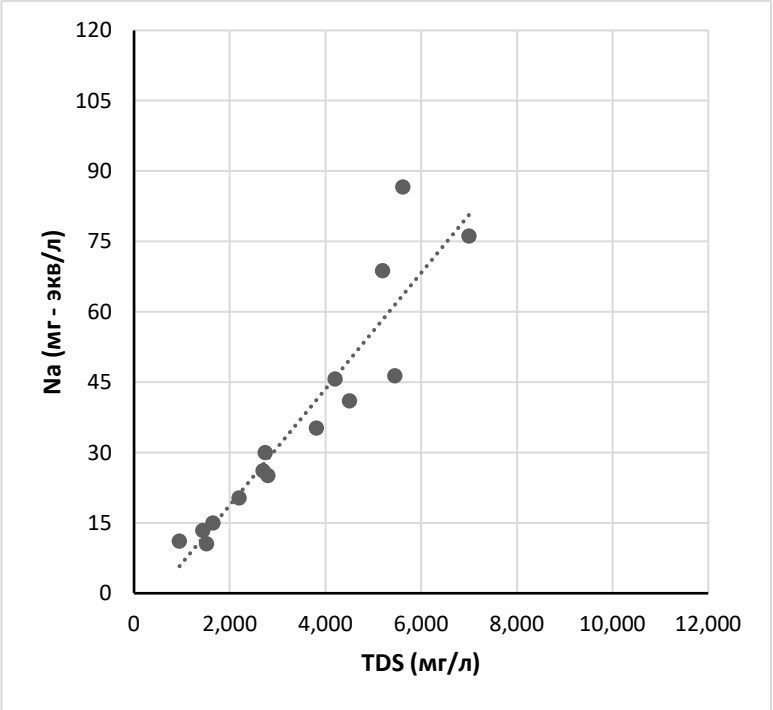

Fig. 4.23, c. Correlation between mineralization (TDS, mg/dm^3) and Na^+ concentration (mg-eq/dm^3) for wells equipped with limestone

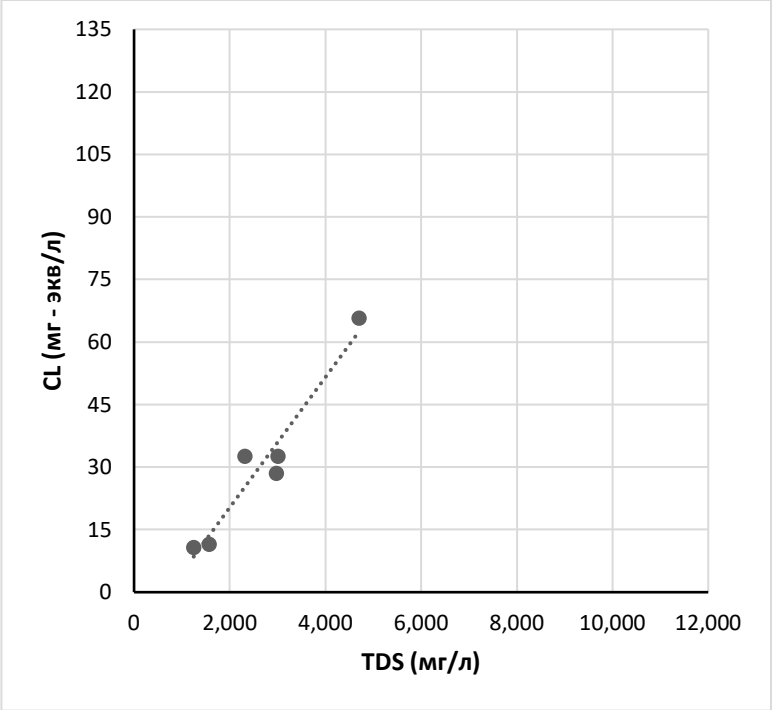

Fig. 4.24, a. Correlation between mineralization (TDS, mg/dm^3) and Cl^- concentration (mg-eq/dm^3) for wells equipped for sandstones

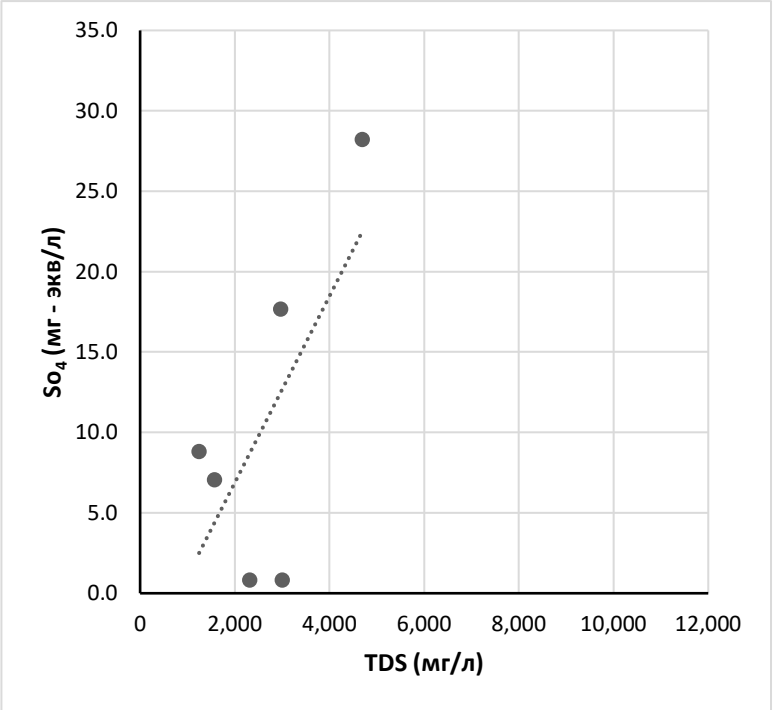

Fig. 4.24, b. Correlation between mineralization (TDS, mg/dm^3) and SO_4^{2-} concentration (mg-eq/dm^3) for wells equipped for sandstones

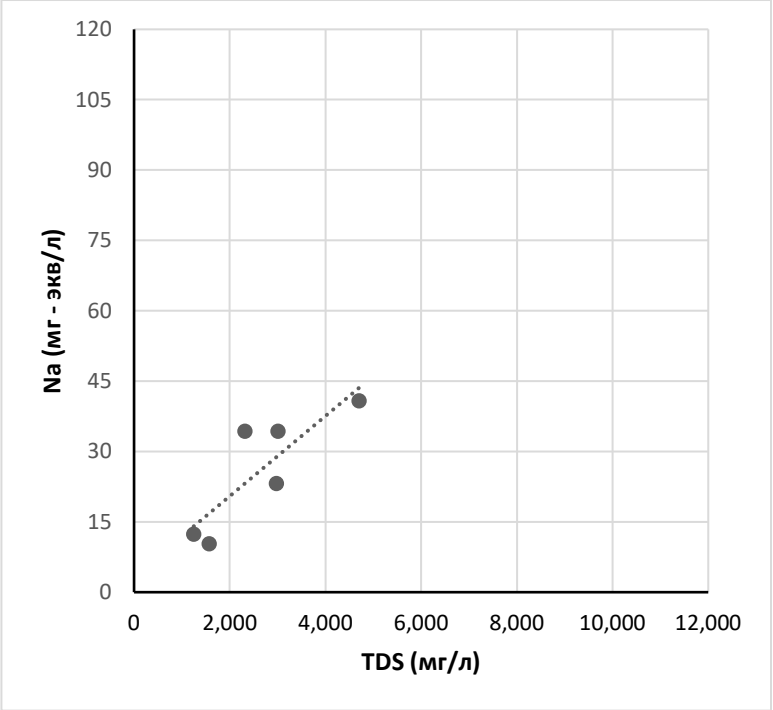

Fig. 4.24, c. Correlation between mineralization (TDS, mg/dm^3) and Na^+ concentration (mg-eq/dm^3) for wells equipped for sandstones

Thus, as in groundwater of Quaternary deposits, in accordance with the ratios of %-equivalent concentrations of macrocomponents (see Tables 4.13-4.18), the main anion determining the mineralization of groundwater in aquifers

of pre-Quaternary deposits - both in limestones and sandstones (at least in brackish waters with a mineralization significantly greater than 1 g/dm3) is Cl^- (with the additional influence of SO_4^{2-}), and the main cation is Na^+.

Figures 4.25 and 4.26 present the correlations between mineralization (TDS) and % equivalent concentrations of all macrocomponents for Upper Cretaceous limestones and Nubian sandstones, respectively. These figures show that in each of the two samples there is a tendency for the percentages of Cl and Na to increase in groundwater, and vice versa, for the percentages of Ca, Mg, SO_4 and HCO^3 to decrease as mineralization increases. That is, once again we can say that the main macrocomponents that determine the mineralization of brackish groundwater in aquifers of pre-Quaternary sediments are Cl^- and Na^+ (as in Quaternary sediments).

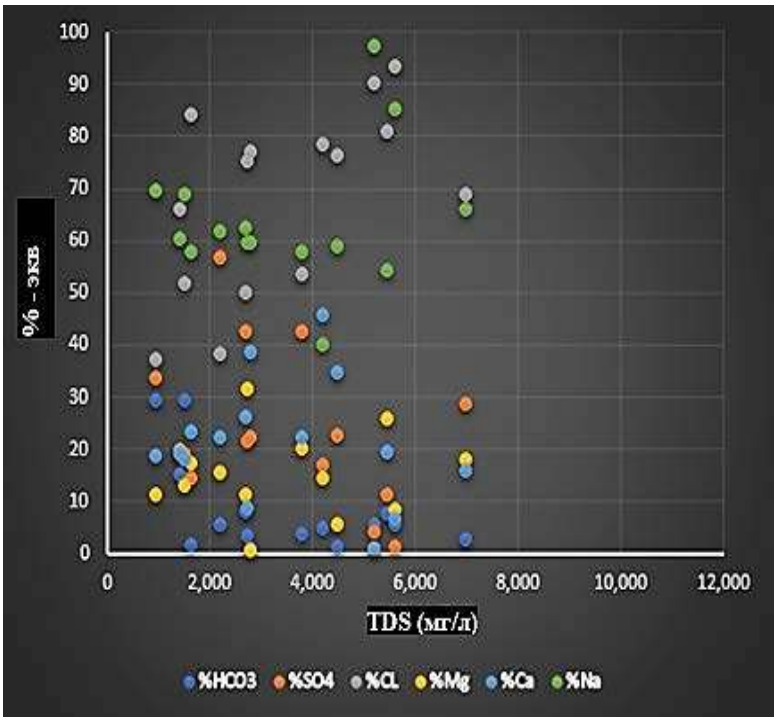

Fig. 4.25. Correlation between mineralization (TDS, mg/dm^3) and concentrations of macrocomponents (in %-eq) for wells in limestone

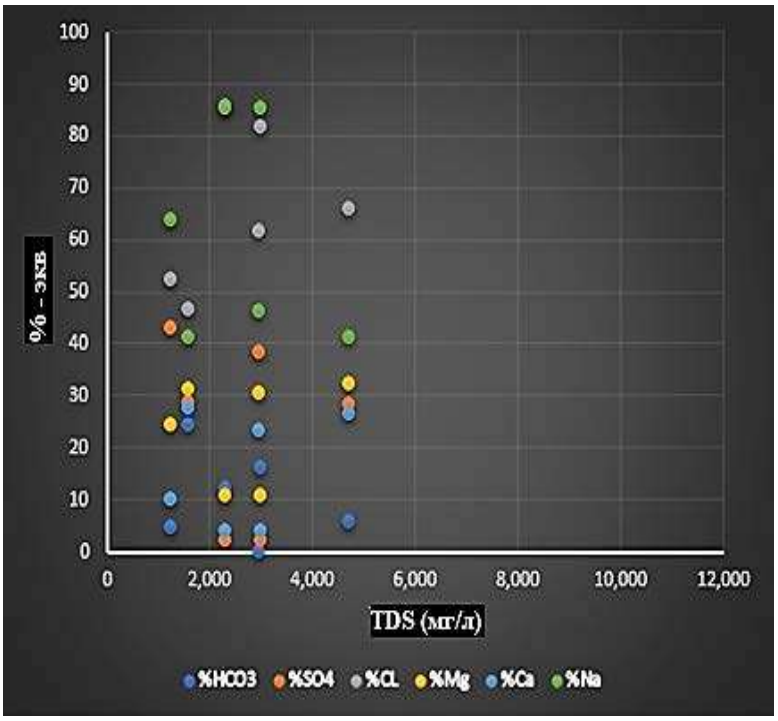

Fig. 4.26. Correlation between mineralization (TDS, mg/dm^3) and concentrations of macrocomponents (in %-eq) for wells in sandstones

Correlation relationships between mineralization values (TDS) and pH values for limestones and sandstones are presented in Figures 4.27 and 4.28. As for waters of Quaternary sediments, no unambiguous correlation is observed in these coordinates for pre-Quaternary aquifers. That is, the formation of acidity in the groundwater environment is a multifactorial process and depends both on the intensity of infiltration or other feeding of horizons, and on the specifics of interactions in the water-rock system at each of the individual sampling sites.

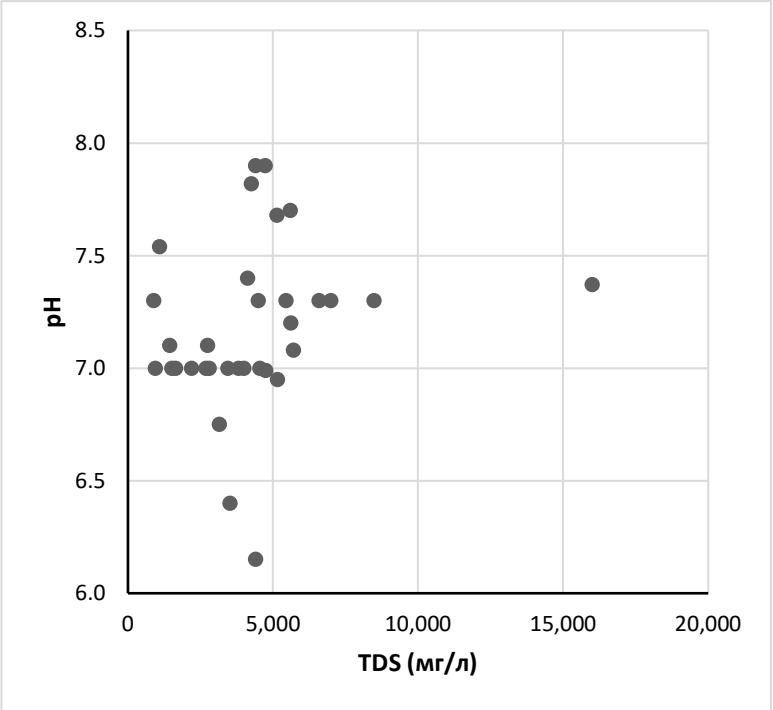

Fig. 4.27. Correlation between mineralization (TDS, mg/dm^3) and pH value for wells equipped with limestone

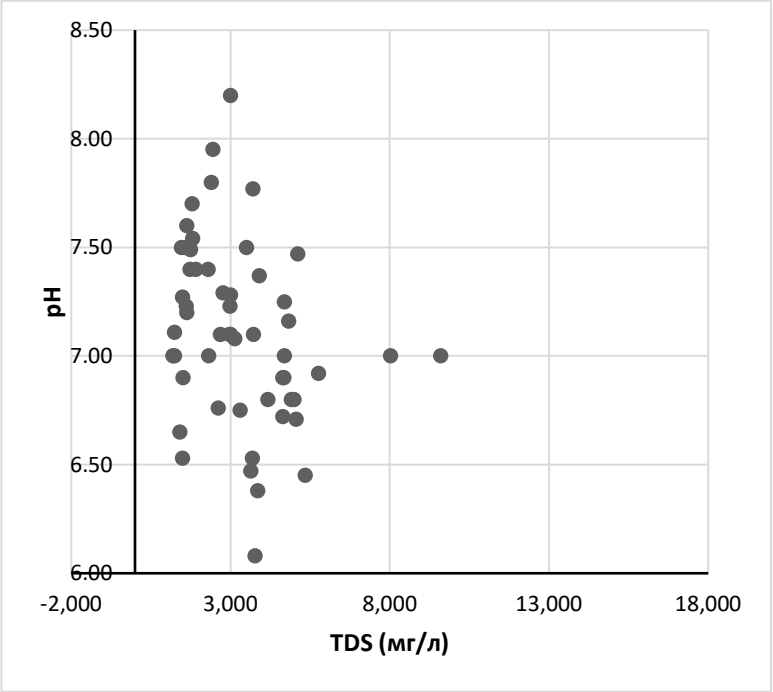

Fig. 4.28. Correlation between mineralization (TDS, mg/dm^3) and pH value for wells equipped with sandstone

Graphs of the dependences of various genetic coefficients on mineralization were also constructed according to the concentration ratios: R_{equ} (see section 3.1); Na^+/Cl^-; SO_4^{2-}/Cl^-; Ca^{2+}/SO_4^{2-}, for which no clear correlation is

observed. As for Quaternary sediments, the values of genetic coefficients vary widely, making it impossible to unambiguously determine the genesis of waters: either sedimentogenic, or due to the evaporation of atmospheric precipitation. The waters of the Upper Cretaceous limestones are characterized mainly by metamorphization coefficients greater than 1 and the sulfate or hydrocarbon-sodium type according to Sulin, which indicates a close connection with infiltration waters. But at some points magnesium chloride and even calcium waters according to Sulin were recorded. Most likely, these are waters of mixed genesis with a significant proportion of sedimentary waters. The waters of the Nubian sandstones are also characterized by a variety of genetic types, but the magnesium chloride type according to Sulin predominates, that is, the proportion of infiltration waters is low, except for points located in the recharge area.

Thus, the waters of pre-Quaternary deposits are the result of the transformation of source waters of different genesis in combination with the processes of precipitation and dissolution of rock-forming minerals, cation exchange and mutual flow.

For wells equipped for pre-Quaternary sediments, for which there was a full set of analyzed hydrochemical indicators, using the PHREEQC program, a calculation of the physico-chemical equilibrium in the groundwater – rock-forming minerals system was carried out. As a result of these calculations, as for groundwater in Quaternary deposits, both for limestones and sandstones, saturation indices (SI) were estimated in relation to the main rock-forming carbonate and sulfate minerals: aragonite, calcite, dolomite, magnesite, gypsum and anhydrite. In total, calculations were performed for limestones (LS) for 13 wells, and for sandstones (SS) - for 9 wells.

Figures 4.29-4.30 show the correlations between mineralization (TDS, mg/l) and saturation index (SI) in relation to calcite for limestones and sandstones, respectively. For the remaining carbonate minerals: aragonite, dolomite and

magnesite, the picture is approximately the same. The saturation index of groundwater in all pre-Quaternary sediments with respect to carbonate minerals varies in a very wide range from -2.5 ÷ -1.5 to +0.5 ÷ +0.8. That is, groundwater in pre-Quaternary deposits can be either undersaturated or oversaturated with respect to carbonate minerals (regardless of the mineral composition of the water-bearing rocks), which obviously indicates the presence of different conditions for the formation of water in different sampled areas. Most likely, the modern chemical composition of these groundwaters is due to the mixing in various proportions of the original saline sedimentogenic water and infiltrative waters, taking into account their evaporation in an arid climate, as well as flows from one aquifer to another and the processes of ion (cation) exchange.

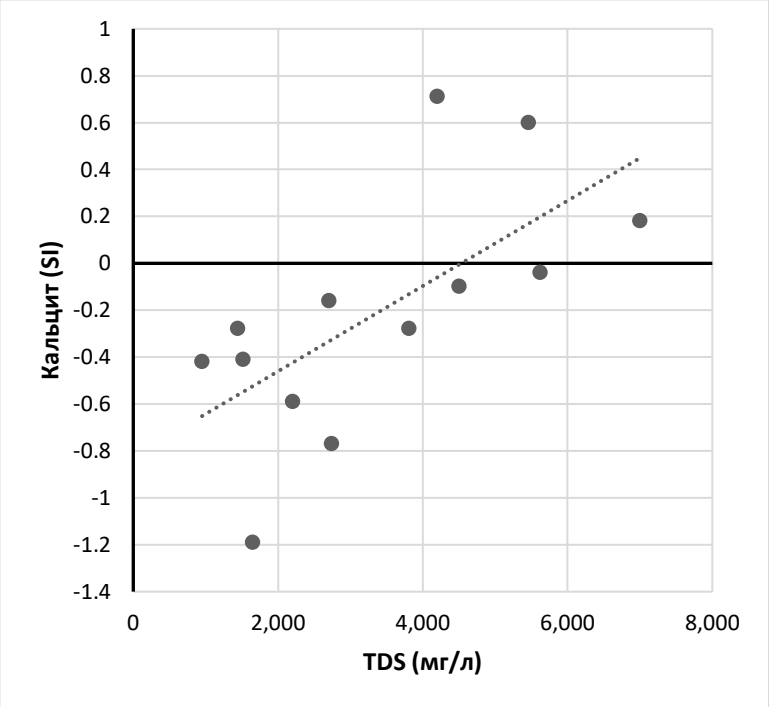

Fig. 4.29. Correlation between mineralization (TDS, mg/dm^3) and saturation index (SI) in relation to calcite for wells drilled on limestone

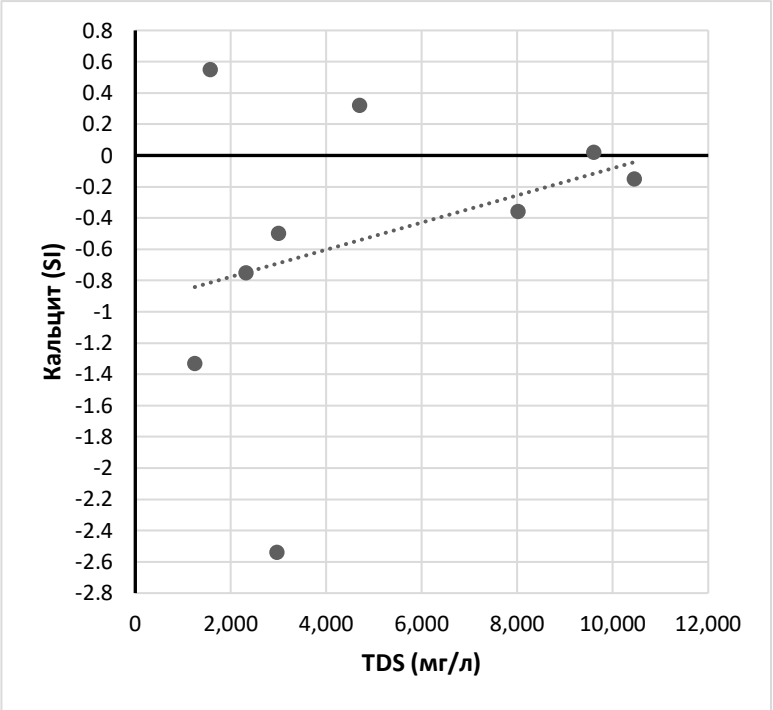

Fig. 4.30. Correlation between mineralization (TDS, mg/dm^3) and saturation index (SI) in relation to calcite for wells drilled on sandstone

At the same time, at least in groundwater developed in limestones, there is a tendency to increase the saturation index (SI) in relation to carbonate minerals as mineralization increases. Due to the fact that infiltrating atmospheric precipitation is undersaturated with respect to carbonate minerals, the lower the degree of dilution of the initial sedimentogenic water by them, the greater the degree of saturation of mixed groundwater with respect to carbonates.

Any obvious relationship between the index of groundwater saturation with respect to carbonate minerals and the sampling depth in pre-Quaternary sediments is not observed in either sandstone or limestone.

In this case, naturally, there is a direct dependence (at least for limestones) of the degree of saturation of groundwater in relation to all carbonate minerals on the pH value. Figures 4.31-4.32, for example, present these correlations for SI in relation to calcite. As already indicated when considering waters of pre-Quaternary sediments, with increasing pH values, the equilibrium between soluble carbonate associated ions and neutral associates in the series $CO_2 – H_2CO_3$

– HCO_3^- – CO_3^{2-} (“carbonate system”) shifts towards the formation of the latter, which leads to an increase degree of saturation of aqueous solutions in relation to all carbonate minerals.

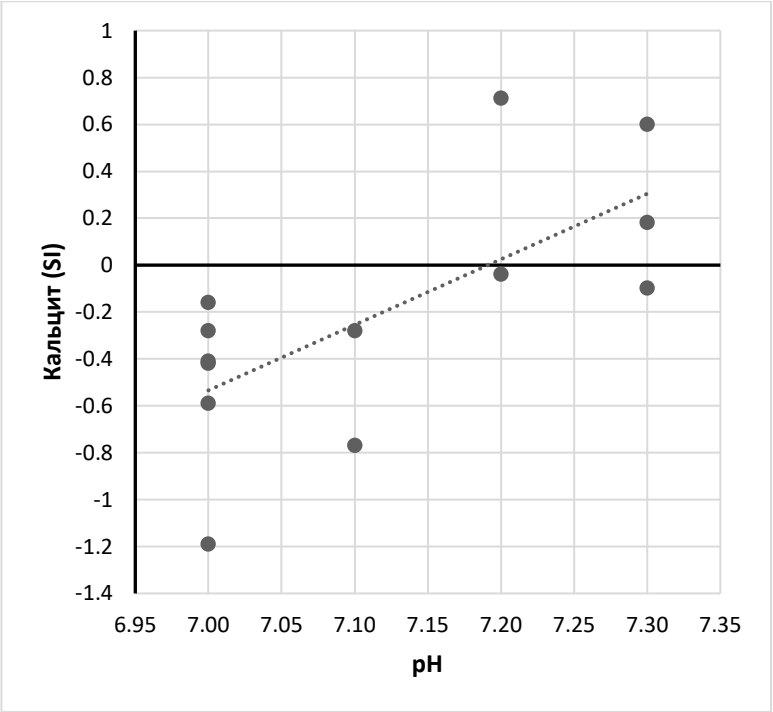

Fig. 4.31. Correlation between the pH value and the saturation index (SI) in relation to calcite for wells equipped with limestone

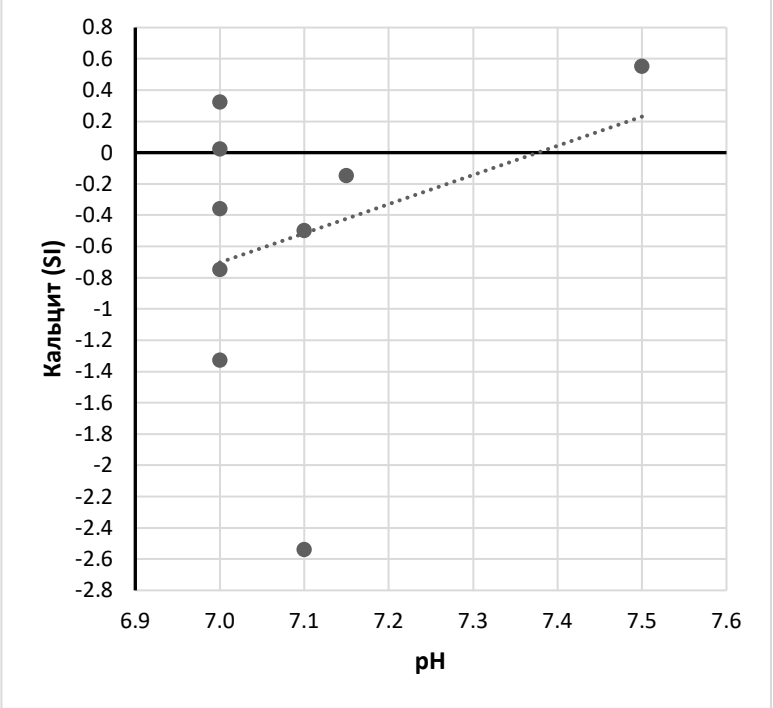

Fig. 4.32. Correlation between the pH value and the saturation index (SI) in relation to calcite for wells equipped with sandstone

Figures 4.33-4.34 present the correlations between mineralization (TDS, mg/l) and saturation index (SI) in relation to gypsum for Upper Cretaceous limestones and Nubian sandstones, respectively. For another sulfate mineral anhydrite, the graphs are similar. As can be seen in these figures, in both limestones and sandstones, the saturation index of groundwater with respect to sulfate minerals is significantly less than zero in all samples. And at the same time, as for groundwater of Quaternary deposits, there is a certain tendency to increase the degree of saturation as the mineralization of groundwater increases, which is in agreement with the above-mentioned tendency to increase the content of sulfates in waters of pre-Quaternary deposits with increasing salinity (Fig. 4.23b and 4.24b).

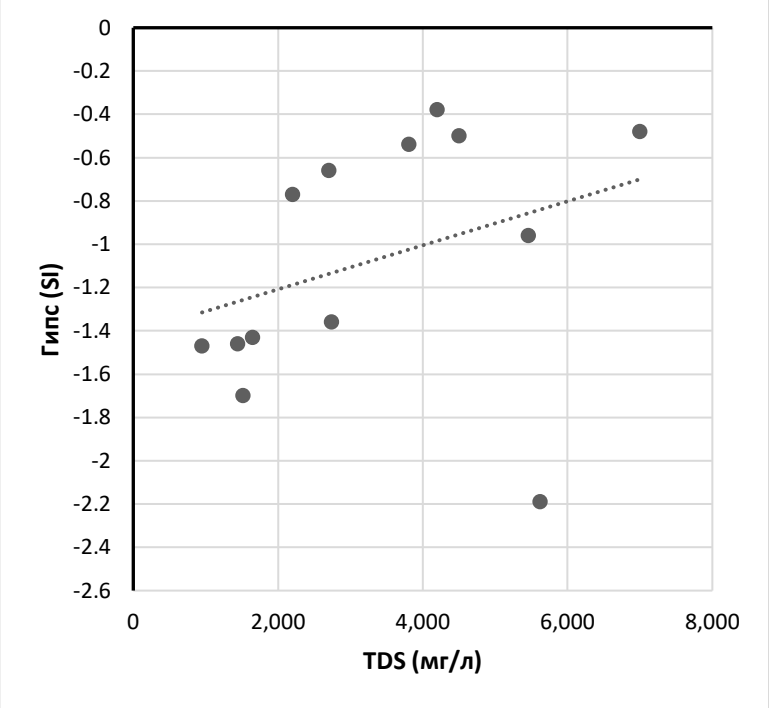

Fig. 4.33. Correlation between mineralization (TDS, mg/dm^3) and saturation index (SI) in relation to gypsum for wells drilled on limestone

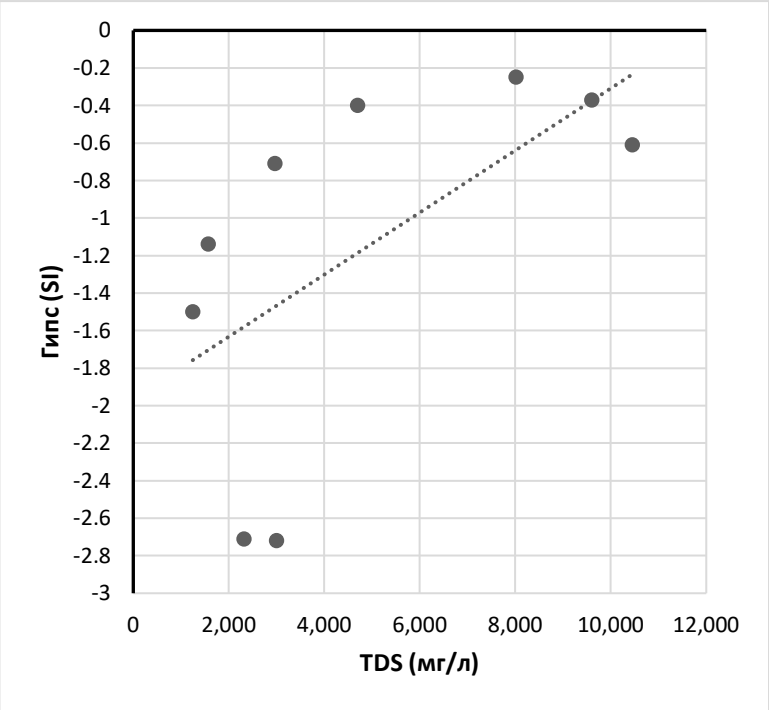

Fig. 4.34. Correlation between mineralization (TDS, mg/dm^3) and saturation index (SI) in relation to gypsum for wells drilled on sandstone

In pre-Quaternary sediments, represented mainly by sandstones and limestones, lenses or inclusions of sulfate minerals are very rarely found, the dissolution of which could lead to an increase in the concentration of sulfates and, accordingly, to high values of the underground saturation index in relation to gypsum and anhydrite. Therefore, low SI values in relation to gypsum and anhydrite are quite natural. It should be noted that the degree of metamorphization of natural waters during the evaporation of atmospheric precipitation does not reach the level at which water becomes saturated with respect to sulfate minerals. It should also be considered natural that, according to the results of studying the chemical composition of groundwater in pre-Quaternary sediments, the degree of evaporation of atmospheric precipitation in North Sinai often does not even reach the level of saturation in relation to much less soluble carbonate minerals.

It is likely that the source of increased concentrations of sulfates in groundwater in pre-Quaternary sediments is water that was either in local zones in direct contact with gypsum or anhydrite, or was initially infiltrated, but with a

relatively high degree of evaporation, as indirectly indicated by a positive correlation of sulfate concentrations and mineralization.

4.3. Zoning of the territory of North Sinai based on groundwater mineralization

Salinity (TDS), as the sum of all substances dissolved in water, is a general indicator of the quality of natural waters from the point of view of their use for drinking, agricultural and cultural water supply. Therefore, identifying areas with acceptable groundwater salinity values is very important, especially in arid regions where groundwater is the only source of water used by local residents, including in North Sinai.

There are several classifications (gradations) of natural waters based on mineralization. For example, the USGS classification uses the following categories:

- Fresh water: less than 1000 mg/dm^3
- Brackish water: 1000 to 10000 mg/dm^3
- Salt water: 10,000 to 35,000 mg/dm^3(mineralization of ocean water)
- Hypersaline: more than 35000 mg/dm^3

Most other classifications fall roughly within these ranges. In Russian terminology, instead of the name “hypersalin”, the name “brine” is usually used.

According to most regulatory documents (WHO, EU, Russia, etc.) applied to assessing the quality of drinking water, these waters must be fresh with a mineralization of less than 1,000 mg/dm^3. It should be noted that under favorable conditions, drinking water usually has a mineralization below 500 mg/dm^3, however, fresh water with higher TDS values is also suitable for drinking, but with some deterioration in organoleptic properties.

The zoning of the territory of North Sinai by mineralization carried out in this work was based on the results of hydrochemical testing of 206 wells equipped

for both Quaternary and pre-Quaternary aquifers [31; 34; 71; 72; 73; 101; and etc.].

In accordance with the range of changes in groundwater mineralization described above in the territory of North Sinai, during the zoning under consideration, a more detailed (compared to the above) categorization was adopted, which is presented in Table 4.19.

Table 4.19- Categorization of mineralization (TDS) of groundwater in North Sinai

No.	category	color	mineralization, mg/dm^3	Name
1	A	●	<1000	fresh
2	B	●	1000 – 3000	slightly salty
3	C	●	3000 – 6000	medium salty
4	D	●	> 6000	highly brackish and salty

Zoning was carried out in a point format: color gradation for each tested well. The results of such zoning are presented in Figure 4.35.

Analysis of the results of zoning of groundwater in North Sinai presented in Figure 4.35 allows us to draw the following conclusions:

Fresh waters (category A), obviously formed due to the supply of infiltrating atmospheric precipitation with a low degree of evaporation, are developed only in Quaternary sediments and only in the areas of El-Arish, Rafah and Sheikh Zuwayid (zones A and SR).

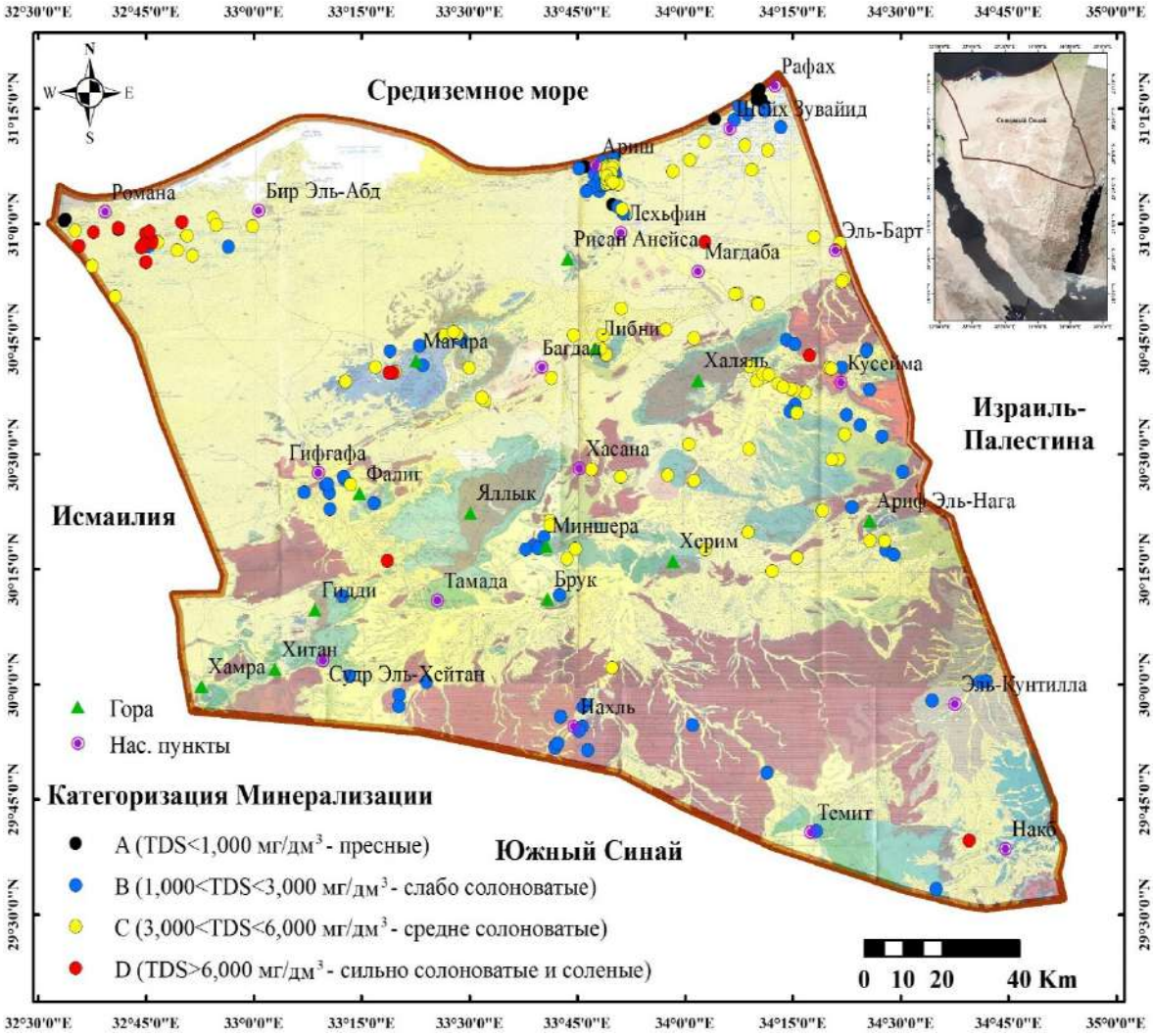

Fig. 4.35. Zoning map of the territory of northern Sinai based on groundwater mineralization

Slightly brackish waters (category B) are found in almost all rocks. In pre-Quaternary deposits, their development zones gravitate towards the peripheral areas of the territory of North Sinai. Moderately brackish waters (category C) are also developed in almost all rocks. In pre-Quaternary deposits, their development zones gravitate towards the central part of the territory of northern Sinai. Most likely, the formation of these waters is also due to the infiltration of atmospheric precipitation, but with a significantly higher degree of metamorphization due to their evaporation in an arid climate. It is also obvious that in the coastal areas of the Mediterranean Sea in Quaternary sediments, such waters are partially formed due to marine intrusions.

Highly brackish and saline waters (category D) in Quaternary sediments are found in large quantities in the Bir El-Abd area (zone_BR); in the eastern regions of El-Arish, Rafah and Sheikh Zuwayid (zones A and SR), such waters were not recorded at all in Quaternary sediments. It is assumed that the occurrence of category D groundwater in the Bir El-Abd area is mainly due to intrusions of seawater from the Mediterranean Sea. In pre-Quaternary sediments of various ages, category D groundwater is observed only in a few wells.

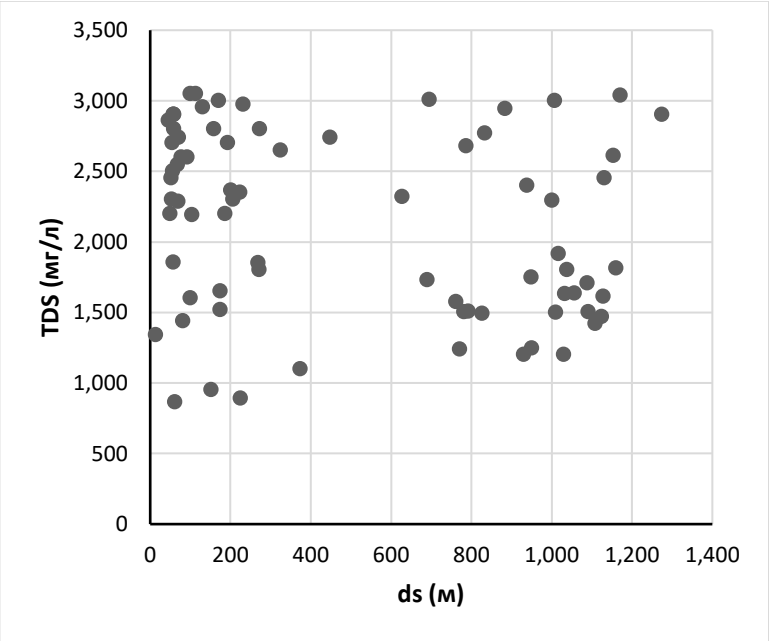

Fig. 4.36. Correlation between mineralization (TDS, mg/dm^3) and well depth (ds, m) for mineralization category B (slightly brackish waters)

These are probably initially sedimentary waters with slight dilution by infiltrating atmospheric precipitation. Indicative in this case is the distribution of groundwater mineralization by depth. If within categories B and C (weak and moderately brackish waters) there is practically no correlation between mineralization and sampling depth (Fig. 4.36, 4.37), then for category D (highly brackish and saline waters) a direct correlation is obvious (Fig. 4.38).

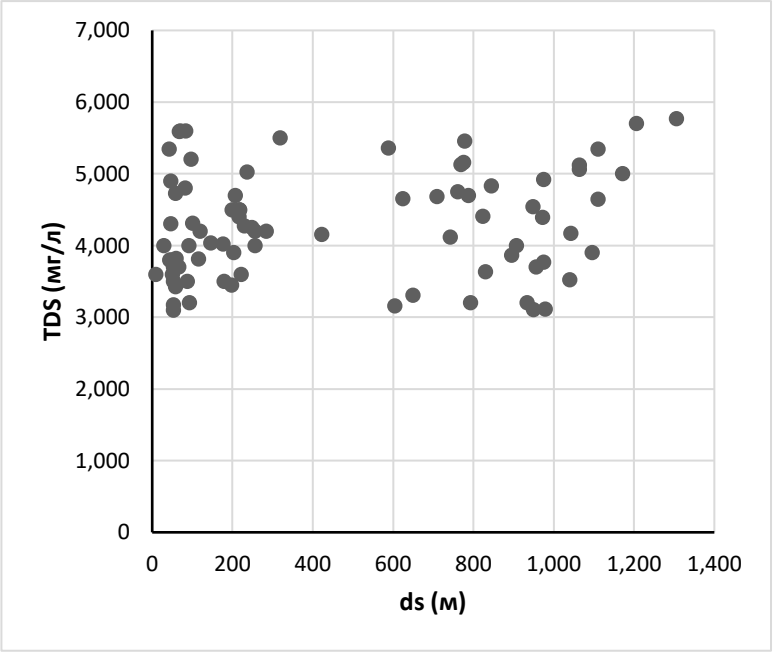

Fig. 4.37. Correlation between mineralization (TDS, mg/dm^3) and well depth (ds, m) for salinity category C (medium brackish waters)

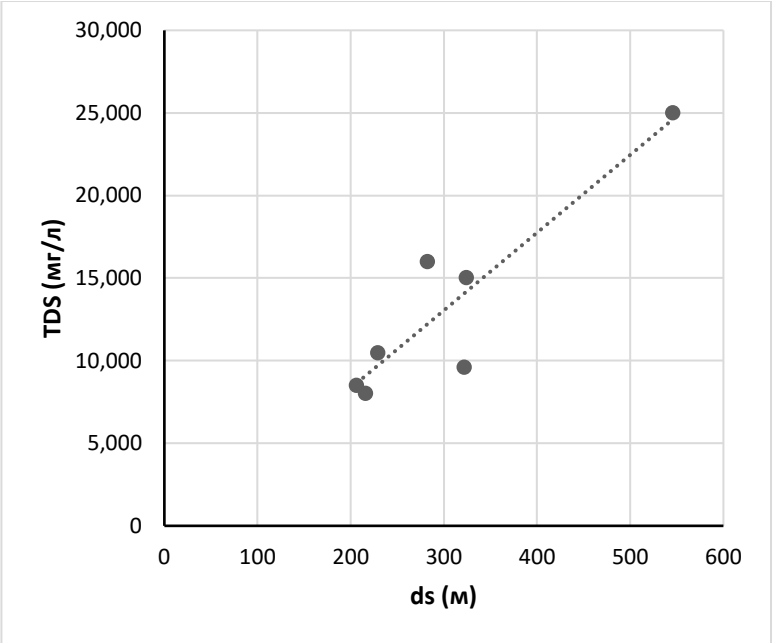

Fig. 4.38. Correlation between mineralization (TDS, mg/dm^3) and well depth (ds, m) for salinity category D (highly brackish and salty waters)

CHAPTER 5. STRUCTURE OF FILTRATION FLOW OF GROUNDWATER IN NORTH SINAI

The characteristics of the structure of groundwater filtration flow for North Sinai presented below are compiled from the totality of the results of all studies previously conducted in this area related to the construction of hydro- and piezoisohypsum maps and the identification of the main directions of filtration flows in various local areas, including in recent years [10; 11; 18; 19; 22; 35; 44; 57; 58; 65; 69; 75; 78; 79; 82; 84; 92; 93; 94; 102; 106; and etc.].

As mentioned above, the basis of the factual base of the research was information on hydrogeological wells contained in the summary report “North Sinai Groundwater Resources Study in the Arab Republic of Egypt” [60], and additionally provided by the Water Research Institute (WRRI) under the Ministry of Irrigation and Water Resources of the Arab Republic of Egypt [7]. As part of this Chapter 4, information on groundwater levels in all existing hydrogeological wells in the North Sinai region has been updated. The result of this systematization was a corresponding database, which collectively included materials from 250 wells [31; 34; 71; 72; 73; 101; and etc.].

As in previous chapters, the groundwater level regime is presented separately: for the Quaternary, Upper Cretaceous-Paleogene and Lower Cretaceous aquifers. In accordance with this division, hydroisohypsum maps (maps of groundwater level distribution in hydrogeological wells) were compiled within North Sinai. The main purpose of constructing these maps is to trace the main directions of natural filtration of groundwater - streamlines perpendicular to the equipotential lines of hydroisohypses (lines of equal pressure of groundwater). In addition, the influence of intensive groundwater pumping on the modern change in the structure of the natural flow of groundwater in the main aquifers is shown at certain points.

5.1. Quaternary aquifer

As already indicated in previous chapters, the distribution of aquifers of significant thickness in Quaternary sediments is limited only to the coastal plain along the Mediterranean Sea - water-saturated, relatively thick Quaternary sediments stretch along the coastal plain in a strip 10 - 15 km wide from the mouth of Wadi El Arish to the Rafah area (Fig. 3.1).

In general, for aquifers of Quaternary sediments for constructing hydroisohypsum maps, the author had data on the position of the static groundwater level (SWL) in 45 wells, of which 33 wells in the Wadi El-Arish area (zone_A) and 12 wells in the Rafah areas and Sheikh Zuwayid (zone_SR).

Using SPSS, statistical estimates were made for the distribution of measured water level elevations in hydrogeological wells (SWL). For Quaternary deposits, various data samples were considered depending on the sampling areas: 1) a general set for all Quaternary deposits (“Quater as a whole”); 2) in the valley of Wadi El Arish (“zone_A”) and 3) in the areas of Sheikh Zuwayid and Rafah (zone_SR). The results of calculating statistical parameters are given in Table 5.1.

Table 5.1- Statistical parameters of the distribution of marks of measured water levels in hydrogeological wells (SWL) in Quaternary deposits for different zones, m-asl

parameter	All	Zone_A	Zone_SR
N	45	33	12
average	1.05	0.30	3.10
median	1.20	0.90	2.60
std. Dev.	2.50	2.10	2.20
minimum	-8.40	-8.40	0.90
maximum	8.10	3.10	8.10

As can be seen from Table 5.1, static groundwater levels in Quaternary sediments within the coastal valley fluctuate in a very narrow range from +8.10 to –8.40 m-asl. (In zone_A from +3.10 to –8.40 m-asl; in zone_SR from +8.10 to

+0.90 m-asl), and negative values are clearly associated with operational wells pumping out groundwater.

It is obvious that in the area of wadi El-Arish, in addition to the main direction of groundwater flow towards the general drain - the Mediterranean Sea, there are also local changes in this flow, due to two factors: 1) the drainage influence of the wadi itself, at least during the driest part of the year and 2) the drainage effect from operational water intake wells (Fig. 5.1). Maximum water levels are naturally observed in the south of the coastal valley, that is, in the area of recharge of Quaternary aquifer from pre-Quaternary aquifers, and also naturally decrease towards the wadi axis, decreasing in general to 0 m-asl along the shore line of the Mediterranean Sea. And the only exceptions to this rule are the locations of water wells, where groundwater levels drop below 0 m-asl.

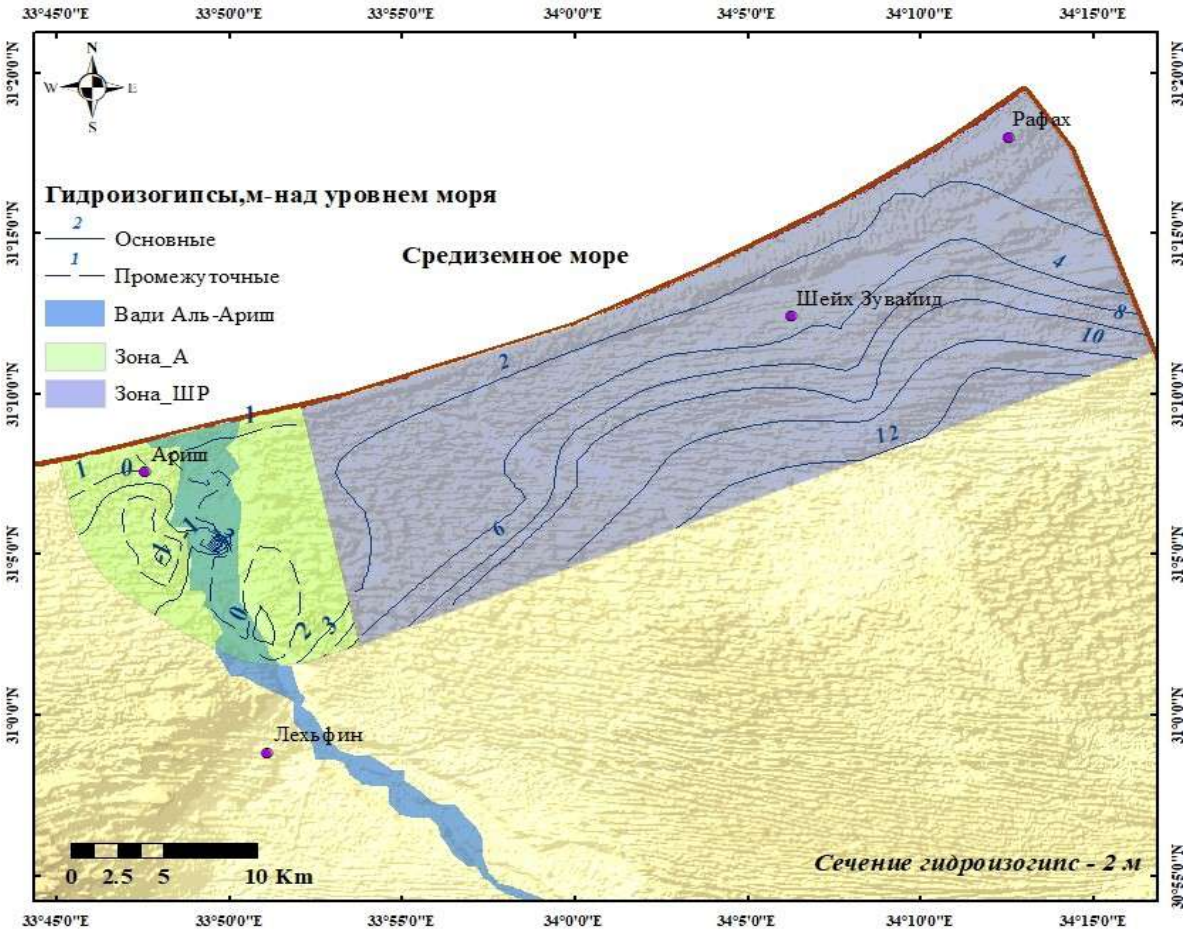

Fig. 5.1. Map of hydroisohypsum in zone A and zone SR

Figure 5.2 shows a typical graph of changes in water level in water intake wells - using the example of well No. A79 in 2016: in January-February (during the maximum flood) the water level was +0.53 m-asl, and by August, to the dry maximum period, decreased to -0.71 m-asl. Clearly, there is an urgent need to develop a plan for the proper management of groundwater resources in the El Arish area during the different seasons of the year.

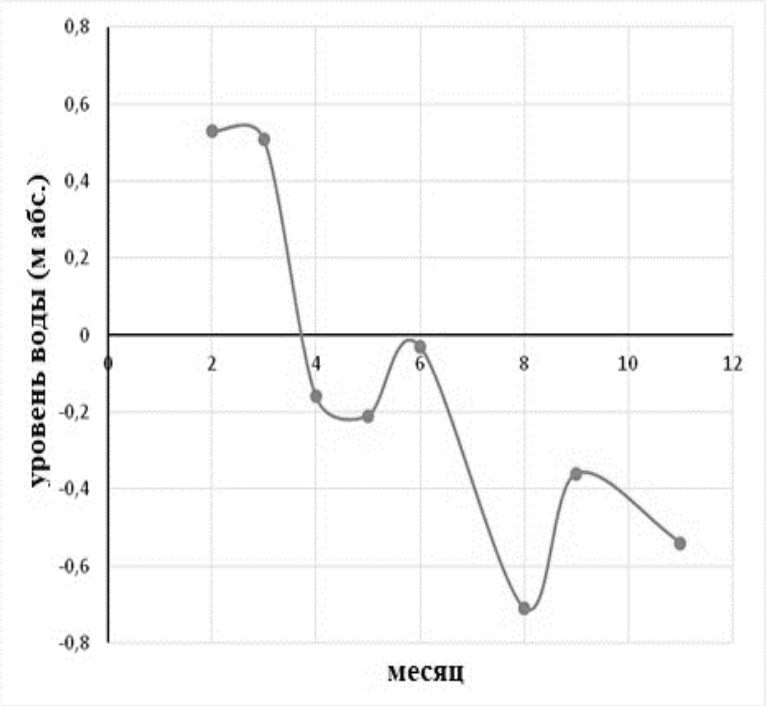

Fig. 5.2. Change in water level in water well No. A79,
located in zone_A

In the Rafah and Sheikh Zuwayid regions (zone_SR), the direction of groundwater flow is determined mainly, as in zone_A, by its movement from the southern border of the development of Quaternary aquifers to the north, to the edge of the Mediterranean Sea (Fig. 5.1). The drainage effect from small wadis is of secondary importance here. And individual water intake wells with low pumping rates are even less important.

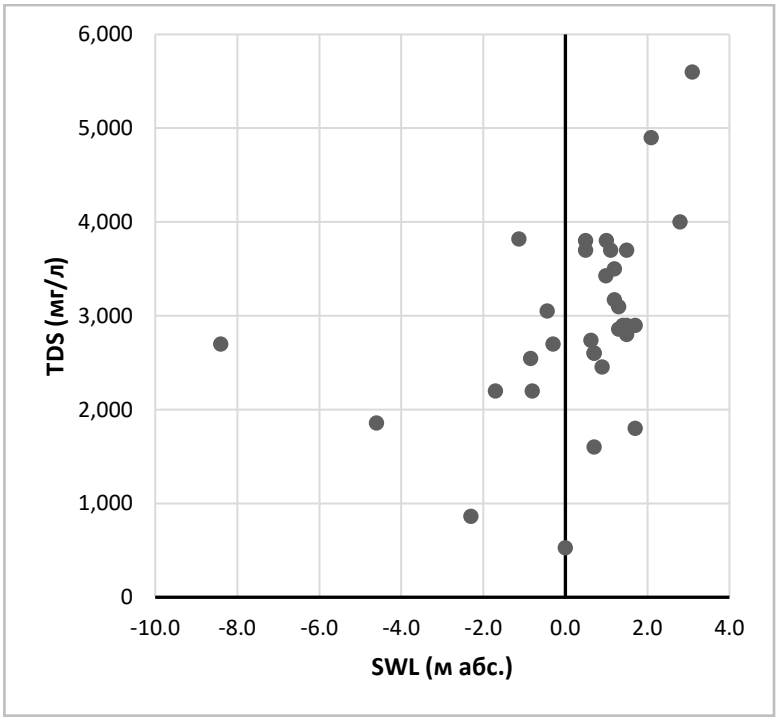

Fig. 5.3. Correlation between salinity (TDS) and static water level in wells (SWL) within zone_A

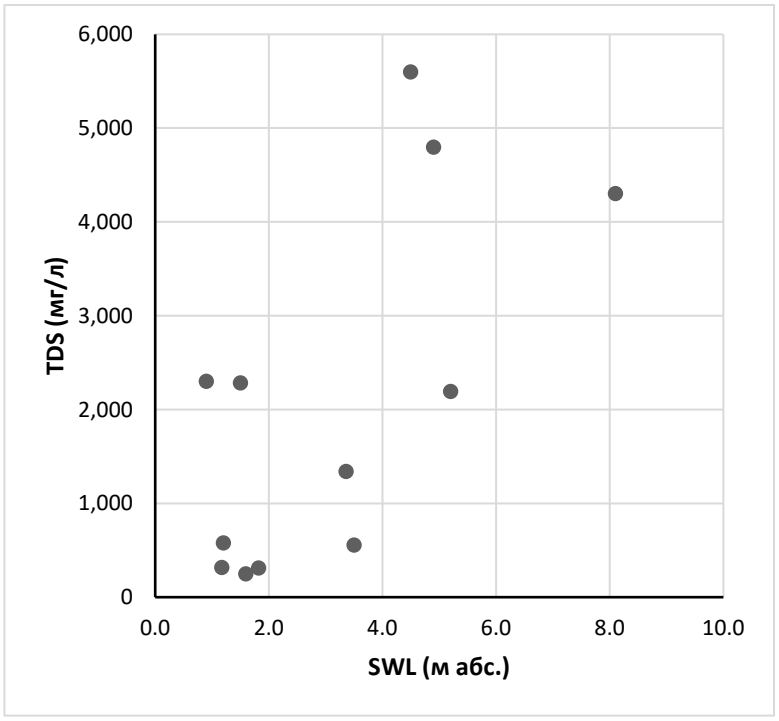

Fig. 5.4. Correlation between salinity (TDS) and static water level in wells (SWL) within zone_SR

It is possible that a decrease in water level in water intake wells may affect the quality of pumped groundwater. To assess this effect for both zones A and SR

– correlation dependences of groundwater salinity (TDS) on the value of water level in wells (SWL) were constructed (Fig. 5.3 and 5.4).

As can be seen in these figures, there is no obvious tendency towards an increase in mineralization at negative or close to 0 m absolute water levels in wells. And, conversely, there is a certain tendency towards an increase in mineralization with an increase in water level in wells with values of the latter greater than 0 m abs. These patterns require further study as relevant factual material accumulates.

5.2. Pre-Quaternary aquifers

Morphologically, the territory of the Sinai Peninsula, represented mainly by pre-Quaternary sediments, consists of two main zones - the Central Plateau and the folded mountains of the Syrian Arc zone. The southern part of Sinai consists of a complex of folded mountains formed by Precambrian igneous and metamorphic rocks; this area is characterized by the highest absolute levels in the Sinai. Therefore, the main direction of flow of groundwater and surface water, coinciding with the direction of flow of surface water in various wadis, is from south to north of Sinai, as well as in the aquifers of Quaternary sediments, to the Mediterranean Sea.

The southern part of the peninsula is a massive plateau, on the eastern and western flanks of which the main flow of groundwater is directed, respectively, to two other general drains, besides the Mediterranean Sea: The Gulf of Aqaba and Suez, which is due to the proximity of the water edges in these gulfs to zero absolute levels. In addition, local fluctuations in groundwater flow are due to the presence of a drainage system of various wadis, the main one being the El-Arish wadi with its tributaries. At the same time, the area in which pre-Quaternary aquifers are developed in northern Sinai is represented by large mountain blocks that belong to the Syrian Arc zone (Gebel Magara, Halal and Yellek), located

along the general axis directed from southwest to northeast. Most of these mountains are primarily composed of limestone, marl and sandstone, ranging in age from the Jurassic to the Upper Cretaceous. These deposits act as water-bearing deposits for aquifers in these areas.

In general, to construct hydroisohypsum maps of aquifers of pre-Quaternary deposits, the author had data on the position of the static groundwater level (SWL) in 106 wells, of which 46 wells were equipped for aquifers in Upper Cretaceous-Paleogene limestones, and in 60 wells equipped on aquifers in the Lower Cretaceous Nubian sandstones.

Using SPSS, statistical estimates were made for the distribution of measured water level elevations in hydrogeological wells (SWL). For pre-Quaternary deposits, various data samples were considered, similar to calculations when analyzing hydrogeochemical information - depending on the age and lithology of the sampled aquifers: 1) a general set for all pre-Quaternary deposits ("Pre-Quaternary as a whole"); 2) aquifers in limestone and 3) aquifers in sandstone. The results of calculating statistical parameters are given in Table 5.2.

Table 5.2- Statistical parameters of the distribution of marks of measured water levels in wells (SWL) for pre-Quaternary aquifers, m-asl

Parameters	All	Limestone K_2+P_g	Sandstone K_1
N	106	46	60
Mean	182	123	227
Median	180	120	224
Std. Dev.	95	69.5	87.5
Minimum	3.1	3.1	23.6
Maximum	420	300	420

As can be seen from this table, the static levels of groundwater in pre-Quaternary deposits, in contrast to the levels in Quaternary deposits within the coastal valley, fluctuate in a very wide range from +400 to +3.1 m-asl. (in the

sample, limestone is from +300 to +3.1 m-asl.; in the sample, sandstone is from +420 to +24 m-asl.) And, thus, even based on these data alone, it can be stated that groundwater pressure gradients (hydraulic slopes) in pre-Quaternary aquifers are significantly higher than in Quaternary aquifers developed in the coastal valley along the edge of the Mediterranean Sea.

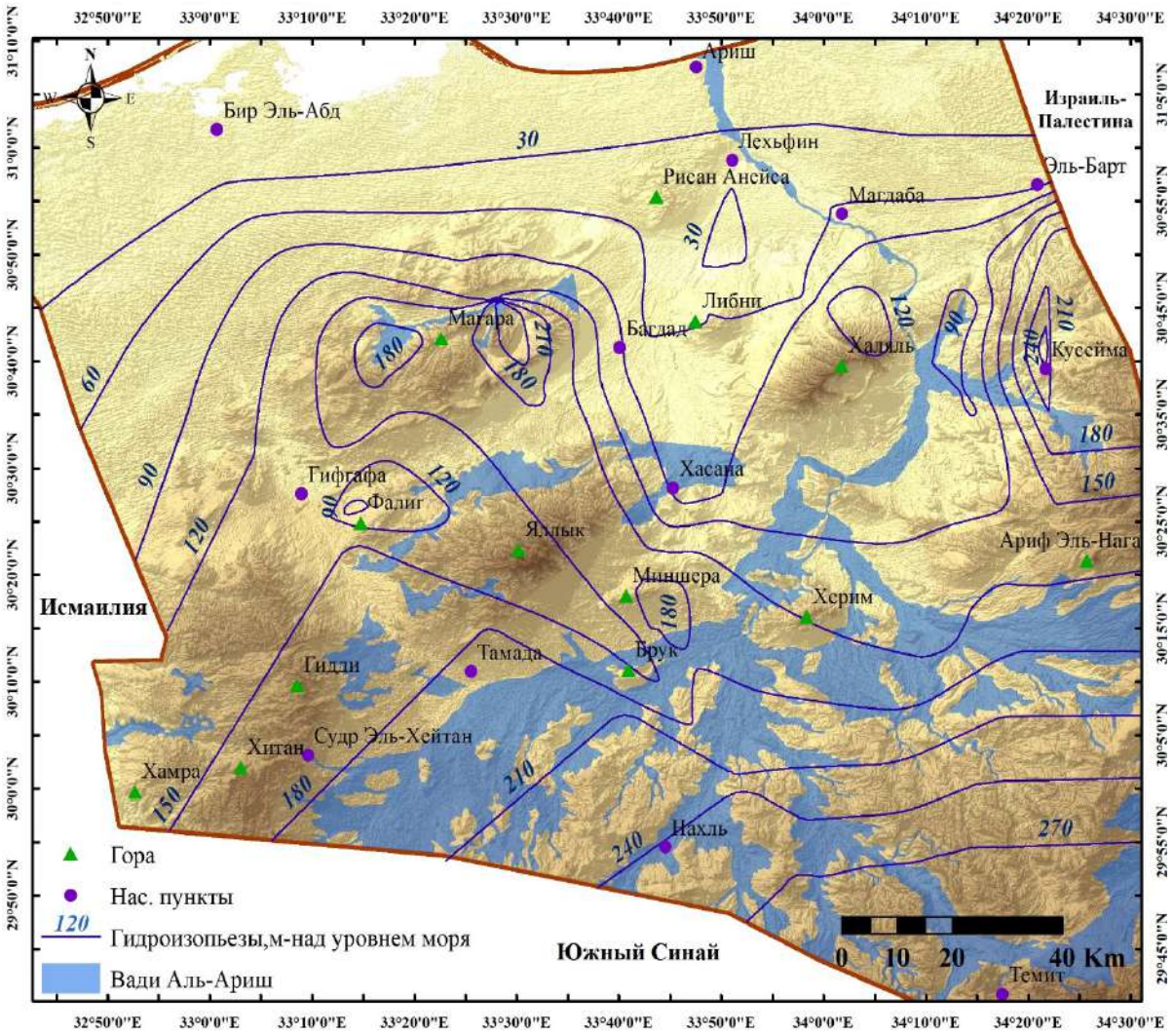

Fig. 5.5. Map of hydroisohypsum of the Upper Cretaceous-Paleogene limestone aquifer

Figures 5.5 and 5.6 show maps of hydroisohypses in aquifers developed in Upper Cretaceous-Paleogene limestone and Lower Cretaceous sandstone, respectively.

As shown in Figure 5.5, in the Upper Cretaceous-Paleogene limestone aquifer, against the background of the general trend described above in the

development of groundwater flow in certain areas, for example, around the settlements of Gebel Faliga, Gebel Halal, Hasana and Risan Aneisa, the groundwater level is significantly lower, than in neighboring areas, which is obviously due to intensive pumping of groundwater from water wells, since here groundwater is the only source of water supply.

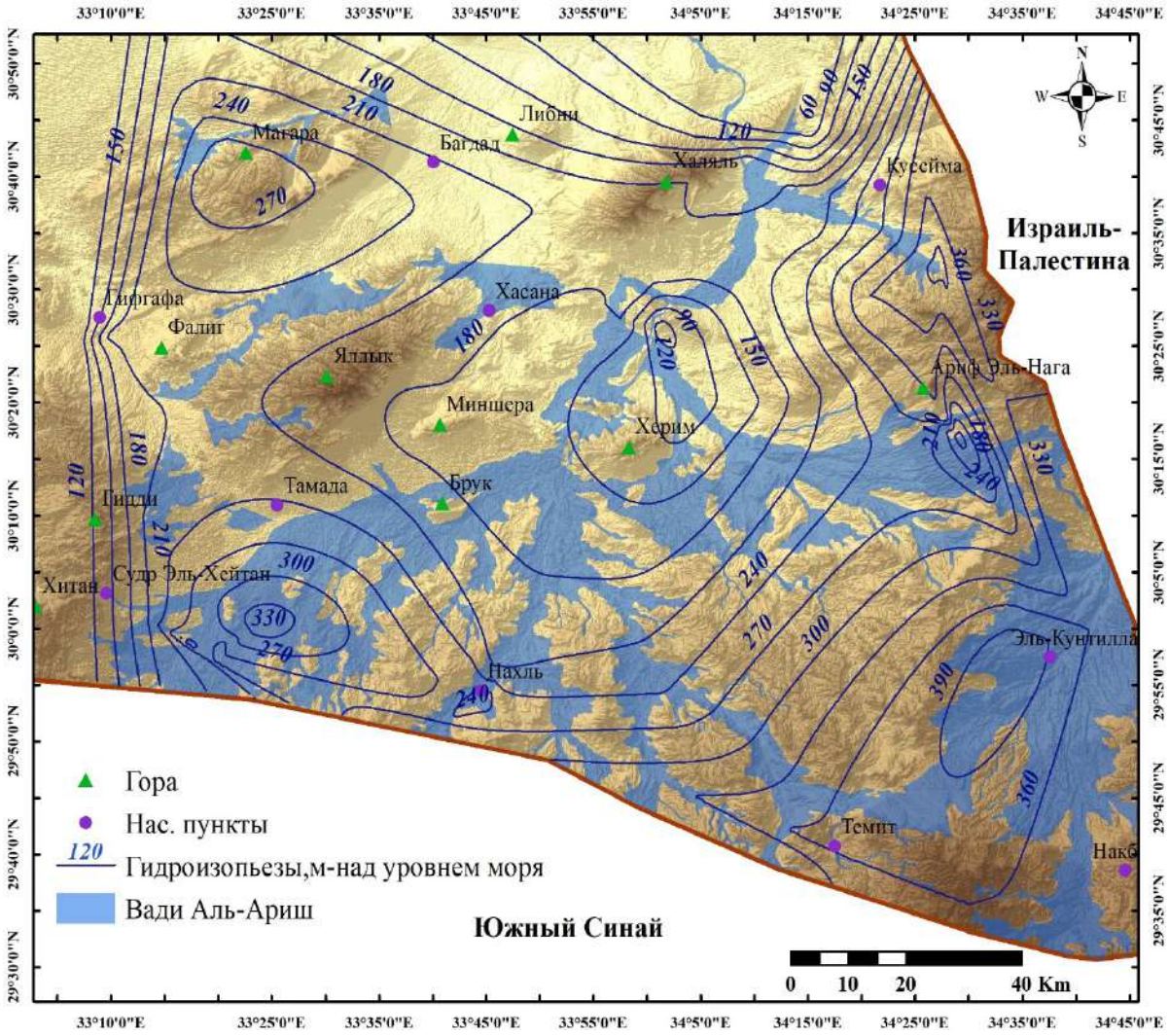

Fig. 5.6. Map of hydroisohypsum of the Lower Cretaceous (Nubian) sandstone aquifer

And, conversely, in the areas of the settlements of Gebel Magara and Qusseima, the water level increases to 200 m above sea level, which should definitely be considered increased compared to the levels in neighboring areas. This is apparently due to the location of these sites in relatively elevated areas, within blocks of limestone, hydraulically isolated from the surrounding zones.

As shown in Figure 5.6, in accordance with the above direction of the general flow from south to north, the highest groundwater levels in sandstones +410 and + 330 m-asl are observed in the El-Kuntilla area in the southeast and in the Sudr El-Heitan area in the southwest of North Sinai; and the lowest levels are about + 50 m-asl northeast of Gebel Halal. And thus, the piezometric surface of the Nubian sandstone aquifer descends approximately from south to north with an average hydraulic slope of about 0.003. At the same time, as in the case of limestones, in certain areas, for example, around the settlement of Gebel Kherim, the groundwater level in sandstones turns out to be noticeably lower than in neighboring areas, which is due to intensive pumping of groundwater from water wells.

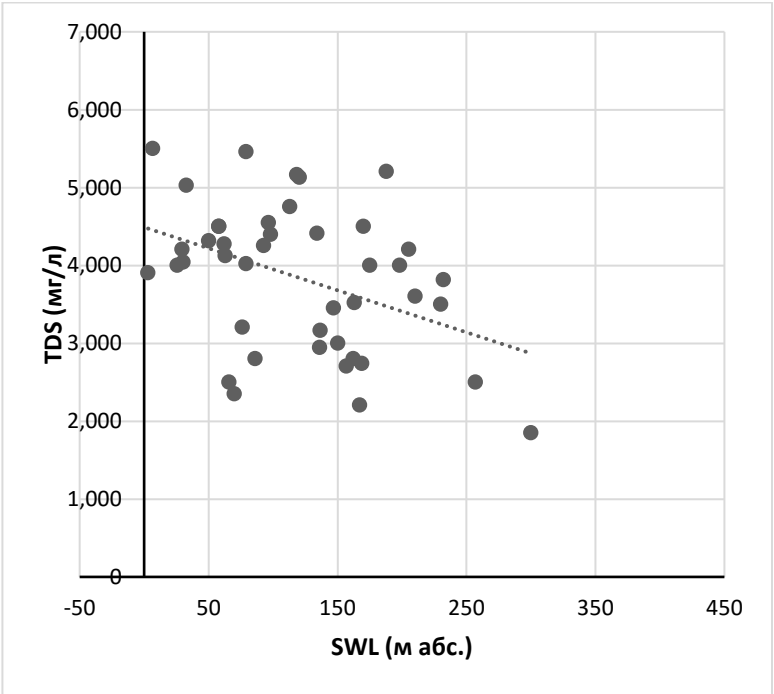

Fig. 5.7. Correlation between salinity (TDS) and groundwater level in wells (SWL) drilled on Upper Cretaceous-Paleogen limestone

As in the case of groundwater in Quaternary deposits, for groundwater developed in Upper Cretaceous-Paleogene limestones and Lower Cretaceous Nubian sandstones, correlation dependences of groundwater salinity (TDS) on the value of water level in wells (SWL) were constructed (Fig. 5.7 and 5.8, respectively). And although an unambiguous relationship is not observed in these

figures, nevertheless, in both graphs one can assume a tendency towards a decrease in mineralization as the absolute level of the tested groundwater increases. Therefore, it is possible that in water intake wells, as the water level decreases, the quality of the pumped water will deteriorate, at least in the direction of increasing salinity.

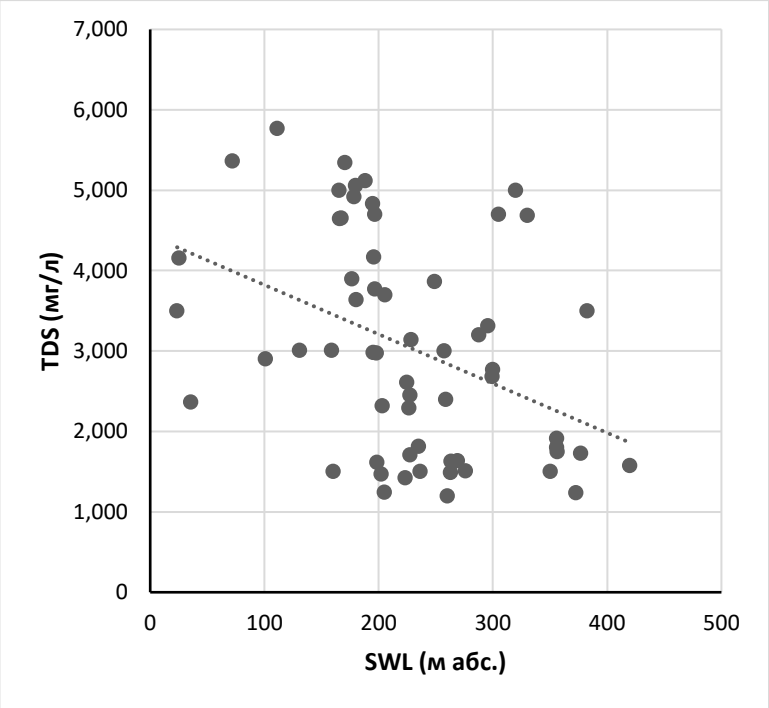

Fig. 5.8. Correlation between salinity (TDS) and groundwater level in wells (SWL) drilled on Lower Cretaceous sandstone

5.3. Generalized structure of groundwater filtration flow within North Sinai

Figure 5.9 shows the generalized structure of groundwater filtration flow within northern Sinai, compiled from the totality of all measurements of groundwater levels in various aquifers lying first from the surface [1; 3; 5].

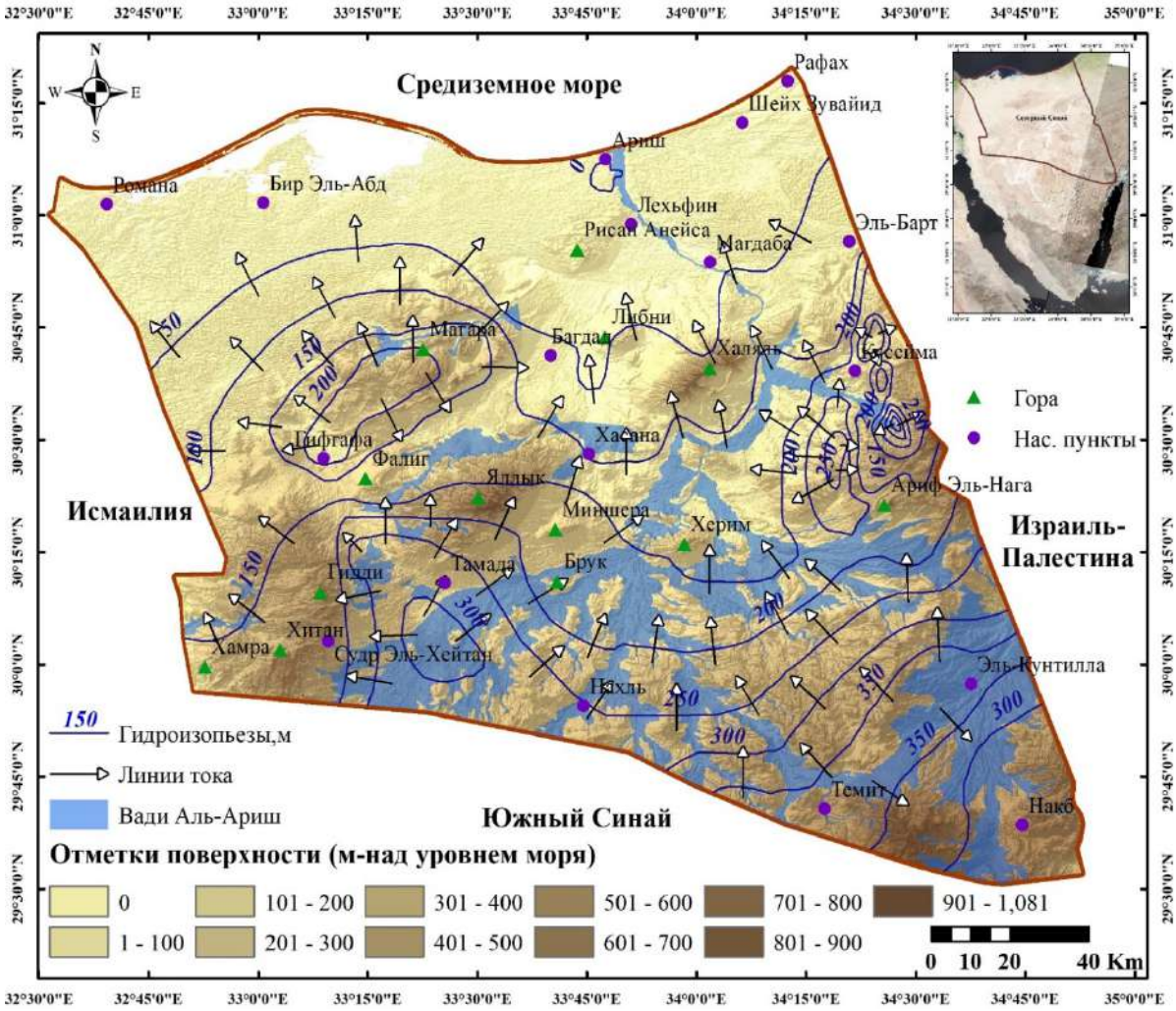

Fig. 5.9. Generalized structure of groundwater filtration flow within North Sinai

As was shown above, for individual aquifers (Fig. 5.1, 5.5 and 5.6), the generalized flow of groundwater, apparently flowing in a sub-horizontal direction from one aquifer to another, is directed mainly from south to north of North Sinai, towards the general drain - Mediterranean Sea, as well as partially in the western and eastern directions, towards the Gulf of Aqaba and Suez (including the Suez Canal). On average, the hydraulic slope of the main filtration flow of groundwater from south to north is about 0.002.

This map naturally reveals the fact that internal, more local groundwater flows are determined by the presence of high and low areas of relief and, as a consequence, low groundwater levels. That is, the general flow of groundwater is directed from areas of their supply, such as the areas of Nakhel, Temed and Sudr El-Heitan, to areas of their discharge, to the Mediterranean Sea, the Gulf of Suez and the Gulf of Aqaba, as well as to the valleys of the main wadi.

CONCLUSION

As a result of the studies described in Chapters 1, 2, 3 and 4, the initially set goals of the hydrogeological study of northern Sinai were achieved:

- the filtration properties of various aquifers were assessed;
- the structure of filtration flow of groundwater in various aquifers was clarified;
- The characteristics of the chemical composition of groundwater in various aquifers are given.

Based on the results of the research, the following conclusions can be drawn:

The distribution of aquifers in Quaternary sediments of significant thickness (up to 100 m) is limited to the coastal plain along the Mediterranean Sea, 10 to 15 km wide. The main water-bearing rocks in the Quaternary aquifer are sand, gravel and kurkar deposits (calcareous sand).

All Quaternary sediments are characterized by very high values of filtration coefficients, averaging tens and even hundreds of m/day. Kurkar and gravel deposits are characterized by a very large scatter of filtration coefficient values - tens of times. Most likely, this is due to different degrees of cementation of these rocks. Sand deposits are more homogeneous from a filtration point of view: the minimum filtration coefficients differ from the maximum by only 2.5−3.5 times.

There is no unambiguous trend in the graphs of correlation dependencies between the filtration coefficient (K) and the depth of the tested well (ds) either for all Quaternary deposits as a whole, or for each of the specified rock varieties.

The thesis presents the areal (in plan) zoning of the territory of development of Quaternary deposits based on the values of filtration coefficients within the coastal plain. From the point of view of water abundance, the development of water supplies due to water-bearing composed of kurkar deposits and gravel

seems most promising in the area of Wadi El Arish, and for water-bearing composed of sand in the areas of the northwestern part of North Sinai.

Static groundwater levels in Quaternary deposits fluctuate in a very narrow range from +8.10 to –8.40 m-asl. Moreover, negative values are clearly associated with operational wells pumping out groundwater.

The main problem with using all groundwater in North Sinai for water supply is its relatively high salinity.

In aquifers in Quaternary deposits, in general, groundwater mineralization in the vast majority of cases ranges from 1900 to 5100 mg/dm^3. There are no unambiguous correlations between groundwater salinity (TDS) and the depth of the tested well (ds). Fresh water with a salinity of less than 1000 mg/dm^3 is found in individual wells drilled into the uppermost of sand deposits (mainly coastal sand dunes) and gravel deposits, which indicates the replenishment of fresh water reserves in these layers due to modern infiltration feeding by atmospheric precipitation.

There were no fundamental differences in the statistical parameters of the distribution of various indicators of the chemical composition of groundwater for all of the specified deposits. All brackish waters are near-neutral or slightly alkaline, on average sulfate-chloride, predominantly calcium-magnesium-sodium. Naturally, a direct linear dependence of mineralization (TDS) on the concentrations of Cl and Na, but on the SO_4 content appears unambiguously. For the remaining macrocomponents, no significant dependence is observed.

Over much of the coastal plain, the PHREEQC-calculated groundwater saturation index (SI) for rock-forming carbonate minerals in Quaternary sediments is substantially less than zero. In this case, there is practically no dependence of saturation on mineralization. Thus, in the formation of the chemical composition of waters, the predominant influence is exerted by infiltration feeding by atmospheric precipitation and/or intrusion of sea water

from the Mediterranean Sea. Moreover, even a relatively high average evaporation rate in an arid climate does not lead to the saturation of groundwater with respect to carbonate minerals. The exception is the groundwater within Wadi El-Arish, which, on the contrary, in the vast majority of cases is saturated or even supersaturated with respect to all carbonate minerals (SI close to or greater than 1). There is also no dependence of saturation on mineralization here. It is obvious that the formation of these waters is determined, first of all, not by the infiltration of atmospheric precipitation during flood periods and not by the intrusions of sea waters, but by the inversion feeding of aquifer directly from Wadi El-Arish during periods of floods, when the water line mark in a temporary watercourse significantly exceeds the level marks groundwater in surrounding areas.

The SI index for all groundwater in Quaternary sediments with respect to sulfate minerals is significantly less than zero. But at the same time, in contrast to the situation with carbonate minerals, there is a certain tendency to increase the degree of saturation as the mineralization of groundwater increases. Probably, the factors for increasing sulfate concentrations here are either the evaporation of infiltrating atmospheric precipitation, or water developed in pre-Quaternary rocks, which enter Quaternary sediments due to subvertical flow from bottom to top or during the process of water outflow from Wadi El-Arish described above.

Pre-Quaternary sedimentary rocks are widespread in North Sinai. Among them are rocks of Jurassic, Lower Cretaceous, Upper Cretaceous and Paleogene. Analysis of the distribution of filtration coefficient values in samples corresponding to the age of the water-bearing rocks turned out to be uninformative: characterized by an extremely large scatter of values and the absence of any correlation with the conditions of occurrence of the sampled intervals.

Pre-Quaternary aquifers are represented mainly by two types of rocks: Upper Cretaceous-Paleogene limestone and Lower Cretaceous Nubian sandstone.

The average and median values of filtration coefficients in limestones and sandstones are values of the same order, but several times and even tens of times less than in Quaternary aquifers. Within each of these samples, a very large scatter is noted: in limestone - from 0.10 to 113 m/day, in sandstone - from 0.13 to 87 m/day. It is obvious that the permeability of all pre-Quaternary sediments is determined not by the filtration properties in porous blocks, but by the intensity of fracturing of the water-bearing rocks. At the same time, the highest values of filtration coefficients (more than 60 m/day) both in limestone and sandstone are observed only to a depth of less than 400 m, and at depths of more than 400 m these values do not exceed 20 m/day at all, amounting to about 5 m/day in limestone and 10 m/day in sandstone.

As for Quaternary deposits, the work presents areal (in plan) zoning of the territory of development of pre-Quaternary deposits based on the values of filtration coefficients, but for the entire territory of North Sinai. In terms of water abundance, the most promising areas for groundwater extraction are the following areas: in the vicinity of Al-Qusaim, Baghdad, Gebel Libni, and Gebel El-Magar for the Upper Cretaceous-Paleogene limestone aquifer and around Al-Qusaim and Gebel Arif El-Naga, and also in Rafah and Sheikh Zuwayid for the Nubian sandstone aquifer.

Static groundwater levels in pre-Quaternary sediments in northern Sinai as a whole, in contrast to levels in Quaternary sediments within the coastal plain, fluctuate in a very wide range from +400 to +3.1 m-asl, which is naturally due to the topography of the territory under consideration.

In the aquifers of pre-Quaternary deposits, in general, the mineralization of groundwater in the vast majority of cases fluctuates approximately in the same range as in Quaternary deposits: from 950 to 7000 mg/dm^3, with unambiguous correlations between groundwater salinity (TDS) and the depth of the sampled wells (ds) are not observed.

There are also no fundamental differences in the statistical parameters of the distribution of various indicators of the chemical composition of groundwater. Both limestone and sandstone contain both practically fresh (about 1000 mg/dm^3) and brackish, near-neutral or slightly alkaline groundwater, on average sulfate-chloride and predominantly sodium. That is, in terms of chemical composition, groundwater in pre-Quaternary aquifers differs little from groundwater developed in Quaternary aquifer.

The groundwater saturation index (SI) in both aquifers of pre-Quaternary sediments in relation to rock-forming carbonate minerals varies in an extremely wide range: from -2.5 ÷ -1.5 to +0.5 ÷ +0.8, that is, groundwater pre-Quaternary sediments can be either undersaturated or oversaturated with respect to carbonate minerals (regardless of the mineral composition of the water-bearing rocks). Any obvious relationship between the saturation index in relation to carbonate minerals and the sampling depth is not observed in either sandstones or limestones, which obviously indicates the presence of different conditions for the formation of groundwater in different sampled areas.

In both the Upper Cretaceous-Paleogene limestone and the Lower Cretaceous sandstone, the saturation index of groundwater with respect to sulfate minerals, as in Quaternary aquifer, is significantly less than zero. And at the same time, there is also a certain tendency to increase the degree of saturation as the mineralization of groundwater increases.

Most likely, the modern chemical composition of groundwater in pre-Quaternary deposits is due to the mixing in various proportions of initial salty sedimentogenic water and infiltrative water, taking into account their evaporation in an arid climate, as well as the flow from one aquifer to another and ion (cation) exchange processes. The source of increased sulfate concentrations is probably water that was either in local zones in direct contact with gypsum or anhydrite (very rare), or initially infiltrated, but with a relatively high degree of evaporation,

which is indirectly indicated by a positive correlation of sulfate concentration and mineralization.

In the work, based on the analysis of hydroisohypsum and hydroisopiesis maps, the main directions of filtration flow of groundwater in various aquifers were identified. The generalized (for all aquifers in total) flow of groundwater, obviously flowing in a sub-horizontal direction from one aquifer to another, is directed mainly from the south to the north of North Sinai, towards the general drain - the Mediterranean Sea, and also partially in the western and eastern directions, towards the Gulf of Aqaba and Suez (including the Suez Canal). On average, the hydraulic slope of the main filtration flow of groundwater from south to north is about 0.002. The direction of internal, more local groundwater flows is determined by the presence of high and low areas of relief and, as a consequence, high and low groundwater levels. In the vast majority of cases, the valleys of numerous wadis act as low areas.

REFERENCES

1. Mohamed Y.S. and Vinograd N.A., (2021). Tracking the natural direction of groundwater flow in North Sinai // From the 23rd XVII Great Geographical Festival, dedicated to the 195th anniversary of the Russian round-the-world trip F.P. Litke (1826-1829) - (St. Petersburg, St. Petersburg State University, Institute of Earth Sciences). C. 205-209. ISBN 978-5-4386-2045-7
2. Mohamed Y.S. and Vinograd N.A., (2021). Zoning of the north of the Sinai Peninsula according to the filtration properties of pre-Quaternary water-bearing rocks // Underground hydrosphere: Materials of the XXIII All-Russian meeting on groundwater in eastern Russia with international participation. – Irkutsk: Institute of the Earth's Crust SB RAS, 2021. –P. 93-95. DOI: 10.52619/978-5-9908560-9-7-2021-23-1-93-95
3. Mohamed Y.S. et al., (2021). Natural and man-made factors in the formation of filtration flows of groundwater in Northern Sinai // Bulletin of Voronezh State University. Series: Geology. No. 4. pp. 71-81. DOI:https://doi.org/10.17308/geology.2021.4/3792
4. Mohamed Y.S., et al., (2020). Assessment of filtration conditions through earthen dams when changing their parameters using the Z_SOIL program // Bulletin of Voronezh State University. Series: Geology. No. 2. pp. 90-97. DOI:https://doi.org/10.17308/geology.2020.2/2863
5. Mohamed Y.S., et al., (2020). Structure of groundwater filtration flows in the North of the Sinai Peninsula. Geology, geoecology, evolutionary geography: Collective monograph. Volume XIX / Ed. EAT. Nesterova, V.A. Snytko. -SPB.: Publishing house of the Russian State Pedagogical University named after. A.I. Herzen. No. 36. pp. 259-262. ISBN 978-5-8064-2986-6.
6. Hydrogeologist's Reference Guide. T.1. (Edited by Maksimov V. M.). M.: Nedra. 1967.
7. Abd El-Aal G.A., (1998). Thesise: Hydrogeology and Land Use Classification of North Sinai Peninsula with the Environmental Impact of Groundwater on Exploitation and Pollution, Egypt.
8. Abd El-Samie S. G. and Sadek M. A., (2001). Groundwater recharge and flow in the Lower Cretaceous Nubian Sandstone aquifer in the Sinai Peninsula, using isotopic techniques and hydrochemistry. Hydrogeology journal of Springer-Verlag, Vol. 09, pp. 378-389. DOI: 10.1007/s100400100140.

9. Abdallah A.M. et al., (2001). Stratigraphy of the Cenomanian and Turonian sequence of El Giddi pass, North West Sinai, Egypt. The 6th conference Geology of Sinai for Development, Ismailia, pp. 211-229.
10. Abdelaziz R. and Bakr M. I., (2012). Inverse Modeling of Groundwater Flow of Delta Wadi El-Arish. Journal of Water Resource and Protection, Vol. 4, pp. 432-438.
11. Abdel-Ghaffar M.K. et al., (2015). Watershed Characteristic and Potentiality of Wadi El-Arish, Sinai, Egypt. International Journal of Advanced Remote Sensing and GIS, Vol. 4, Issue 1, pp. 1070-1091.
12. Abdel-hady A.A., and Fursich F.T., (2014). Macroinvertebrate Palaeo-communities from the Jurassic succession of Gebel Maghara, Sinai, Egypt. Journal of African Earth Sciences, Vol. 97, pp. 173-193.
13. Abdel-Rahman A.A. et al., (2010). Geoelectrical Exploration to Delineate the Groundwater Occurrence in Risan Unayzah Area, North Sinai. The 6th International Symposium on Geophysics, Tanta, Egypt, pp. 144-152.
14. Abdel-Raouf O., (2014). Investigation of groundwater flow heterogeneity in fractured aquifers (Case study: Qusiema area, North Sinai). International Journal of Water Resources and Environmental Engineering, Vol. 6(11), pp. 279-286.
15. Abdel-Shafy H.I. and Kamel A.H., (2016). Groundwater in Egypt Issue: Resources, Location, Amount, Contamination, Protection, Renewal, Future Overview. The Egyptian Journal of Chemistry, Vol. 59, No. 3, pp. 321- 362.
16. Abdulhadya Y.A., and Sayedb A.S., (2018). Evaluation of Hydrochemical Facies and Ionic Ratio of Al-Salam Canal Water and Its Relation with Watery Extracted Soil and Water Table, North Sinai, Egypt. Octa Journal of Environmental Research, Vol. 6(2), pp. 052-074.
17. Abo El-Fadl M.M., (2018). Monitoring of water - rock interaction and its impact on groundwater salinization at El Goura area, Northeast Sinai, Egypt. Journal of Current Science International-CRW, Vol. 07, Issue 02, pp. 279-292.
18. Abouelmagd A. et al., (2014). Paleoclimate record in the Nubian Sandstone Aquifer, Sinai Peninsula, Egypt. Journal of Quaternary Research Vol. 81, pp. 158–167.
19. AbuBakr M. et al., (2013). Use of radar data to unveil the paleolakes and the ancestral course of Wadi El-Arish, Sinai Peninsula, Egypt. Journal of Geomorphology Vol. 194, pp. 34–45.
20. Afify A.M. et al., (2019). Contribution to the stratigraphy and sedimentology of the Upper Jurassic – lower Eocene succession of the Mitla–El Giddi stretches, west Central Sinai, Egypt. Journal of African Earth Sciences, No. 125, pp. 48-68.

21. Aggour, T. A. et al., (2007). Geology of Water Resources at Wadi Geraia Basin, Sinai, Egypt. Egyptian Journal of Geology, Vol. 51, pp.177-204.
22. Al-Gamal S.A. and Sadek M., (2015). An assessment of water resources in Sinai Peninsula, using conventional and isotopic techniques, Egypt. International Journal of Hydrology Science and Technology, Vol. 5, No. 3, pp. 241-257.
23. Allam A., and Khalil H., (1988). Geology and stratigraphy of the Arif El-Naqa area, Sinai, Egypt. Journal of Geology Sciences, No. 32, Vol. 1-2, pp. 199-218.
24. Arad A., and Kafri U., (1980). Hydrogeological Inter-Relationship between the Judea Group and the Nubian Sandstone Aquifers in Sinai and the Negev. Israel Journal of Earth-Sciences, Vol. 29, pp.67-72.
25. Arnous M.O., (2016). Groundwater potentiality mapping of hard-rock terrain in arid regions using geospatial modelling: example from Wadi Feiran basin, South Sinai, Egypt. Hydrogeology Journal of Springer Vol. 24, pp. 1375–1392.
26. Attia O.E., (1998). Evolution of El Sheikh Zuweid modern brine, north Sinai, Egypt. Journal M.E.R.C. of Ain Shams University, Earth Sciences, Vol. 12, pp. 188-204.
27. Barseem M.S., (2011). Delineating the Conditions of Groundwater Occurrences in the Area South Baloza, Romana Road, North West Sinai, Egypt. Egyptian Geophysical Society (EGS) Journal, Vol. 9, No. 1, pp. 135-143.
28. Bekhit H. M., (2015). Sustainable groundwater management in coastal aquifer of Sinai using evolutionary algorithms. Journal of Procedia Environmental Sciences, Vol. 25, pp. 19-27.
29. Carling P. et al., (2009). Unsteady 1D and 2D hydraulic models with ice dam break for Quaternary mega-flood, Altai Mountains, southern Siberia. Journal Global and Planetary Change. DOI: 10.1016/j.gloplacha.2009.11.005.
30. Carling P. et al., (2009). Unsteady 1D and 2D hydraulic models with ice dam break for Quaternary mega-flood, Altai Mountains, southern Siberia. Journal Global and Planetary Change. DOI: 10.1016/j.gloplacha.2009.11.005.
31. Climate Change Research Institute database - National Water Research Center - Ministry of Water Resources and Irrigation. The Arab Republic of Egypt. www.mwri.org.eg (In Arabic) checked in 06.06.2021.
32. Comte J. C. et al., (2016). Challenges in groundwater resource management in coastal aquifers of East Africa: Investigations and lessons learned in the Comoros Islands, Kenya, and Tanzania. Journal of Hydrology, Vol. 5, pp. 179–199.

33. Dada P. O. O. et al., (2016). Effects of soil physical properties on soil loss due to manual yam harvesting under a sandy loam environment. Journal of international soil and water conservation research, Vol. 4, pp. 121-125.
34. Database of the Egyptian General Authority for Mineral Resources, (2018). El Weili - Cairo. The Arab Republic of Egypt.
35. Effat H.A. and Hegazy M.N., (2012). Mapping potential landfill sites for North Sinai cities using spatial multicriteria evaluation. The Egyptian Journal of Remote Sensing and Space Science, Vol. 15, Issue 2, pp. 125-133.
36. El Alfy M., (2010). Integrated geostatistics and GIS techniques for assessing groundwater contamination in Al Arish area, Sinai, Egypt. Arab Journal of Geosciences, Vol. 5, pp. 197-215.
37. El-Alfy M., and Merkel B., (2006). Hydrochemical Relationships and Geochemical Modeling of Groundwater in Al Arish Area, North Sinai, Egypt. Journal of American Institute of Hydrology, Vol. 22, No. 1-4, pp. 47-62.
38. El-Beialy S.Y. et al., (2010). Palynology of the Mid-Cretaceous Malha and Galala formations, gebel El Minshara, North Sinai, Egypt. Journal SEPM (Society for Sedimentary Geology), Vol. 25, pp. 517-526.
39. Elbeih S. F., (2015). An overview of integrated remote sensing and GIS for groundwater mapping in Egypt. Ain Shams Engineering Journal, Vol. 6, pp. 1–15.
40. El-Bihery M. A. and Lachmar T. E., (1994). Groundwater quality degradation as a result of overpumping in the delta Wadi EI-Arish area, Sinai Peninsula, Egypt. Journal of Environmental Geology, Vol. 24, pp. 293-305.
41. Elewa H. H. et al., (2013). Runoff Water Harvesting Optimization by Using RS, GIS and Watershed Modelling in Wadi El-Arish, Sinai. International Journal of Engineering Research & Technology (IJERT), Vol. 2, Issue 12.
42. Elewa H.H., and Qaddah A.A., (2011). Groundwater potentiality mapping in the Sinai Peninsula, Egypt, using remote sensing and GIS-watershed-based modeling. Hydrogeology Journal of Springer-Verlag, Vol. 19, pp. 613–628.
43. El-Kashouty M. et al., (2011). Characterization of the aquifer system in the northern Sinai Peninsula, Egypt. Journal of Environmental Chemistry and Ecotoxicology, Vol. 4(3), pp. 41-63.
44. El-Rayes A.E. et al., (2017). Morphotectonic controls of groundwater flow regime and relating environmental impacts in Northwest Sinai, Egypt. Arab Journal of Geosciences, Vol. 10, pp. 401-420.

45. El-Samanoudi M.A. et al., (2011). Assessment of Groundwater Resources in North Eastern Sinai Peninsula Constrained by Mathematical Modeling Techniques. Fifteenth International Water Technology Conference, IWTC-15 2011, Alexandria, Egypt.
46. Embaby A.A., and El-Barbary S.M., (2011). Evaluation of Quaternary aquifer for agricultural purposes in northwest Sinai, Egypt. Journal of American Science, Vol. 7(3), pp. 344-361.
47. Fathy K. et al., (2014). Gravity observations at Sinai Peninsula and its geophysical and geodetic applications. NRIAG Journal of Astronomy and Geophysics, Vol. 2, pp. 223-233.
48. Feldman H.R. et al., (2012). Taxonomy and Paleobiogeography of late Bathonian Brachiopods from gebel Engabashi, Northern Sinai. Journal of Paleontology, Vol. 86, Issue 2, pp. 238-252.
49. Gad M. I. and Khalaf S., (2015). Management of Groundwater Resources in Arid Areas Case Study: North Sinai, Egypt. Journal of Water Resources, Vol. 42, No. 4, pp. 535-552.
50. Geriesh M.H. et al., (2015). Geoenvironmental Impact Assessment of El-salam Canal on the Surrounding Soil and Groundwater Flow Regime, Northwestern Sinai, Egypt. CATRINA Journal the Egyptian Society for Environmental Sciences, Vol. 12 (1), pp. 17-29.
51. Gheith H. M. and Sultan M. I., (2000). Assessment of the renewable groundwater resources of Wadi El-Arish, Sinai, Egypt: modelling, remote sensing and GIS applications. Journal of Remote Sensing and Hydrology, No. 267, pp. 451-454.
52. Ghoubachi S.Y., (2013). Contribution to the hydrogeology of the Lower Cretaceous aquifer in east Central Sinai, Egypt. Journal of King Saud University – Science, Vol. 25, Issue 2, pp. 91-105.
53. Heinl M. and Brinkmann P. J., (1989). A groundwater model of the Nubian aquifer system. Journal of Hydrological Sciences, Vol. 34, No. 4.
54. https://www.youm7.com
55. Ibrahim E.H. et al., (2018). Geoelectric study for Quaternary groundwater aquifers in northwest Sinai, Egypt. https://www.researchgate.net/publication/23810031.
56. Idris H., (2000). Short account of groundwater as the source for famous springs in Egypt. Hydrogeology, 1 T., 76, pp. 389-404.
57. Issar A. and Bein A., (1972). On the Ancient Water of the Upper Nubian Sandstone Aquifer in Central Sinai and Southern Israel. Journal of Hydrology, Vol. 17, pp. 353-374.

58. Issar A.S. and Bruins H.J., (1983). Special Climatological Conditions in the Deserts of Sinai and the Negev during the Latest Pleistocene. Elsevier Science Journal of Palaeogeography, Palaeoclimatology, Palaeoecology, Vol. 43, pp. 63-72.
59. Jamel A. A., (2016). Analysis and Estimation of Seepage through Homogenous Earth Dam without Filter. Diyala Journal of Engineering Sciences, Vol. 09, No. 02, pp. 38-94. https://www.iasj.net/iasj?func=article&aId=113108.
60. Japan International Cooperation Agency (JICA), (1992). Main report: North Sinai Groundwater Resources Study in the Arab Republic of Egypt. https://www.jica.go.jp/english/
61. Jun-Feng F. U. and Sheng, J. A., (2009). Study on Unsteady Seepage Flow through Dam. Elsevier journal of hydrodynamics, Vol. 04, No. 21, pp. 499-504. DOI: 10.1016/S1001-6058(08)60176-6.
62. Jun-Feng F. U. and Sheng, J., (2009). A Study on Unsteady Seepage Flow through Dam. Elsevier journal of hydrodynamics, Vol. 04, No. 21, pp. 499-504. DOI: 10.1016/S1001-6058(08)60176-6.
63. Khaled M.A. et al., (2016). Geoelectrical and hydrogeological study to delineate the geological structures affecting the groundwater occurrence in Wadi El Khariq Basin, Northwest El Maghara, north Sinai, Egypt. Arab journal of Geosciences- Springer, DOI 10.1007/s12517-015-2286-5.
64. Kosinova I. I. and Kustova N. R., (2008). Teoriya i metodologiya geoekologicheskikh riskov [Theory and methodology of geoecological risks]. Vestnik Voronezhskogo gosudarstvennogo universiteta. Seriya: Geologiya. = Proceedings of Voronezh State University. Series: Geology, no 2, pp. 189-197 (In Russ.)
65. Maged M. E. et al., (2016). Estimation of flash flood using surface water model and GIS technique in Wadi El-Azariq, East Sinai, Egypt. Journal of Natural Hazards and Earth System Sciences, manuscript under review for the journal.
66. Magesh N. S. et al., (2012). Delineation of groundwater potential zones in Theni district, Tamil Nadu, using remote sensing, GIS and MIF techniques. Journal of Geoscience Frontiers, Vol. 3, No. 2, pp. 189-196.
67. Mekawy M.S., (2012). Unusual Factor Affecting the Preservation of Fossils from Northern Sinai, Egypt. Journal of Earth Science Climate Change, Vol. 3, Issue 3, doi:10.4172/2157-7617.1000121.

68. Mekawy M.S., (2013). Taphonomy of Aptian-Albian Beds in the Gebel Mistan, Maghara Area, Northern Sinai, Egypt. Journal of Earth Science Climate Change, Vol. 4, Issue 2, ISSN:2157-7617.
69. Milewski A. M., (2008). Remote Sensing Solutions for Estimating Runoff and Recharge in Arid Environments. Dissertations, 795. http://scholarworks.wmich.edu/dissertations/795
70. Mingqian Li et al., (2019). Hydrochemical Evolution of Groundwater in a Typical Semi-Arid Groundwater Storage Basin Using a Zoning Model. Water Journal, Vol. 11, No. 1334.
71. Ministry of State for Environmental Affairs - Environmental Affairs Agency, North Sinai Governorate - Environmental Affairs Administration, (2007). Environmental characterization of North Sinai Governorate. North Sinai Governorate. The Arab Republic of Egypt. (In Arabic)
72. Ministry of Water Resources and Irrigation, (2016). "Atlas of Climate Changes for the Sinai Peninsula". Nile Corniche - Imbaba. The Arab Republic of Egypt. www.mwri.org.eg (In Arabic) checked in 06.06.2021.
73. Ministry of Water Resources and Irrigation, (2017). "Atlas of torrents of the valleys of the Sinai Peninsula". Nile Corniche - Imbaba. The Arab Republic of Egypt. www.mwri.org.eg (In Arabic) checked in 06.06.2021.
74. Mohamed A.I., and Hassan M.A., (2017). Mapping of Groundwater Quality in Northern Sinai Using GIS Technique. Merit Research Journal of Agricultural Science and Soil Sciences, Vol. 5(2), pp. 024-039.
75. Mohamed L. et al., (2015). Structural Controls on Groundwater Flow in Basement Terrains: Geophysical, Remote Sensing, and Field Investigations in Sinai. Springer journal of Surv. and Geophys, DOI 10.1007/s10712-015-9331-5.
76. Mohamed Ya. Sh. et al., (2021). Justification for Effective Water Planning and Management in the North of the Sinai Peninsula, Egypt // Journal Bioscience Biotechnology Research Communications. Vol. 14, No. 03, pp. 986-992. DOI: http://dx.doi.org/10.21786/bbrc/14.3.13
77. Moustafa A.R., and Khalil S.M., (1995). Rejuvenation of the Tethyan passive continental margin of northern Sinai: deformation style and age (Gebel Yelleq area). Journal of Tectonophysics- Science Direct, Vol. 241, Issue 3-4, pp. 225-238.
78. Omran E., (2016). A stochastic simulation model to early predict susceptible areas to water table level fluctuations in North Sinai, Egypt. The Egyptian Journal of Remote Sensing and Space Science Vol. 19, Issue 2, pp. 235-257.

79. Peters E. et al., (2018). Tracers Reveal Recharge Elevations, Groundwater Flow Paths and Travel Times on Mount Shasta, California. Journal of Water, Vol. 10, No. 97.
80. Ramadan S. M. et al., (2013). Effect of Aswan High Dam (AHD) Storage on The Integrated Management of Water Resources in Egypt. The Egyptian Int. J. of Eng. Sci. and Technology, Vol. 16, No. 3, pp. 1517-1524.
81. Reddy V. R. et al., (2018). A Water–Energy–Food Nexus Perspective on the Challenge of Eutrophication. Journal of Water, Vol. 10, No. 101.
82. Rosenthal E. et al., (1990). Definition of groundwater flow patterns by environmental tracers in the multiple aquifer system of southern Arava Valley, Israel. Journal of Hydrogeology, Vol. 117, pp. 339-368.
83. Rosenthal E. et al., (2007). The hydrochemical evolution of brackish groundwater in central and northern Sinai (Egypt) and in the western Negev (Israel). Journal of Hydrology-Sience Direct, Vol. 337, pp. 294– 314.
84. Ruiz G., (2015). Estimation of the groundwater recharge in the aquifer of the Mexico City. Journal Procedia Environmental Sciences, Vol. 25, pp. 220 – 226.
85. Salem M. G. and El-Sayed E. A. H., (2017). Historical Satellite Data Analysis to Enhance Climate Change Adaption and Hydrologic Models in Egypt. Journal of Power and Energy Engineering, No. 5, pp. 56-71.
86. Santosh N. et al., (2016). Slope Stability Analysis with Geo5 Software for Malin Landslide in Pune (Maharashtra). Global Journal of Engineering Science and Researches. ISSN 2348 – 8034. http://www.gjesr.com/Issues%20PDF/TECHNOPHILIA-2016%20-%20Jaihind%20Polytechhnic,%20Kuran,%20February,%202016/3.pdf.
87. Seleem T. A., (2013). Analysis and Tectonic Implication of DEM-Derived Structural Lineaments, Sinai Peninsula, Egypt. International Journal of Geosciences, Vol. 4, pp. 183-201.
88. Senanayake I. P. et al., (2016). An approach to delineate groundwater recharge potential sites in Ambalantota, Sri Lanka using GIS techniques. Journal of Geoscience Frontiers, Vol. 7, pp. 115-124.
89. Shata A.A., (1982). Hydrogeology of the Great Nubian Sandstone basin, Egypt. Quarterly Journal of Engineering Geology and Hydrogeology, Vol. 15, pp. 127-133.
90. Smith S. E. et al., (1997). Locating regions of high probability for groundwater in the Wadi El-Arish Basin, Sinai, Egypt. Journal of African Earth Sciences, Vol. 25, No. 2, pp. 253-262.

91. Strzepek K. M. et al., (1996). Vulnerability assessment of water resources in Egypt to climatic change in the Nile Basin. Journal of Climate Research, Vol. 6, pp. 89-95.
92. Sultan A.S. et al., (2013). The Use of Geophysical and Remote Sensing Data Analysis in the Groundwater Assessment of El Qaa Plain, South Sinai, Egypt. 5th International Conference on Water Resources and Arid Environments (ICWRAE 5), Riyadh, Saudi Arabia pp. 292-305.
93. Sultan M. et al., (2002). Origin and recharge rates of alluvial ground waters, Eastern Desert, Egypt. https://www.researchgate.net/publication/255270881
94. Sultan M. et al., (2011). Modern recharge to fossil aquifers: Geochemical, geophysical, and modeling constraints. Journal of Hydrology Vol. 403, pp. 14–24.
95. Szczesny J. and Truty A., (2004). Dam surveillance and maintenance – general approach and case studies. http://www.symposcience.eu/exl-doc/colloque/ART-00001147.pdf.
96. UNEP. (2010). Africa Water Atlas. Division of Early Warning and Assessment (DEWA). United Nations Environment Programme (UNEP). Nairobi, Kenya.
97. Valenzuela L., (2016). Design, construction, operation and the effect of fines content and permeability on the seismic performance of tailings sand dams in Chile. Obras y Proyectos, Vol. 19, pp. 6-22. http://200.14.96.130/index.php/obrasyproyectos/article/view/116.
98. Vengosh A., and Rosenthal E. (1993). Saline Groundwater in Israel: Its Bearing on the Water Crisis in the Country. ELSEVIER Journal of Hydrology, Vol. 156, pp. 389-430.
99. Wahid A. et al., (2016). Geospatial Analysis for the Determination of Hydro-Morphological Characteristics and Assessment of Flash Flood Potentiality in Arid Coastal Plains: A Case in Southwestern Sinai, Egypt. Journal Earth Sciences Research, Vol. 20, No. 1, pp. E1-E9.
100. Wanas H. A., (2008). Cenomanian rocks in the Sinai Peninsula, Northeast Egypt: Facies analysis and sequence stratigraphy. Journal of African Earth Sciences, Vol. 52, pp. 125-138.
101. Water Resources Research Institute database - National Water Research Center - Ministry of Water Resources and Irrigation. The Arab Republic of Egypt. www.mwri.org.eg (In Arabic) checked in 06.06.2021.
102. Weinberger G. and Rosenthal E., (1998). Reconstruction of natural groundwater flow paths in the multiple aquifer system of the northern Negev (Israel), based on lithological and structural evidence. Springer-Verlag Hydrogeology Journal, Vol. 6, pp. 421–440.
103. Xu Y. Q. et al., (2003). Optimal hydraulic design of earth dam cross section using saturated–unsaturated seepage flow model. Journal Advances in Water Resources, Vol. 26, pp. 1–7. PII: S03 0 9-1 7 08 (0 2)0 01 2 4- 0.

104. Yeh H. et al., (2016). Mapping groundwater recharge potential zone using a GIS approach in Hualian River, Taiwan. Journal Sustainable Environment Research, Vol. 26, pp. 33-43.

105. Yousef A.F., and El Shenawy I.A., (2000). Environmental Monitoring of North Sinai with Emphasis on Factors Affecting the Salinity of some Sediments. Journal ICEHM2000, Cairo University, Egypt, pp. 91- 101.

106. Zhou Y. et al., (2013). Upgrading a regional groundwater level monitoring network for Beijing Plain, China. Journal Geoscience Frontiers Vol. 4, pp. 127 – 138.